January 2008

Hydrogeological characterization of baseflow to Jacob's Well spring, Hays County, Texas

Sarah Cain Davidson

Hydrogeological characterization of baseflow to Jacob's Well spring, Hays County, Texas

by

Sarah Cain Davidson, B.S.

Thesis

Presented to the Faculty of the Graduate School of

The University of Texas at Austin

in Partial Fulfillment

of the Requirements

for the Degree of

Master of Science in Geological Sciences

The University of Texas at Austin

December 2008

Hydrogeological characterization of baseflow to Jacob's Well spring, Hays County, Texas

Approved by
Supervising Committee:

Philip C. Bennett, supervisor

John M. Sharp, Jr.

David R. Maidment

Acknowledgements

I first want to first thank my advisor, Philip Bennett, for his guidance and advice, and the rest of the Bennett Lab group for their feedback and support. Second, this study would not exist without the financial and logistical support of the Hays Trinity Groundwater Conservation District. Andrew Backus, Al Broun, Doug Wierman, and Leslie Llado provided me with invaluable background information, well owner contacts, and advice about fieldwork. Holly Field and Wesley Schumacher were helpful and enthusiastic field assistants. Additional important logistical support and background information came from Marcus Gary, Gregg Tatum and the rest of the cave diving team, and David Baker.

Thanks to the many well owners of Wimberley who went out of their way to let me dig around in their sheds, provided me with well construction information, and sat out in the hot Texas sun to chat with me about the project. Special gratitude to the two who helped me battle a swarm of wasps and taught me how to change a tire on a pickup.

Thanks to Jay Banner and Larry Mack for assisting me in the slow process of measuring strontium isotope ratios, and to Nate Miller for running my samples for cations. Jack Sharp, Bridget Scanlon, and David Maidment offered additional advice on this project and during my time at UT.

Thanks also to everyone at Loomis Partners and the Texas Water Development Board, especially Robert Mace and Clif Ladd, for introducing me to work in geology and water resources; and to Jim Sansom, Bob Bluntzer, and Chock Woodruff for introducing me to central Texas field geology.

Lastly, I would not be writing this without the love and support of my friends and family, especially Mom, Dad, Larry, Ted, and Alex. Thanks guys.

December 5, 2008

Abstract

Hydrogeological characterization of baseflow to Jacob's Well spring, Hays County, Texas

Sarah Cain Davidson, M.S.Geo.Sci.

The University of Texas at Austin, 2008

Supervisor: Philip C. Bennett

Jacob's Well is a karst spring that discharges from the Trinity aquifer in central Texas. Ongoing development and increased groundwater pumping in the area around the spring are thought to be impacting the volume of discharge at the spring—however, the source of spring discharge is poorly understood. The goals of this study are to characterize the chemistry of springflow and nearby surface waters and groundwaters and to identify the source or sources of water that contribute flow to the spring under low flow conditions.

The spring is located in the Middle Trinity aquifer within the Lower Cretaceous Trinity Group in central Texas. The Trinity Group is composed of alternating terrestrial and marine deposits, with most groundwater flow occurring through secondary porosity in the carbonate units. The cave leading up to the spring consists of at least two water-filled conduits that have been mapped down into the Cow Creek Limestone and several hundred meters to the north and northwest of the spring outlet.

Water samples and measurements of water levels and chemical field parameters were collected at 48 study sites representing stream, spring, and well waters over a 250-km^2 area around the spring from May–September 2008. The area was in drought throughout this period and the results thus represent low flow conditions. Samples were analyzed for major and trace ions, organic and inorganic carbon, and isotopes of O, H, and Sr. Modeling using PHREEQC was used to calculate whether realistic phase changes in known aquifer minerals could explain the chemical differences between sampled waters along hypothesized flowpaths.

Water levels indicate that groundwater flows generally to the southeast within the study area. Chemical analyses of water samples show three chemical types: (1) Ca-Mg-HCO_3 waters, which make up all spring water, all surface water, and most ground water samples; (2) high TDS Ca-Mg-SO_4 ground waters; and (3) high TDS Na-Mg-Ca-SO_4 ground waters. Measured element concentrations, strontium isotope data, and geochemical modeling results indicate that the high TDS waters most likely come from the upper member of the Glen Rose Limestone downgradient from the spring (type 2) and from the Hosston Formation in the Lower Trinity aquifer (type 3).

Physical and chemical properties of the sampled waters were used to define which well and stream samples might represent water within the area contributing to baseflow at the spring. Water samples taken from seven sites north and west of the spring were found to represent possible sources of springflow during the study period. These findings suggest the possibility of two distinct flowpaths connecting the aquifer to Jacob's Well: (1) flow to the southeast within the Cypress Creek watershed along the regional groundwater flow path estimated from water level measurements, and (2) flow to the east along fracture or conduit paths that cross the surface divide between the Upper Blanco River and Cypress Creek watersheds.

Table of Contents

List of Tables

List of Figures

Introduction

Spring waters that flow from karst aquifers across Central Texas support unique ecosystems, are popular recreation areas, and help to meet water demands. The drought-prone climate of the area, combined with rapid population growth, have lead to declines in discharge in many of these springs and have raised concerns about whether flow can be sustained.

One of these springs is Jacob's Well, a karst spring that discharges from the carbonate Trinity aquifer in Wimberley, Texas. It is a popular area swimming hole, and historically has provided perennial flow to the Blanco River, which flows southeast through Wimberley and over the Edwards aquifer. However, increased groundwater pumping related to residential development in the area could threaten baseflow in the spring, particularly during drought. Flow in the spring ceased for the first time on record in 2000 (Price 2008).

To assess possible effects of groundwater pumping and drought on springflow, researchers and groundwater managers must have an understanding of the provenance and characteristics of baseflow waters, which provide water to wells and springs between rainfall events (Atkinson 1977). In addition, the chemistry and chemical variability of springflow can be used to infer flow regimes within carbonate aquifers (Shuster and White 1971, Scanlon and Thrailkill 1987, Dreiss 1989, Lakey and Krothe 1996). Knowledge of basefow conditions is useful for evaluating how spring discharge changes under high flow conditions or during and after storm events, a common focus of existing studies of chemistry in karst spring waters (Lakey and Kroth 1996, Lee and Krothe 2001, Desmarais and Rojstaczer 2002, Perrin *et al*. 2003, Birk *et al*. 2004, Vesper and White 2004, Winston and Criss 2004, Doctor *et al*. 2006, Perrin *et al*. 2007, Li *et al*. 2008).

Many of these studies assume that baseflow, non-event water has a constant chemistry—and, presumably, a constant source (e.g. Dreiss 1989). However, if this assumption is not justified by knowledge of baseflow chemistry it discounts the possibility of changes in the source of baseflow due to seasonal water-level fluctuations or other variability. In some systems the baseflow has been studied and found to represent a constant source (Shuster and White 1971, Lee and Krothe 2001). In others, researchers have found that seasonal variation in water chemistry can be significant (Shuster and White 1971), in some cases exceeding the variation caused by individual storms (Desmarais and Rojstaczer 2002).

The purpose of this study is to characterize the chemistry of water in and around Jacob's Well and to use this information to identify the source or sources of baseflow to the spring. Possible sources include water from one or more formations within the Trinity aquifer and surface water from the Blanco River. DeCook (1960) attributes water discharging from Jacob's Well to the lower member of the Glen Rose Limestone. The Texas Water Development Board groundwater database lists the spring as being sourced from the Cow Creek Limestone (TWDB 2008). And results of a 2006 University of Texas study indicated that water discharging at Jacob's Well was likely coming from a losing section of the Blanco River (Steinhauer *et al*. 2006). This study tests these hypotheses using water chemistry and water level data collected during the spring, summer, and fall of 2008.

Study area description

The spring studied here, known as Jacob's Well, is located in the City of Wimberley in southwestern Hays County, Texas. Discharge from the spring provides the sole source of perennial flow to Cypress Creek, which flows into the Upper Blanco River about eight km downstream. The study area covers about 250 km^2 in and west of Wimberley in the Hill Country of south-central Texas, so named for its rugged, hilly terrain (Figure 1). The area is within the Blanco River watershed, with elevations ranging from about 250 to 470 m above mean sea level (amsl).

CLIMATE AND VEGETATION

The Köppen-Geiger climate classification system classifies the study area as temperate with hot summers (Peel 2007). In Blanco, Texas, approximately 30 km west-northwest of the spring, the average annual temperature is 19ºC. Based on a period of record from 1971 to present, average maximum monthly temperatures reach 35ºC in August, and average minimum monthly temperatures reach 1ºC in January. Average annual precipitation is 890 mm, with most rain occurring in May, June, and October. Figure 2 shows measurements of precipitation and temperature over the last five years (NCDC 2008).

Soils in the area are predominantly shallow, well drained, gravelly clays and loams (USDA SCS 1984). Prairie grasses, live oak, and juniper (known locally as cedar) make up much of the vegetation in the area (Ashworth 1983). In drainages and other places where water is accessible, common trees include cottonwood, cypress, sycamore, and willow (DeCook 1960). Relationships between vegetation, soils, and underlying geologic formations allow surface geology in the area to be mapped using the distribution of vegetation in the area (Cuyler 1931, DeCook 1960, Grimshaw 1970).

LAND USE AND DEVELOPMENT IN WIMBERLEY

The Village of Wimberley originated as a sawmill built in 1848 by European settlers (DeCook 1960). Most agriculture in the area consists of cattle, sheep, and goat ranching (DeCook 1960, Ashworth 1983), with ranches used primarily for beef cattle (USDA SCS 1984). Crops are commonly grown in river valleys (DeCook 1960) and consist predominantly of grass, feed crops, and orchards (Ashworth 1983). Development for tourism and recreation near Wimberley began by the 1950s (DeCook 1960), and beginning in the late 1960s, tracts of land historically used for ranching in the area were being divided to allow for residential developments and seasonal tourist resorts (USDA SCS 1984, Muller and McCoy 1987). More recently, with the expansion of major cities in the region, the Hill Country is undergoing increased suburban development (Fahlquist and Ardis 2004).

Land use over most of the study area is classified as forest, grass, and scrub, which includes significant amounts of land used to graze livestock. The most significant developed areas are the cities of Blanco in the northwest and Wimberley in the southeast, including the area around Jacob's Well. Wetlands are located along the Upper Blanco River and along Cypress Creek downstream from Jacob's Well (Figure 3) (USGS 2003, Homer *et al*. 2004).

Between 1940 and 2000, the population of Hays County grew from around 15,000 to nearly 98,000 (USCB 1993, 2003). Population projections estimate that by 2060 the county's population will grow to nearly half a million, a 400 percent increase (Figure 4). Similar population increases are expected for the area around Jacob's Well. The population served by the three primary public water suppliers in Wimberley—the Wimberley Water Supply Company, Woodcreek subdivision, and Woodcreek Utilities, Inc.—is expected to grow from 8,300 in 2000 to 38,400 by 2060 (TWDB 2007) (Table

1). Total water demand for the three public water suppliers in the Wimberley area is projected to rise from 1,200 acre-feet (1.5 million m^3) in 2000 to 5,900 acre-feet (7.3 million m^3) in 2060, and additional demand will come from development outside the service area of these suppliers (TWDB 2007).

GEOLOGIC SETTING

Jacob's Well is located within the Lower Cretaceous Trinity Group, which forms the hydrogeologically distinct Trinity aquifer. The geology in and near the study area has been described by DeCook (1960), Grimshaw (1970), Ashworth (1983), Hammond (1984), and Muller and McCoy (1987).

Stratigraphy and depositional history

In the study area, the Trinity Group overlies a southeast-dipping, eroded surface of Paleozoic age, comprised of the mostly metamorphosed rocks of the Ouachita system (Flawn and others 1961). It is covered in southeastern Hays County by the younger Fredericksburg Group rocks that make up the Edwards aquifer (Ashworth 1983, Muller and McCoy 1987). The Trinity Group is divided into six formations that alternate between terrestrial sedimentary units and shallow marine carbonates. From oldest to youngest, these are the Hosston Sand (also known as the Sycamore Sand), Sligo Limestone, Hammett Shale (also known as the Pine Island Shale), Cow Creek Limestone, Hensel Sand, and Glen Rose Limestone (Stricklin *et al*. 1971). An additional unit, the Bexar Shale, is located between the Cow Creek Limestone and Hensel Sand in some areas (Forgotson 1957, Muller and McCoy 1987). The Glen Rose Limestone is subdivided into a lower member and an upper member (Stricklin *et al*. 1971) and outcrops over most of the study area (Figure 5).

Stratigraphic nomenclature in the literature does not always follow that described above. In a number of publications, different combinations of these formations are referred to collectively as members of the Travis Peak and Pearsall formations (Hill 1901, Imlay 1945, Forgotson 1957, Muller and McCoy 1987, Barker *et al*. 1994). Imlay (1945) places the Sligo and Hosston formations below the Trinity Group, in the Durango and Nuevo Leon groups of the Coahuila Series of Mexico. To complicate things further, the Sycamore Sand has been equated to both the Hammett Shale (Hill 1901, DeCook 1960) and Hosston formations (Stricklin *et al*. 1971). The more specific names introduced above are used here in order to avoid confusion, to follow the revision of Lozo and Stricklin (1956) that removes the Travis Peak Formation from stratigraphic terminology, and because the literature provides sufficient detail in local stratigraphy. Figure 6 provides a generalized stratigraphic section using this terminology.

In what is now central Texas, the Trinity Group formations were deposited during the Lower Cretaceous in terrestrial and shallow marine settings during a predominantly transgressive phase. The ocean transgressed from the southeast, allowing deposition of marine carbonates, while the erosion of the Llano Uplift in the northwest supplied siliciclastic sediments to the area that make up the Hosston Sand, Hammett Shale, and Hensel Sand. Each unit generally thickens and dips to the southeast, away from the bedrock structural high in the northwest (Stricklin *et al*. 1971). Some of the earliest detailed descriptions of the Lower Cretaceous deposits in central Texas are provided by Hill (1891, 1901) and Taff (1892).

The Hosston Sand forms the base of the Trinity Group and is composed of sediments, derived primarily from the Llano uplift in the northwest, that filled in an uneven surface of folded Paleozoic units. The unit is composed of conglomerate, sandstone, and claystone beds. These sediments consist predominantly of quartz sand,

along with dolomite, glauconite, and larger clasts of rocks from the Llano Uplift (Stricklin *et al*. 1971). In eastern Hays County, the unit is composed of shale and sandstone (DeCook 1960). Near the study area, estimated thickness of the Hosston Sand ranges from 120–150 m (Imlay 1945, DeCook 1960), and a well log within the study area indicates the Hosston Formation is 50 m thick (Hammond 1984).

Downdip to the southeast, the sediments of the Hosston Sand grade into the Sligo Limestone. Regionally, the lower part of the unit is composed of dolomite, siltstone, and fine-grained limestone, while the upper part of the unit consists of coarser-grained carbonates (Stricklin *et al*. 1971). Near the study area, this unit contains alternating beds of limestone and shale in the lower part and thick limestone in the upper part and is about 70 m thick (DeCook 1960). Within the study area, the Sligo Formation is about 18 m thick (Hammond 1984).

The Hammett Shale disconformably overlies the Sligo Limestone. It consists of a calcareous and dolomitic shale interbedded with limestone, dolomite, sand, and red beds (Stricklin *et al*. 1971). In northern Hays County, the unit is composed of conglomerate and crossbedded tan and red sand (DeCook 1960, referred to in text as the "Sycamore sand member of Hill"). This unit is approximately 15–20 m thick in and near the study area (Imlay 1945, DeCook 1960, Hammond 1984).

Overlying the Hammett Shale is the Cow Creek Limestone. The unit is a calcarenitic, bioclastic limestone that contains quartz sands and beds of shell fragments (Stricklin *et al*. 1971). In Hays County, the unit is described as a fine-grained limestone at the base, overlain by massive, detrital, and dolomitic limestone (DeCook 1960). In the vicinity of the study area, the formation is an estimated 18–23 m thick (Imlay 1945, DeCook 1960, Hammond 1984). Limited caves and karst features are known to exist in the formation (Veni 1994).

The Hensel Sand (commonly, but incorrectly, spelled Hensell Sand) overlies the eroded top of the Cow Creek Limestone and is predominantly made up of sands deposited in alluvial and near-shore marine environments. The alluvial deposits, found only in the updip part of the formation, include a basal layer of fine-grained limestone and dolomite overlain by clay, sand, and gravel. The marine deposits are composed predominantly of sand-rich dolomite beds (Stricklin *et al*. 1971). Updip alluvial sediments include conglomerate, sand, silt, red clay, and limestone beds (Forgotson 1957, Ashworth 1983). Downdip, these terrestrial deposits grade into marine beds predominantly composed of calcareous shale and thinly bedded limestone that are known as the Bexar Shale (Forgotson 1957, Ashworth 1983). In Hays County, the unit consists primarily of fine-grained sand, siltstone, and marly limestone that fines downdip (DeCook 1960). Estimates of the thickness of the Hensel Sand in and near the study area range from 13–26 m (Imlay 1945, DeCook 1960, Hammond 1984).

The Glen Rose Limestone is the seaward extension of the Hensel Sand (Barnes 1948, Stricklin *et al*. 1971). Regionally, the unit consists of two members. The base of the lower member is composed of massive limestone with areas of reef rocks made up largely of rudist and coral fossils (Stricklin *et al*. 1971). Reef deposits are located in western Hays County within the study area, including "the Narrows" in the Blanco River valley (Lozo and Stricklin 1956). The unit grades upwards into thinner beds of dolomite, dolomitic shale, clay, and fine-grained limestone (Stricklin *et al*. 1971). The member contains extensive cave systems and other karst features (Veni 1994). The top of the lower member of the Glen Rose Limestone is separated from the upper member by a marker bed of iron-stained limestone, known locally as the corbula bed, that is rich in fossils of *Corbula martinae*. This bed is typically less than 0.3 m thick and is laterally continuous over thousands of square kilometers (Whitney 1952, Stricklin *et al*. 1971).

The upper member of the Glen Rose Limestone is composed of resistant beds of dolomite, marl, and limestone that alternate with non-resistant beds of calcareous clay. At the base of the member, a zone of collapsed breccia has filled in a layer of gypsum that has been largely leached from the formation. A second collapse zone is located in the center of the member, where another layer of evaporites has been largely dissolved (Stricklin *et al*. 1971). In general, this member is more poorly karsted than the lower member, although it is known to contain significant caves near the top of the unit (Veni 1994).

Descriptions of the Glen Rose Limestone in Hays County are very similar to the detailed regional description above. Grimshaw (1970) provides a detailed stratigraphy of outcrops of the Glen Rose Limestone over a portion of western Hays County that overlaps much of the study area. In general, the lower member of the Glen Rose Limestone crops out within the Blanco River and Cypress Creek drainages, and the upper member is present at higher elevations (Figure 5). Within the study area, the lower member of the Glen Rose Limestone reaches 61–76 m thick (DeCook 1960, Hammond 1984) and the upper member reaches 122 m thick (DeCook 1960, Grimshaw 1970).

Since the time Trinity Group formations were deposited, groundwater flow through the limestones and evaporites in the Trinity Group has caused dissolution that has created secondary porosity in the form of cavities and solution channels. Sinkholes within streambeds and dissolution cavities are especially common in the Glen Rose Limestone, and the Cow Creek Limestone is often described as honeycombed in outcrop. The orientation of cavities and conduits reflects jointing patterns in the limestone (Ashworth 1983). Within the several study area, several known caves are located within the lower member of the Glen Rose Limestone (Grimshaw 1970).

Erosion, primarily by the flow of streams that flow southeast through the Hill Country, has removed most of the overlying Edwards Group rocks (Barker *et al*. 1994), deposited quaternary alluvium in local drainages (Grimshaw 1970), and created today's topographic relief by cutting into the Trinity Group formations (Barker *et al*. 1994). In particular, erosion of the resistant beds of the upper Glen Rose Limestone has resulted in a characteristic terraced or "stairstep" pattern of topography in the area (Hill 1901, Grimshaw 1970, Stricklin *et al*. 1971).

Structure

The Hill Country is located south of the Llano Uplift, east of the Edwards Plateau, and northwest of the Gulf Coastal Plain (Stricklin *et al*. 1971) (Figure 7). The Llano Uplift is an area about 160 km in diameter in which Precambrian metamorphic and igneous rocks are raised hundreds of meters above their level in the surrounding area and form a structural dome, exposing these rocks at the surface in some places (Sellards 1932). The San Marcos arch is another significant structural feature in the study area. The arch is a broad anticline that plunges southeast, away from the Llano Uplift. Across the axis of the anticline, the tops of geologic formations become more shallow and the units become thinner (Adkins 1932). The study area is also located on the northwest edge of the Balcones Fault Zone, which runs perpendicular to the San Marcos Arch and is made up predominantly of northeast-southwest trending normal faults. Displacement is generally down to the southeast (Weeks 1945).

Although the main faults of the Balcones Fault Zone are located outside the study area (Weeks 1945), several smaller faults are present that are part of the same system and share the same characteristics. Faults generally trend northeast-southwest (DeCook 1960, Ogden *et al*. 1986), and measured dips are typically over 60 degrees (DeCook 1960). Measured displacements range from 6 to 84 m down to the south and southeast. One of

these faults, Jacob's Well Fault, is located about 275 m downstream of the spring (Figure 5) (Grimshaw 1970, Ogden *et al*. 1986).

Observed joints in the area generally trend northeast-southwest and northwest-southeast. The orientation of faults and joints appears to control drainage within the area (Grimshaw 1970, Ogden *et al*. 1986). Measured fracture orientations in the lower Glen Rose Formation are bimodal, tending to trend northeast-southwest (40–79º) or northwest-southeast (120–159º) (Veni 1994). Wermund *et al*. (1978) found similar results in measurements of fractures in the Edwards Limestone, southwest of the study area.

HYDROGEOLOGY

The hydrogeology of Hays County, Texas has been described by Turner (1938), DeCook (1960), Ashworth (1983), Muller and McCoy (1987), and Broun *et al*. (in press). Monitoring programs administered by the Hays Trinity Groundwater Conservation District, Texas Water Development Board, Texas Commission on Environmental Quality, and U.S. Geological Survey provide additional records of information about well construction, water levels, and water chemistry.

Jacob's Well

DeCook (1960) and Brune (1981) describe Jacob's Well as a spring created by faulting that has arranged the Glen Rose Limestone against relatively impermeable rock, thus forcing groundwater to flow upward. Spring water discharges from a conduit opening in the lower Glen Rose Limestone. Cave divers have mapped two main water-filled conduit passages that lead several hundred meters north and northwest of the spring opening (Figure 8) (Gary 2007). Below the cave opening, the main conduit extends down into to the Cow Creek Limestone, reaching a depth of about 41 m below the water table over approximately 50 m (Figure 9).

Gauging equipment installed at the spring has recorded information about spring flow, temperature, and conductivity since April 2005. The equipment was installed by the U.S. Geological Survey (gauge 08170990) approximately 15 m below the main conduit opening (Figure 9). Data collected at the gauge show that spikes in discharge during and after rain events correspond to decreases in specific conductivity (Figure 10) and temperature and increases in turbidity. The average discharge over the period of record at the gauge is 220 L/s. However, this is largely due to above average rainfall in 2007—the average discharge rates for 2005, 2006, 2007, and 2008 were 150, 45, 553, and 69 L/s, respectively. Six measurements of spring discharge measured between 1924 and 1974 vary from 68–170 L/s, with the lowest measurement occurring in 1955 (Brune 1981), near the end of the most severe drought of the last 100 years (Mace et al. 2000).

Trinity aquifer

The Trinity Group formations have long been recognized as an important source of water supply (Hill 1901). The Trinity aquifer is composed of three distinct aquifer units, based on differences in their hydrogeologic characteristics, that form a leaky, primarily confined aquifer system (Ashworth 1983). The Lower Trinity aquifer overlies relatively impermeable pre-Cretaceous rocks beneath the Trinity Group (Barker *et al*. 1994) and includes the Hosston Sand and Sligo Limestone. The Middle Trinity aquifer, separated from the Lower Trinity aquifer by the Hammett Shale, includes the Cow Creek Limestone, Hensel Sand, Bexar Shale, and the lower member of the Glen Rose Limestone. The Upper Trinity aquifer consists of the upper member of the Glen Rose Limestone (Ashworth 1983). The Trinity aquifer is also recognized as part of the larger Edwards-Trinity regional aquifer system, which comprises Cretaceous-age units that underlie 109,000 km^2 of west-central Texas. In addition to the Trinity aquifer, this

regional system includes the Edwards-Trinity (Plateau) aquifer to the west and the Edwards aquifer to the east (Barker *et al*. 1994).

Within the study area, the approximate thickness of the Lower Trinity aquifer increases to the southeast, from around 46 m east of the City of Blanco to almost 122 m where Cypress Creek joins the Blanco River at Wimberley. The thickness of the Middle Trinity increases to the southeast, from about 91 m at the City of Blanco to over 140 m at Wimberley (Ashworth 1983), and the Upper Trinity aquifer reaches approximately 120 m thick in the study area (Grimshaw 1970). A regional map by Ardis and Barker (1993) indicates that the saturated thickness in the Trinity aquifer prior to significant groundwater development ranged from 122 to 305 m in the study area.

In Hays County, the Trinity aquifer is recharged by infiltration of direct precipitation over outcrop areas, infiltration of surface water in losing portions of streams, and interformational flow (DeCook 1960). Specifically, DeCook (1960) notes that the Blanco River is a likely source of significant recharge where it crosses the lower Glen Rose Limestone upstream from Wimberley.

Water in the aquifer system moves primarily to the southeast, in the direction of the regional dip (DeCook 1960), with slower vertical movement downward between the aquifers (Muller and McCoy 1987, Muller 1990). Several published maps depict the potentiometric surface in the study area (Kunianski 1990, Bush *et al*. 1993, Veni 1994). These maps indicate regional flow to the east and southeast. However, while regional groundwater flow is perpendicular to the equipotentials, anisotropy in aquifers can lead to flowpaths that do not follow this surface. For example, flow can be diverted to the northeast along faults within the Edwards Balcones Fault Zone (Abbot 1977, Maclay and Small 1986). The potentiometric gradient created by these diversions is not discernible on regional maps (Bush *et al*. 1993).

Over an area of the Trinity aquifer extending from Hays County in the northeast to Uvalde County in the southwest, Ashworth (1983) used available aquifer test information to calculate average transmissivities of $1.4x10^{-3}$ m^2/s in the Lower Trinity aquifer and $2.4x10^{-4}$ m^2/s in the Middle Trinity aquifer. Little information was available for the Upper Trinity aquifer, but the Ashworth (1983) assumed the transmissivity is significantly lower in this part of the aquifer. Ogden *et al*. (1986) calculated transmissivities of $1.9x10^{-6}$ and $2.0x10^{-6}$ m^2/s for two wells in the Glen Rose aquifer within a few kilometers of the study area. Based on pump tests in 13 wells over approximately the same area, Hammond (1984) estimated transmissivities ranging from $2.3x10^{-5}$–$2.3x10^{-3}$ m^2/s and hydraulic conductivites ranging from $3.5x10^{-7}$ to $3.5x10^{-5}$ m/s. In addition, Hammond (1984) calculated that the velocity of groundwater flow in the Trinity aquifer west of the study area ranges from $1.1x10^{-7}$ to $6.9x10^{-7}$ m/s (3.4 to 21.9 m/yr).

Measurements of storage coefficients based on pumping tests in the Sligo, Hosston, Cow Creek, and Hensel formations by Ashworth (1983) range from $2x10^{-5}$ to $7x10^{-4}$. In addition, porosity estimates based on laboratory core analyses average 16 percent in the Hosston Formation (15 measurements), 19 percent in the Cow Creek Limestone (27 measurements), 24 percent in the Hensel Sand (28 measurements), and 21 percent in the lower member of the Glen Rose Formation (Ashworth 1983). The lower member of the Glen Rose Limestone contains more secondary porosity than the upper member (Ashworth 1983, Veni 1994).

In western Hays County, groundwater ranges from fresh to slightly saline (Muller and McCoy 1987). It is generally hard and high levels of SO_4 are common. Samples from in and around Dripping Springs, 15 km north of the study area, showed that SO_4 concentrations were higher in the lower member of the Glen Rose than in the upper

member (Muller 1990). However, Hammond (1984) and Veni (1994) proposed that high SO_4 levels found in some wells within the lower Glen Rose Limestone were caused by leakage of water from the evaporites in the upper Glen Rose Limestone through poorly constructed wells. Another study by DeCook (1960) found that water was more saline in the Glen Rose Limestone than within the rest of the aquifer. Compared to the more well-known Edwards aquifer, located downgradient from the Trinity aquifer, the Trinity contains higher concentrations of SO_4, Cl, and total dissolved solids (TDS), and fewer detections of NO_3, pesticides, and volatile organics (Bush *et al*. 2000).

Carbonate aquifer geochemistry

Water movement in carbonate aquifers is often dominated by flow through fractures and dissolution cavities, with slower diffuse flow and the majority of water storage occurring in the rock matrix (Atkinson 1977). Because of this complexity, determining flowpaths by methods that assume darcian flow and aquifer homogeneity provide an incomplete or misleading picture of these systems. Alternatively, tracing flowpaths using water chemistry does not require precise knowledge of where conduits and fractures are located in an aquifer (Shuster and White 1971, Scanlon and Thrailkill 1987). This study uses a combination of physical and chemical methods, but focuses largely on the chemistry of waters in the study area.

CARBONATE GEOCHEMISTRY

The primary control on the chemistry of most natural waters, including the Trinity aquifer, is the interaction of these waters with carbonate minerals (Langmuir 1997). Calcite ($CaCO_3$), the predominant mineral in limestone, dissolves into and precipitates from water through the reaction

$$CaCO_3 + H_2O + CO_2 \leftrightarrow 2HCO_3^- + Ca^{2+} \quad (1)$$

The availability of CO_2 plays a large role in regulating carbonate geochemistry. In equilibrium with the atmosphere, the partial pressure of CO_2 gas (P_{CO_2}) is $10^{-3.5}$ atm. Biological activity in soils can significantly raise the P_{CO_2} in soil waters, making them undersaturated with respect to calcite (Appelo and Postma 2005). The addition of CO_2 to water pushes eq. 1 to the right, causing calcite dissolution, through the following reactions and associated constants:

$$CO_{2(g)} \rightarrow CO_{2(aq)} \qquad K_H = 10^{-1.5} = \frac{(H_2CO_3)}{(P_{CO_2})} \quad (2)$$

$$CO_{2(g)} + H_2O \rightarrow H_2CO_3 \qquad K_{a,1} = 10^{-6.3} = \frac{(H^+)(HCO_3^-)}{(H_2CO_3^*)} \qquad (3)$$

$$H_2CO_3 \rightarrow H^+ + HCO_3^- \qquad K_{a,2} = 10^{-10.3} = \frac{(H^+)(CO_3^{2-})}{(HCO_3^-)} \qquad (4)$$

$$HCO_3^- \rightarrow H^+ + CO_3^{2-} \qquad K_{a,2} = 10^{-10.3} = \frac{(H^+)(CO_3^{2-})}{(HCO_3^-)} \qquad (5)$$

$$CaCO_3 \rightarrow Ca^{2+} + CO_3^{2-} \qquad K_{sp} = 10^{-8.35} = (Ca^{2+})(CO_3^{2-}) \qquad (6)$$

(The concentration of H_2CO_3 is typically much less than that of $CO2_{(aq)}$, and the two species are commonly summed and expressed as H_2CO_3 (Appelo and Postma 2005).) If water with a P_{CO_2} higher than that of the atmosphere discharges at the surface, CO_2 will degas from the water by

$$H^+ + HCO_3^- \rightarrow H_2CO_3^* \rightarrow H_2O + CO_{2(g)} \qquad (7)$$

This process pushes eq. 1 to the left, causing calcite precipitation. These reactions lead to a decrease in dissolved HCO_3 and Ca, a decrease in P_{CO_2}, an increase in pH, and increased saturation with respect to calcite (Usdowski *et al*. 1979).

Other minerals common to carbonate aquifers, such as dolomite and evaporites, can have additional effects on groundwater chemistry. The solubility of these minerals, described by their equilibrium solubility product constant, or K_{sp}, largely determines their influence on groundwater chemistry (Table 2).

Dolomite ($CaMg(CO_3)_2$), a common carbonate mineral, does not precipitate under most common conditions. When dolomite dissolves, as shown in the following equation (Appelo and Postma 2005),

$$CaMg(CO_3)_2 + 2CO_2 + 2H_2O \leftrightarrow Ca^{2+} + Mg^{2+} + 4HCO_3 \qquad (8)$$

it releases Ca and causes calcite precipitation, which removes Ca from the water but not Mg. This process leads to a relative increase in Mg, and thus a decrease in the Ca/Mg ratio, along a flowpath.

Evaporite minerals, such as gypsum ($CaSO_4 \bullet 2H_2O$), anhydrite ($CaSO_4$), and halite (NaCl), are more soluble than calcite and dolomite and will further affect the amount and type of dissolved solids in carbonate groundwaters. For example, anhydrite will dissolve in water that is at equilibrium with respect to calcite through the reaction (Stumm and Morgan 1996)

$$CaSO_4 \rightarrow Ca^{2+} + SO_2^{-4} \quad (9)$$

thereby adding Ca to the water and causing calcite to precipitate as in eq. 1 (Appelo and Postma 2005).

Where limestone, dolomite, and gypsum or anhydrite are present, a process called dedolomitization can take place that causes dolomite to be replaced by calcite in the rock and concentrations of Ca, Mg, and SO_4 in water to increase (Back and Hanshaw 1971, Plummer 1977, Back *et al*. 1983). Dissolving gypsum or anhydrite adds Ca to the water and causes calcite to precipitate, thus removing Ca and CO_3 from the water, which makes the water undersaturated with respect to dolomite and promotes more dolomite dissolution and the resulting chemical change (Appelo and Postma 2005):

$$Ca^{2+} + CaMg(CO_3)_2 \leftrightarrow 2CaCO_3 + Mg^{2+} \quad (10)$$

In an aquifer at equilibrium with both calcite and dolomite, the Mg/Ca ratio will be approximately 0.8 (and the Ca/Mg ratio will be approximately 1.35) according to the mass action equation (Stumm and Morgan 1996)

$$K = \frac{(Mg^{2+})}{(Ca^{2+})} = \frac{K_{dol}}{(K_{cc})^2} = \frac{10^{-17.09}}{(10^{-8.48})^2} = 0.8 \quad (11)$$

KARST HYDROGEOLOGY

The dissolution of carbonate rocks commonly forms extensive systems of enlarged fractures and conduits that make highly productive aquifers. Carbonate minerals have high solubility, and areas of secondary porosity will tend to increase over time if

there is a source of circulating groundwater undersaturated with respect to calcite. Eventually, carbonate dissolution can create systems of conduits through which turbulent flow occurs, dominating groundwater flow in carbonate aquifers (e.g. Stringfield and Le Grand 1966, Thrailkill 1968). The extent and rate of carbonate dissolution is dependent on many factors, including the composition and temperature of aquifer waters (Thrailkill 1968); the presence of multiple waters mixing in the aquifer (Wigley and Plummer 1976, Smart *et al*. 1988); geologic structures such as faults, joints, and bedding planes (Stringfield and Le Grand 1966, Thrailkill 1968); biological activity (Engel *et al*. 2004); and lithology and mineralogy (Rauch and White 1977).

Karst springs are used frequently as a focus of studies on the hydrogeology of karst aquifers (e.g. Shuster and White 1971, Deines *et al*. 1974, Krothe and Libra 1983, Scanlon and Thrailkill 1987, Padilla *et al*. 1994, Lakey and Krothe 1996, Lee and Krothe 2001, Desmarais and Rojstaczer 2002, Maloszewski *et al*. 2002, Perrin *et al*. 2003, Vesper and White 2004, Perrin *et al*. 2007, Li *et al*. 2008). These springs can serve as major discharge points for regional flow through carbonate aquifers; thus, physical and chemical measurements of spring discharge represent conditions within the entire portion of the aquifer that provides discharge to the spring (Shuster and White 1971, Scanlon and Thrailkill 1987, Dreiss 1989).

Methods

Data collected for this study include water sampling from wells, stream waters, and discharge from Jacob's Well. In addition, measurements of water levels and site elevation provide evidence of water level changes throughout the study area and study period. Laboratory analyses of water samples provide measurements of dissolved major and trace ions, dissolved organic and inorganic carbon, and isotope ratios of Sr, O, and H.

WATER LEVEL SURVEY

To map the potentiometric surface of the study area, site locations were surveyed and water levels collected at Jacob's Well, 37 wells, and 6 surface water sites between May and July of 2008. Multiple water level measurements were made in seven wells for the study, and monthly water level measurements for seven study wells were made as part of a water level monitoring program conducted by the Hays Trinity Groundwater Conservation District.

Site locations were determined using a Trimble GeoExplorer3 GPS and corrected for psuedorange and carrier phase errors using data collected at a Continuously Operating Reference Station in Austin, TX (available online from the Texas Department of Transportation and National Geodetic Survey) and the software GPS Pathfinder Office, Version 3.10. The resulting location coordinates have an average horizontal precision of ±0.12 m, an average vertical precision of ±0.16 m, and an average accuracy of around ±0.25 m.

Water levels in wells were measured prior to water sampling to minimize well drawdown caused by running the well pump. Several methods were used to estimate the depth to water below ground level, including a Sonic water level meter (Model 200, Ravensgate Corporation), a steel tape, and an e-line. In order to avoid catching the e-line

in a homeowner well, the Sonic water level meter was used at most locations; a second measurement was made with a steel tape where possible. In addition, the Hays Trinity Groundwater Conservation District provided several water level measurements taken using the same methods as part of a static water level survey within a few days of sampling. The water level at Jacob's Well was measured using a gauge meter posted in the main pool of the spring.

FIELD SAMPLING

Water chemistry data in this study are from samples taken at Jacob's Well, 33 wells, and 6 surface water sites along the Upper Blanco River from May to September, 2008 (Figure 11). Wells sampled are primarily domestic wells and include several municipal and stock wells. Table 3 shows available information on study wells and associated well numbers for those study wells that are included in water well databases administered by the Texas Water Development Board and Texas Commission on Environmental Quality. Reported hydrostratigraphic units are from available drillers' logs, TCEQ (2007), Broun pers. comm. (2008), and TWDB (2008). Wells were chosen based on location, amount of available construction information, and accessibility. Samples were taken at two or three timepoints from eight wells and one stream site, and Jacob's Well was sampled nine times, approximately biweekly, over the study period. In addition, three samples were collected from points within the cave leading to Jacob's Well spring during a cave diving expedition in August (Figure 8).

At each groundwater sampling site, the sampling point was that nearest to the well head and before any water treatment, although in a few cases water was collected after a sediment filter. In most cases the nearest sampling point was after a pressure tank. Well discharge was directed through 6.4 or 9.5 mm (1/4–3/8 inch) vinyl tubing at ~1–2 L/min into a 1-L Nalgene bottle and pH, dissolved oxygen, and temperature measurements were

recorded on flowing water using an Accumet AP74 dissolved oxygen/temperature data meter (Fischer Scientific) and an Accumet AP62 portable pH/mV meter (Fischer Scientific). Stable values were obtained, typically after running water for 10–20 min, prior to sample collection. In addition, a V-2000 Multi-analyte Photometer was used to measure concentrations of dissolved oxygen below 1 mg/L, H_2S, Fe, PO_4, and NH_4 using colorimetry (Chemetrics).

Samples collected for alkalinity, anion, cation, and carbon analysis were filtered to 0.2 μm in the field using membrane filters. Samples for oxygen isotope and carbon analysis were collected without headspace in glass bottles. Samples for other analyses were collected in polyethylene bottles; those for cations were acid-washed. Samples for cation analysis were acidified with ultrapure 2% HNO_3 to a pH below 2 and all other samples were refrigerated.

At stream sampling sites, values of pH, dissolved oxygen concentration, and temperature were measured across a transect of the stream to evaluate variability of the water at the sampling site. A grab sample of water was then collected from below the surface of the water at a point along the transect that showed average conditions based on these measurements. Sample processing and storage procedures were the same as described above.

To sample discharging spring waters at Jacob's Well, weighted plastic tubing attached to a peristaltic pump (Masterflex E/S Portable Sampler, Cole-Parmer Instrument Company) was dropped to the bottom of the main ledge of the cave, approximately 7 m below the water surface. Sampling, processing, and storage procedures were the same as those used for groundwater sampling.

LABORATORY ANALYSES

Samples were analyzed for major and trace elements; dissolved organic carbon (OC), dissolved inorganic carbon (IC), and total dissolved nitrogen; and isotopes of O, H, and Sr. With the exception of O and H isotopes, all analyses were completed at The University of Texas at Austin.

Chemical composition

Concentrations of HCO_3 in samples were determined by titration in the laboratory, typically within 10 hours of sample collection. Each sample was titrated to a 4.5 endpoint with 0.1 N HCl using a 702 SM Titrino auto titrator (Metrohm). It is assumed that all carbonate in the samples was HCO_3 because the pH of all but one sample was less than 8.4, the range within which carbonate alkalinity should be as HCO_3 in natural waters.

Concentrations of other major anions (Cl, SO_4, F, NO_2, and NO_3) were measured by single column ion chromatography using a Waters 501 HPLC pump and Waters 717plus autosampler. Measurements of Cl, SO_4, and F are from a Waters Model 430 Conductivity Detector, and measurements of NO_2 and NO_3 are from a Waters 486 Tunable Absorbance Detector (all components from Millipore). Phosphate concentrations were measured using the spectrophotometric ascorbic acid method (APHA *et al*. 1976, method 4500-P E).

Concentrations of OC, IC, and total nitrogen were measured using an Apollo 9000 Combustion TOC/TN Analyzer (Teledyne Tekmar). The machine converts organic or inorganic carbon to CO_2 and then measures the carbon concentration in the gas with a nondispersive infrared detector (Teledyne Tekmar Co. 2003). To measure dissolved nitrogen, the machine converts all nitrogen except N_2 to NO_2 and measures the

concentration in the gas using a chemiluminescence photodiode detector (Teledyne Tekmar Co. 2002).

Environmental isotopes

Isotopes of certain elements provide a variety of ways to characterize groundwater systems. In this study, isotopes of Sr, O, and H help identify water provenance and flowpaths.

$^{87}Sr/^{86}Sr$

The $^{87}Sr/^{86}Sr$ ratio provides a useful way to characterize the rock-water interactions and chemical evolution of groundwater systems, as described in Smalley *et al*. (1988), Franklyn *et al*. (1991), Musgrove and Banner (1993), Banner *et al*. (1994), Bishop *et al*. (1994), Katz and Bullen (1996), Oetting *et al*. (1996), Jørgensen and Banoeng-Yakubo (2001), Harrington and Herczeg (2003), Musgrove and Banner (2004), and Barbieri *et al*. (2005). The isotope ^{87}Sr is the daughter product of ^{87}Rb. Although Sr and Rb are not major rock-forming elements, Sr commonly substitutes for Ca in calcium-bearing minerals and can substitute for K in potassium feldspar, while Rb can substitute for K in potassium-bearing minerals (Faure and Powell 1972). The abundance of ^{87}Sr tends to vary in rocks, while the abundance of ^{86}Sr is constant. Isotopes of Sr do not fractionate though other geological processes. The $^{87}Sr/^{86}Sr$ ratio is thus a function of the original $^{87}Sr/^{86}Sr$ ratio in the minerals in a rock and the amount of ^{87}Rb decay that has occurred since the rock formed. This ratio can serve as a way to distinguish waters coming from formations that contain otherwise similar chemical characteristics (McNutt 2000).

Samples for $^{87}Sr/^{86}Sr$ isotope measurement were prepared by drying down approximately 2 mL of sample and 0.1 mL 7N HNO_3 in a Teflon vial. The dried sample

was then dissolved in 3N HNO_3, and strontium was isolated using a strontium-specific resin (Eichrom). Measurements of $^{87}Sr/^{86}Sr$ were made by a Thermo Triton thermal ionization mass spectrometer (Thermo Scientific). The samples were run with the standard NIST-SRM-987, which has an $^{87}Sr/^{86}Sr$ ratio of 0.710249 (2σ=0.000011, 12 values), giving the results an external precision of ±0.000011‰. The exponential fractionation law was used to correct for fractionation.

$\delta^{18}O$ and $\delta^{2}H$

The isotopic ratios $^{2}H/H$ and $^{18}O/^{16}O$ provide a way of comparing and discerning the cause of changes in water chemistries that is commonly used in groundwater studies (Bakalowicz *et al*. 1974, Moser and Stichler 1975, Musgrove and Banner 1993, Katz and Bullen 1996, Lakey and Krothe 1996, Jones *et al*. 2000, Jørgensen and Banoeng-Yakubo 2001, Maloszewski *et al*. 2002, Perrin *et al*. 2003, Winston and Criss 2004, Barbieri *et al*. 2005, Doctor *et al*. 2006, Simsek *et al*. 2008). Isotope ratios of $^{2}H/H$ and $^{18}O/^{16}O$ are reported as the per mille (‰) enrichment relative to the ratios measured in standard mean ocean water (SMOW):

$$\delta_{sample} = \frac{R_{sample} - R_{SMOW}}{R_{SMOW}} \times 1000 \tag{12}$$

where R_{sample} is the measured isotopic ratio and R_{SMOW} is the isotopic ratio of the standard. SMOW is defined using an isotopic water standard from the National Institute of Standards and Technology (formerly the National Bureau of Standards) (Craig 1961a). Craig (1961b) found that these isotopic ratios plot linearly for meteoric waters globally according to the equation

$$\delta^{2}H = 8 \times \delta^{18}O + 10 \tag{13}$$

Where meteoric waters have been partially evaporated, kinetic fractionation causes the slope of the line to decrease to around five (Craig 1961b). In addition, ^{18}O and

^{2}H are conservative isotopes, enriched relative to lighter isotopes by evaporation but not measurably fractionated through other processes in groundwater systems, and can be used to assess aquifer recharge sources and source water mixing (Kendall *et al*. 1995, Jones *et al*. 2000).

Measurements of $^{18}O/^{16}O$ and $^{2}H/H$ were made using a DeltaPlus XP mass spectrometer interfaced to a Thermo Gas Bench II at the University of New Hampshire Stable Isotope Laboratory. The sample values were calibrated with Vienna Standard Mean Ocean Water (VSMOW) as 0‰, GISP as -24.8‰, and SLAP as -55.5‰.

GEOCHEMICAL MODELING

The aqueous geochemical modeling program PHREEQC for Windows (Parkhurst and Appelo 1999) and AquaChem (Version 5.1) (Schlumberger Water Services 2007) were used to calculate additional geochemical parameters and evaluate possible groundwater mixing and flowpaths using the collected data.

To characterize redox conditions in the sample waters to accurately speciate and model water chemistry in PHREEQC, Eh values were calculated using the Nernst equation (Nernst 1904, Appelo and Postma 2005):

$$Eh = E^{0} + \frac{RT}{nF}\ln\frac{(D_{ox})^{d}}{(B_{red})^{b}} \text{ for the half-reaction } bB_{red} \rightarrow dD_{ox} + ne^{-} \qquad (14)$$

where R is the gas constant, T is temperature (K), n is the number of electrons transferred in the half-reaction, F is Faraday's constant, and E^{0} is the expected standard electrical potential. These values were then converted to pe using

$$pe = 16.9Eh \text{ at } 25°C \qquad (15)$$

Two modeling methods, inverse mass balance modeling and forward reaction-path modeling, were used in this study. Inverse mass balance models allow users to evaluate whether a possible source water/s might have evolved into a final water along a

hypothesized flow path (Plummer and Back 1980, Plummer *et al*. 1990, Parkhurst and Appelo 1999). Given the chemical compositions of the source and final waters, the model will calculate possible mass transfer reactions—such as mineral precipitation or dissolution—that could account for the chemical differences between the waters. Assumptions used in inverse mass balancing are that (1) the waters chosen are located along the same flow path, (2) water chemistries are not affected by diffusion, dispersion, or time, and (3) the modeled phase changes represent plausible reactions in the groundwater system being studied (Zhu and Anderson 2002).

Forward reaction-path modeling was used to check solutions calculated by inverse modeling and to calculate phase changes to explain the evolution of rainwater to groundwater. These models make calculations to predict the water chemistry that would result from chemical reactions, such as (1) the dissolution or precipitation of given amounts of mineral or gas phases or (2) bringing the water to a given saturation index relative to mineral or gas phases. In a successful forward model, the calculated water chemistry will resemble that of the final water, thus confirming the modeled reactions and phase changes as possible reactions occurring along the actual flowpath (Parkhurst and Plummer 1993).

The mineral and gas phases used for modeling include albite, anhydrite, calcite, CO_2(g), dolomite, illite, kaolinite, potassium feldspar, and quartz. In addition, phase changes in H_2O and halite were used to simulate evaporative concentration of rainwater prior to infiltration. Chloride and B were used to balance the model and dolomite, potassium feldspar, albite, and anhydrite were not allowed to precipitate.

Results

A total of 66 water samples and 56 water level measurements were collected in the study area between May and September 2008 (Figure 11). Water samples include 9 from the main outlet of Jacob's Well, 3 from the conduit leading to Jacob's Well, 8 from sites along the Upper Blanco River, and 46 from well sites. Site locations and water level measurements are summarized in Table 4, and results of chemical analyses are shown in Tables 5, 6, 7, and 8. Measurements of $^{87}Sr/^{86}Sr$ ratios are listed in Table 9. The figures here and in the discussion include only one sample from each stream and well site. Results of additional sampling at some sites are listed in these tables.

HYDROGEOLOGY

Site locations and measured water levels are listed in Table 4. Figure 12 shows the approximate potentiometric surface based on these measurements. Where multiple measurements were made, the earliest measurement was used in order to minimize the time period that the map represents. The map shows that groundwater flow in the study area is generally to the southeast, consistent with other studies in the area (Kunianski 1990, Bush and others 1993, Veni 1994). Three samples, from sites CHA, MCM, and SPR, have water levels significantly lower than those in surrounding wells. As discussed below, it is likely that these wells are screened within the Lower Trinity aquifer and the lower water levels signify downward groundwater movement from the Middle Trinity aquifer.

Of the seven wells in which multiple (two or three) water level measurements were made during the study period, two showed increases (mean=2.6 m), three showed decreases (mean=-8.2 m), and two showed no change. Monthly water level measurements made by the Hays Trinity Groundwater Conservation District between April and

September, 2008, show declines between April and September in seven study wells (Figure 13).

The water level at Jacob's Well during sampling times varied about 0.2 m during the study period, corresponding to a range in discharge of 24–82 L/s (Table 10). Data from USGS gauging equipment installed at the spring show a gradual decrease in spring flow from over 300 L/s at the beginning of October 2007, a wetter than normal year, to well below 100 L/s throughout the study period (Figure 14).

WATER CHEMISTRY

Table 5 summarizes pH, temperature, and major element concentrations from all water samples. Waters throughout the study area, including all samples from Jacob's Well, are predominantly Ca-Mg-HCO_3 type, as shown on Figure 15. The general distribution of chemical type is similar to that from a regional study of the Trinity aquifer by Fahlquist and Ardis (2004).

Most samples contained concentrations of trace elements below instrument detection limit, with the exception of Ba, Cu, and Zn (Table 6). More than 10 samples contained measurable concentrations of Fe, Mn, Ni, Pb, Rb, Sn, Ti, and U. Levels of nutrients—including NO_3, NO_2, NH_3, and PO_4—in the sampled waters are generally low (Tables 5, 6, and 7). All samples contained phosphate levels below the method detection limit, and most samples contained NO_2 concentrations below instrument detection limit.

Values of $\delta^{18}O$ and $\delta^{2}H$ measured in 41 samples range from -4.49–3.57‰ (Table 6). The external precision of the measurements is ±0.30‰. The $^{87}Sr/^{86}Sr$ ratios measured in 6 water samples range from 0.70776–0.70865 (Table 9). Each $^{87}Sr/^{86}Sr$ value represents the average of 160 measurements. The external precision of the measurements is ±0.000011‰. These results are similar to those reported in Lambert *et al*. (2000) for 17

samples taken from Trinity aquifer groundwaters in Medina and Bandera counties, TX, approximately 100 km southwest of the study area (range=0.70746–0.70846).

Jacob's Well

Analyzed samples from Jacob's Well show that water chemistry in the spring varied little over the study period. TDS in the samples ranged from 467–502 mg/L, and the concentrations of major cations and anions remained fairly constant (Figures 15 and 16a, Table 5a).

Data recorded at the USGS gauge in the spring that serve as proxies for water chemistry, including records of turbidity, specific conductivity, and temperature, were recorded continuously throughout the study period and also show fairly stable conditions (Table 10, Figure 14). Specific conductivity ranged from 559–574 μS/cm at 25ºC, and turbidity ranged from 0.00–0.92 formazin nephelometric units (Anderson 2008). Water temperature was about 21ºC throughout the study period.

Concentrations of most trace elements in the samples from Jacob's Well are below instrument detection limit (Table 7a). Low concentrations of Mn, Ba, Zn, and Sn are found in most samples from the spring. The first sample taken at the spring, on 5/19/08, contained the highest concentrations of Mn, Ni, Ba, Zn, Cs, Cu, Ti, and U of all the spring samples. The sample taken on 7/22/08 was the only spring sample to contain measurable Fe (0.24 μmol/L).

Nutrient levels in the spring samples are also low. None had detectable levels of PO_4, and only one had a detectable concentration of NO_2. Nitrate concentrations are below 50 μmol/L in all spring samples, and NH_3 levels are all 8 μmol/L or lower. Levels of OC range from 20–230 μmol/L (Tables 5a, 6a, and 7a).

Two samples from Jacob's Well were analyzed for oxygen and hydrogen isotopes, and one sample was analyzed for its $^{87}Sr/^{86}Sr$ ratio. Values of $\delta^{18}O$ (-3.5 and

-3.6‰) and δ^2H (-24.2 and -26.9‰) are depleted relative to most stream water samples and enriched relative to most groundwater samples (Table 6). The $^{87}Sr/^{86}Sr$ ratio measured in Jacob's Well, 0.70777, is not significantly different from those measured in wells NEW and LED and at stream site UBR1 (Table 9).

Saturation indices calculated in PHREEQC show that samples from the spring are all undersaturated with respect to anhydrite, dolomite, and barite. All samples but two are undersaturated with respect to calcite; the remaining two are slightly above saturation with respect to calcite. Values of P_{CO_2} range from $10^{-1.7}$–$10^{-1.3}$ atm (Table 8a).

Stream water

Stream water samples are Ca-Mg-HCO_3 and Mg-Ca-HCO_3 type and contain 327–494 mg/L TDS (Table 5b). The stream samples have higher pH than the spring and well samples. The concentrations of major elements are similar to those in the spring waters (Figures 16a and 16b)—however, samples from sites UBR1, UBR2, UBR3, and UBR4 contain lower levels of Ca and higher levels of Si than all spring and well samples, and lower levels of HCO_3 than all spring samples and nearly all well samples (Table 5).

Stream water samples generally contain low concentrations of trace elements and nutrients (Tables 5b, 6b, and 7b). The sample from site UBR5 is an exception, showing high concentrations of Fe and As. Measurements of NO_2 and PO_4 are below detection limit, and NH_3 concentrations are all below 20 μmol/L. Nitrate concentrations from sites UBR1, UBR2, UBR3, and UBR4 are below 10 μmol/L, lower than in all spring samples and most well samples. Concentrations of OC range from 40–360 μmol/L, with the lowest concentrations occurring at sites UBR5 and UBR6.

Measurements of $\delta^{18}O$ (-3.50–3.57‰) and δ^2H (-26.01–6.52‰) show that oxygen isotopes in samples from sites UBR1, UBR2, UBR3, and UBR4 are enriched considerably relative to all spring and well samples (Table 6, Figure 17). A stream water

$^{87}Sr/^{86}Sr$ ratio—0.70777—measured in a sample from site UBR1, is not significantly different from $^{87}Sr/^{86}Sr$ ratios measured at Jacob's Well and at well sites NEW and LED (Table 9).

Calculated saturation indices indicate that stream samples are all supersaturated with respect to calcite and dolomite and undersaturated with respect to anhydrite and barite. Values of P_{CO_2} are between $10^{-3.3}$ and $10^{-2.0}$ atm (Table 8b).

Groundwater

The major element compositions of most sampled well waters are Ca-Mg-HCO_3 type (fresh groundwaters). In addition, there appear to be two high SO_4, saline groundwater endmembers. One endmember (saline endmember 1), represented by sites VAS and JAN, is characterized by high concentrations of SO_4, Ca, and Mg. The other endmember (saline endmember 2), represented by sites CHA, BUR, and SPR, also contains relatively high levels of Cl, K, and Na, and low levels of HCO_3. The major element compositions of sites GLE, GRA, and WC12 fall between the fresh and saline types (Figures 15 and 16c–e, Table 5c).

Trace element concentrations in groundwater samples vary. In general, the most prevalent trace elements include Ba, Cu, Fe, Rb, and Zn (Table 7c). Site SWM contains the highest measured levels of Cu, Fe, and Mn in all study samples—2.4, 6.6, and 1.4 μmol/L, respectively—and the highest total concentration of trace elements. Samples from site LED contain the second highest concentration of trace elements. Wells representing the saline endmembers, along with sites GRA and GLE, contain higher Rb levels (above 0.09 μmol/L) than all other study samples.

In general, nutrient concentrations in well samples are low (Tables 5c, 6c, and 7c). Phosphate concentrations in all well samples were below the method detection limit. Levels of NO_2 in well samples are below 2 μmol/L, with the exception of site SPR, which

contained 3 and 18 μmol/L. The highest levels of NO_3 in all study samples occur in wells GRA (131 and 113 μmol/L), BUR (162 μmol/L), and SWH (684 μmol/L). Other well samples contain 4–84 μmol/L of NO_3. Concentrations of OC in well samples range from 1.2 mmol/L at site ROH to 0.01 mmol/L at site PAT (Table 6c).

Oxygen isotope ratios were measured in 33 well samples, and $^{87}Sr/^{86}Sr$ ratios were measured in 4 well samples. Measured values of $\delta^{18}O$ range from -4.49–-3.35‰, and values of $\delta^{2}H$ range from -30.51–-25.19‰ (Table 6c). Ratios of $^{87}Sr/^{86}Sr$ measured in samples from sites CHA, NEW, LED, and VAS range from 0.70776–0.70866 (Table 9). The $^{87}Sr/^{86}Sr$ ratios measured at sites NEW and LED do not differ significantly from ratios measured in spring and stream samples.

Calculated saturation indices indicate that most well samples are undersaturated with respect to barite, calcite, and dolomite, and that all well samples are undersaturated with respect to anhydrite (Table 8c). Samples from sites CHA, GRA, HAR, LED, NEW, SPR, SUT, SWH, VAS, and WC12 are at saturation or slightly supersaturated with respect to calcite. Sites GRA, GOT, SAN, SPR, and WC12 are at saturation or slightly supersaturated with respect to barite. Wells HAR, GRA, NEW, SPR, SWH, VAS, and WC12 are saturated or slightly above saturation with respect to dolomite. Calculated values of P_{CO_2} range from $10^{-2.1}$–$10^{-0.8}$ atm.

Discussion

The chemistry of water samples collected in the study area show a variety of water types, including spring water, surface water, and three groundwater endmembers. Previous reports have identified waters from the lower member of the Glen Rose Formation (DeCook 1960), the Cow Creek Limestone (TWDB 2008), and the Upper Blanco River (Steinhauer *et al*. 2006) as possible sources of springflow to Jacob's Well. Additional waters in the local aquifer system include groundwater from the Hensel Sand, the Lower Trinity aquifer, and the Upper Trinity aquifer.

Precipitation was substantially lower than normal during the study period (Table 11)—therefore, the results of this study are interpreted to represent drought conditions. Sections of the Upper Blanco River, including sites UBR2 and UBR3, were not flowing when sampled in June; water at these sites had dried up completely by September.

GROUNDWATER FLOW AND WATER TABLE FLUCTUATIONS

As mentioned above, groundwater flow in the study area is generally to the southeast. Although the density of water-level measurements is limited, the results show it is possible that the Upper Blanco River and Cypress Creek are gaining in the eastern part of the study area and upgradient from Jacob's Well (Figure 12). Downstream from Jacob's Well, water levels indicate that Cypress Creek is losing. Chemistry of two of the upstream sites on the Upper Blanco River (sites UBR2 and UBR3) suggests that they represent water that was locally perched at the time of measurement, in which case the actual water table for the Trinity aquifer would be lower than the recorded measurements.

Wells from which more than one water level measurement is available over the study period show some evidence of water level declines during the study period. Wells SWH, SWM, and WC21 show steady declines from April through September. In

addition, two measurements taken at site WC12 show a 20 m drop in the water level between May and September; measurements made by the owners of this well over the study period indicate a continuous water level decline through the study period (Figure 13). However, multiple water level measurements at other sites, such as CYJ and GRA, show variable change or very little change.

Interpreting hydrographs from wells sampled only a few times over several months do not necessarily provide conclusive evidence of water level changes. While water level differences might indicate a rising or lowering of the water table, they might also represent temporary drawdown in the vicinity of the well caused by groundwater pumping in the well or nearby wells prior to the measurement.

REDOX INDICATORS

Measurable levels of dissolved O_2 in most waters sampled indicate that the study waters are generally aerobic (Table 5). However, well MCM contained no dissolved O_2 and wells CHA, GLE, HOM, VAS, ROH, GRA, BUR, and PAT contained less than 1 mg/L, indicating relatively reduced conditions.

One indicator of potential reducing conditions is the concentration of reductants such as OC. Langmuir (1997) suggested that waters not in direct contact with atmospheric oxygen that contain more than 4 mg/L (333 μmol/L) of OC typically become anaerobic as this organic matter decays. In deep groundwaters or other systems where oxygen can only be added by diffusion and mixing, smaller amounts of OC can cause the microbial reduction of dissolved O_2 (Langmuir 1997). Waters that contain more than 4 mg/L of OC include samples from stream sites UBR1, UBR2, UBR3 and wells GOT, ROH, and VAS. Two other wells with low dissolved O_2, CHA and GRA, in addition to one sample from Jacob's Well, contain 2 mg/L (167 μmol/L) or more of OC (Tables 5 and 6). Samples from several of the sites listed above also contain measurable amounts of

dissolved Mn, another indicator of reducing conditions. These include stream sites UBR1, UBR2, UBR3, UBR4, UBR5 and wells BUR, CHA, GRA, ROH, SPR, and VAS.

Based on the descriptions above, the more reduced waters in the study area seem to be associated with surface water processes or location in the aquifer. The reduced conditions in stream waters and wells ROH, PAT, HOM, and WS4—all located near the Upper Blanco River (Figure 11)—might be caused by microbial consumption of O_2 related to the influx of fresh organic matter in the stream that extends to the nearby groundwater (Langmuir 1997). Other reduced groundwater samples are possibly from parts of the aquifer that do not receive high rates of recharge and are largely cut off from atmospheric oxygen. Several samples that show reducing conditions, including those from CHA, SPR, WC12, and MCM, are from wells 152 m deep or greater. In addition, wells BUR, CHA, GLE, SPR, and VAS represent the two high SO_4 saline endmembers, and wells GRA and WC12 represent waters that lie between the freshwater and saline endmembers on Figure 15, indicating possible mixing with or evolution toward these saline endmembers. As is discussed below, some of these more saline waters are probably older and from lower permeability portions of the aquifer.

JACOB'S WELL

In general, the chemistry in spring waters at Jacob's Well varied little over the study period (Tables 5a and 6a). Much of the variation in element concentrations from samples taken at the spring outlet is within a possible five percent measurement error caused by instrument error and differences due to slight variations in the sampling point during each sampling. In addition, calculated saturation indices show that all spring samples are near saturation with respect to calcite and dolomite. These characteristics indicate that baseflow to the spring during drought periods comes from a continuous source, likely along a diffuse flowpath (Shuster and White 1971).

Spring samples taken from Jacob's Well during a slightly wetter period in 2006 (Steinhauer *et al*. 2006) show similar chemistry to those measured for this study. Accounting for a five percent measurement error, the samples from this study contain approximately 50 μmol/L more Cl and 10 μmol/L NO_3 than in 2006. This suggests more evaporation prior to the infiltration of recharge water in the 2008 samples, but not a chemically different source water between the two study periods.

Samples taken from within the two main conduits in the cave leading up to the spring (Figure 8) provide information about possible chemical reactions and water mixing taking place as baseflow travels toward the spring outlet. Cave divers have described palpable differences in the temperature of water in different parts of the cave during higher flow periods (Gary pers. comm. 2008), and preliminary data from temperature transducers installed at the cave sampling points between October 2007 and August 2008 indicate that the water temperature at site B1 is very slightly cooler than at the other locations (Hays Trinity Groundwater Conservation District pers. comm. 2008).

Two samples taken along the main conduit, at cave sites A1 and A2, show minor differences in chemistry along the flowpath of the conduit (Table 5a, Figure 8). Calculated saturation indices indicate that the water becomes more saturated with respect to anhydrite and more undersaturated with respect to calcite and dolomite along this conduit (Table 8a). However, increases in concentrations of Ca and Mg from site A1 to A2 suggest possible dissolution of calcite and dolomite, which should increase saturation relative to these minerals (Table 5a). It is possible that the abnormally low value of HCO_3 for the sample from site A2 (Table 5a), probably an error and the most likely cause of the high positive charge balance for this sample (Table 8a), affected the calculated saturation indices.

Samples from cave sites A2 and B1, representing the two main conduits leading to the spring, show minor differences—assuming a potential measurement error of five percent, the sample from conduit B contains more HCO_3 and SO_4 and less NO_3 and Na than the sample from conduit A (Table 5a). Inverse modeling in PHREEQC indicates that a mixture of 90 percent water from conduit A and 10 percent water from conduit B, along with the dissolution of 0.24 mmol/kg of calcite, can explain the chemistry of water at the spring outlet (Table 12). Alternatively, mixing calculations performed using Aquachem found that the chemistry of the sample measured at the spring ledge on the day of cave sampling is best explained by a mixture of 84 percent water from conduit A and 16 percent from conduit B (Table 13). These models suggest that conduit A is the primary contributor of flow to the spring outlet during low flow periods and that mixing waters could cause dissolution in parts of the aquifer during low flow periods.

It is likely that more significant changes in water chemistry at the spring, and therefore source waters, occur during storm events. The data collected by the gauging equipment at the spring show that precipitation events are correlated to increases in discharge and turbidity and decreases in temperature and specific conductivity (Figures 10 and 14). Although some variation in the gauge data is likely due to human interference caused by swimmers at the spring and pumping in nearby municipal wells (Hays Trinity Groundwater Conservation District pers. comm. 2008), such interference should be minimal in the daily averages shown in Figure 14. The trends in the gauging data suggest that precipitation events lead to an influx of fresher water with higher suspended sediment loads, likely along fast conduit flowpaths.

SURFACE WATER

Due to the low flow in the Upper Blanco River throughout the study period, stream samples most likely represent baseflow from groundwater. Identifying which of

these samples represent surface water that has spent considerable residence time in the stream and which represent recent, local groundwater input can help characterize the surface water during the study period and interpret how it might differ during wetter periods.

Sites UBR2 and UBR3 were not flowing at the time of sampling; samples from site UBR1 were taken above an impoundment in the stream that was likely receiving limited inflow during the study period. Local landowners described sites UBR4 and UBR5 as being springfed.

Because the stream travels through carbonates upstream from the study area, surface waters should still be Ca-Mg-HCO_3 type, but can also be expected to have several distinguishing characteristics. Surface waters at or near equilibrium with the atmosphere will have higher pH, lower P_{CO_2} ($10^{-3.5}$ atm at equilibrium), and lower concentrations of Ca and HCO_3 than groundwaters, as described by eqs. 1 and 7.

The P_{CO_2} of stream samples ranges from $10^{-3.3}$ atm at site UBR1 to $10^{-2.0}$ atm at site UBR5 (Table 8). These high values of P_{CO_2}, in addition to the decrease in P_{CO_2} over time in multiple samples from site UBR1, indicate that the stream samples represent groundwater discharge approaching equilibrium with atmospheric P_{CO_2} and not water derived from precipitation. Samples from sites UBR5 and UBR6 have pH values and concentrations of HCO_3 and Ca most similar to those in spring waters and some groundwaters, suggesting that these represent local groundwater input (Figure 18, Table 5). The low levels of HCO_3 and Ca relative to most groundwaters and spring waters at sites UBR1, UBR2, UBR3, and UBR4 suggest that samples from these sites represent waters that have spent a longer time at the surface.

Another important characteristic of the stream waters is the extent to which they have undergone evaporation. Waters that have spent considerable time in the stream,

either by traveling downstream or by ponding in the streambed, will become concentrated by evaporation, leading to increased concentrations of conservative elements, such as Cl and B, and TDS. Stream water samples from sites UBR1, UBR2, UBR3, and UBR4, are considerably enriched in $\delta^{18}O$ and $\delta^{2}H$, which should increase as the lighter ^{16}O and H isotopes preferentially evaporate, increasing the $^{18}O/^{16}O$ and $^{2}H/H$ ratios. The slope of the regression line on Figure 18 is 4.35 (r^2=0.99), similar to that found for partially evaporated meteoric waters by Craig (1961b) (Table 6b).

Interpreting how the stream waters interact with the groundwater system, and potentially springflow at Jacob's Well, depends in part on the cause of this evaporation. If the evaporation took place as surface water traveled downstream under typical low flow conditions, then the samples represent water that could potentially recharge the aquifer. If the evaporation took place after water ponded in the streambed, then these waters might be more highly evaporated water than typical surface waters. In addition, extended ponding would take place in an impermeable part of the channel and thus not represent possible recharge to the aquifer.

Given the physical and chemical descriptions above and the data in Tables 5b, 6b, and 7b and Figures 17 and 18, samples from sites UBR5 and UBR6 likely represent local groundwater flow into gaining sections of the stream; samples from sites UBR2 and UBR3 are likely highly evaporated surface water that originated primarily as groundwater discharge; the sample from site UBR4 is likely a mixture of older and more recent groundwater discharge; and the samples from site UBR1 are probably the most representative of typical surface waters approaching equilibrium with atmospheric P_{CO_2} under low flow conditions.

In June 2006, Steinhauer *et al*. (2006) collected samples from stream sites UBR3, UBR5, and UBR6. At each site, samples collected for this study contained more Cl and

SO_4 than in 2006. At sites UBR5 and UBR6 (cations were not measured in the 2006 sample from site UBR3), samples collected for this study also contained more Ca, Mg, and TDS than in 2006. These differences suggest that in 2008, surface waters were more highly evaporated than in 2006, or that the samples collected in 2006 contained a larger proportion of dilute rainwater. In addition, from 2006 to 2008, HCO_3 concentrations increased at sites UBR3 and UBR6 and decreased at site UBR5. Calculated values of P_{CO_2} were higher at site UBR3 and lower at sites UBR5 and UBR6 in 2008 than in 2006. These changes in P_{CO_2} and HCO_3 indicate that water from site UBR3 was closer to equilibrium with the atmosphere in 2006 than in 2008, while water from site UBR5 was closer to equilibrium with the atmosphere in 2008. Samples could be closer to equilibrium with the atmosphere because they contain a larger component of rainwater or, if they are composed of groundwater discharge, because they have had a longer time at the surface to allow outgassing of CO_2.

GROUND WATER

Because most well completion records are incomplete or unavailable, most well samples cannot be associated *a priori* to a known formation or aquifer. In addition, because most wells used for water supplies are screened in more than one formation—including those that are reported to draw from a specific hydrostratigraphic unit (Table 3)—samples can represent a mixture of water from multiple parts of the aquifer. For these reasons, the source of sampled waters must be deduced largely by using the measured water chemistry and knowledge of the aquifer geology.

As described above, the results of groundwater samples show three major chemical endmembers: low TDS Ca-Mg-HCO_3 waters (fresh endmember), high TDS Ca-Mg-SO_4 waters (saline endmember 1), and high TDS Na-Mg-Ca-SO_4 waters (saline endmember 2) (Figures 15 and 16, Table 5c). Each of these chemical endmembers also

seems to have a distinct $^{87}Sr/^{86}Sr$ ratio, with the two saline endmembers containing higher $^{87}Sr/^{86}Sr$ ratios than those measured in fresh groundwaters, spring waters, and stream waters (Table 9).

Fresh endmember

The fresh groundwater endmember contains less than 500 mg/L TDS, is composed primarily of dissolved HCO_3 and Ca, and has low levels of the conservative element Cl. Samples that most represent this water type include those from sites HAR, HOL, and NEW (Table 5c). Most groundwater samples, as well as stream and spring water samples, group near this endmember (Figure 15).

This endmember most likely represents recent meteoric water that has interacted with carbonates, primarily limestones, in the aquifer. PHREEQC was used to speciate the chemistry of a rainwater sample from Sonora, Texas, about 270 km west-northwest of the study area (NADP 2007), and then model what possible phase changes could explain the evolution of this rainwater to water from site NEW. Modeling results show that the evolution of rainwater to that sampled at site NEW can be explained by evaporating 99 percent of the rainwater and then dissolving calcite and dolomite, ingassing CO_2, and precipitating a relatively small amount of anhydrite (Table 14). The phase changes in calcite, dolomite, and $CO_2(g)$ are expected reactions in a dilute, meteoric water recharging and flowing through a carbonate aquifer (eqs. 1–6, Appelo and Postma 2005). However, because both waters are undersaturated with respect to anhydrite, this mineral did not precipitate along the flowpath—the chemical change is more likely attributed to a slight difference in the SO_4 concentration of the actual precipitation that evolved to the water sampled at site NEW compared to the rainwater sample used here.

Saline endmember 1

Saline endmember 1 is characterized by high levels of Ca, SO_4, and Mg; more than 2000 mg/L TDS; and Cl, Na, and K concentrations similar to the fresh endmember. The most likely explanation for these waters, represented by wells VAS and JAN, is that that they represent meteoric water that is interacting with carbonates and evaporites and evolving by dedolomitization (eq. 10), probably in the upper member of the Glen Rose Limestone.

Several lines of evidence point to this interpretation. First, although the saline endmember 1 waters have high TDS, the low concentrations of Cl, Na, and K closely resemble those of the fresh groundwaters (Table 5c). In addition, the Ca/Mg ratios in these waters are within the range found in the fresh groundwaters—assuming a homogenous distribution of calcite and dolomite within the aquifer, this ratio should decrease with increasing residence time, as described above. The Ca/Mg ratios from site VAS are some of the highest of all the study samples, indicating a relatively short residence time (Table 8).

Second, samples from sites VAS and JAN contain the highest concentrations of SO_4 and three of the four highest concentrations of Sr in all study samples (Table 5). High concentrations of SO_4 are expected in waters dissolving gypsum or anhydrite, and high concentrations of Sr are often found in these minerals because of the occurrence of celestite ($SrSO_4$), a result of Sr substituting for Ca in gypsum (Playá and Rosell 2005). This explanation is supported by the strong correlation between Sr and SO_4 concentrations in the study samples (r^2=0.85, Figure 19).

Third, simple calculations indicate that evaporite dissolution is a likely cause of the high element concentrations in the endmember waters. Waters in the presence of evaporites should be close to saturated with respect to gypsum and anhydrite. The

calculated gypsum saturation indices suggest that wells VAS and JAN are approaching saturation with respect to gypsum (Table 8, Figure 20). Also, on Figure 21a, the 1:2 line indicates the concentrations of HCO_3 and Ca+Mg expected if these parameters can be explained entirely by calcite dissolution. Most of the samples plot along or near this line. However, the saline endmember 1 samples plot above it, indicating there is an additional source of Ca for the water. To test whether gypsum dissolution could be providing the additional Ca, the concentration of SO_4 can be subtracted from that of Ca+Mg and plotted as in Figure 21b. On this figure, samples VAS and JAN plot much closer to the 1:2 line.

Third, inverse modeling with PHREEQC supports the hypothesis that the aquifer rocks interacting with these samples are undergoing dedolomitization. Model results show that the chemical differences between rainwater from Sonora, Texas (NADP 2007) and water sampled at site VAS can be explained by evaporating 99 percent of the rainwater and then dissolving dolomite and anhydrite, ingassing CO_2, and precipitating calcite (Table 14). These phase changes, along with high concentrations of Ca, Mg, and SO_4, are characteristic of dedolomitization (Back and Hanshaw 1971, Plummer 1977, Back *et al*. 1983, Appelo and Postma 2005).

While these samples might represent waters from any part of the aquifer containing both carbonates and evaporites, the most likely source is the upper member of the Glen Rose Limestone. This unit is known to contain beds of evaporites (Stricklin *et al*. 1971). In addition, wells VAS and JAN are within the outcrop area of the upper member of the Glen Rose Limestone (Figure 5), and so the wells are potentially screened within the formation. Two wells that plot as intermediate between fresh groundwaters and saline endmember 1 waters on Figure 15, WC12 and GLE, are also within the outcrop area of this member of the Glen Rose Limestone.

Saline endmember 2

Saline endmember 2 samples contain 1500–1800 TDS, including high levels of Ca, Cl, Na, Mg, and SO_4 compared to the fresh endmember. This endmember—represented by samples from sites CHA, BUR, and SPR—probably represents older meteoric groundwater interacting with carbonate and silicate minerals, probably in the Lower Trinity aquifer.

The Ca/Mg ratios in these samples are among the lowest measured (0.9–1.0; the well sample average is 2.2) (Table 8), indicating a long residence time in contact with dolomite relative to other sampled waters. In addition, if the high levels of Na and Cl in these samples (Table 5, Figure 22) are due to evaporation prior to infiltration, they could be explained by a different source of recharge, such as waters that infiltrated during a different time period.

The chemistry of these waters also indicates that they have interacted more with silicate minerals than the other sampled waters, suggesting rock-water interaction with silicate terrestrial deposits that are found in the Hosston, Hammett, and Hensel formations (DeCook 1960, Stricklin *et al*. 1971). Interaction with silicate minerals in these formations would explain the high Si and K concentrations and Na/Cl ratios in the saline endmember 2 samples (Tables 5c and 8c). The high levels of Na relative to Cl (Na/Cl>1.5) can be explained by albite dissolution, as proposed by Barbieri *et al*. (2005). In addition, the Na and Cl concentrations in these waters plot along a mixing line between fresh waters and water known to be from the Hosston Formation, which is within the Lower Trinity aquifer, proposed by Oetting *et al*. (1996).

The $^{87}Sr/^{86}Sr$ ratios measured in sample waters support this interpretation. All $^{87}Sr/^{86}Sr$ values measured in sample waters are below 0.710, within the range typical for unaltered carbonate rocks with a marine origin (Table 9) (McNutt 2000). However, the

$^{87}Sr/^{86}Sr$ ratio from site CHA is significantly higher than those measured in other sample waters and higher than measured $^{87}Sr/^{86}Sr$ ratios in whole rock samples from the Middle and Lower Trinity aquifers (Figure 23; Koepnick *et al*. 1985, Woronick 1985). In general, interaction with both carbonate and silicate minerals is a possible explanation for the higher $^{87}Sr/^{86}Sr$ in this sample. Granitic, metamorphic, and detrital sedimentary rocks can have $^{87}Sr/^{86}Sr$ ratios that can reach well above the highest values measured in study samples (Franklyn *et al*. 1991, Harrington and Herczeg 2003, Bickle *et al*. 2005). This is because Rb commonly substitutes for K in silicate minerals, leading to more decay of ^{87}Rb to ^{87}Sr and thus higher concentrations of ^{87}Sr relative to ^{86}Sr (Faure and Powell 1972). The strong correlation between K and Rb in the study samples (r^2=0.97, y=1.04x-3.54) and high levels of both elements in samples from CHA, SPR, and BUR support this explanation (Tables 5 and 7, Figure 24).

Inverse modeling with PHREEQC provides estimates of phase changes that could explain evolution from fresh endmember waters to saline endmember 2 waters. Starting with a fresh groundwater, the chemistry in saline endmember 2 waters can be explained by dissolution of anhydrite, dolomite, albite, potassium feldspar, and halite and precipitation of calcite, kaolinite, and quartz (Table 12). Halite is not thought to be present in the aquifer—a more likely explanation is that the water was concentrated by evaporation prior to infiltration, as discussed above. Also, while most saline endmember 2 samples are supersaturated with respect to quartz, it is likely that some of the modeled quartz precipitation is accounted for by other reactions not modeled here.

Physical evidence supports the possibility that these samples are from the Lower Trinity aquifer. Based on well depth and local stratigraphic data, the wells at all three sites are drilled down to the Lower Trinity aquifer (Broun, pers. comm. 2008) and thus can potentially be drawing water from this part of the aquifer (Table 3). In addition, the

water level elevations measured at sites CHA and SPR are significantly lower than those in nearby wells, indicating they are part of a hydraulically separate unit (Table 4, Figure 12), and groundwater is thought to move downward within the Trinity aquifer (Muller and McCoy 1987, Muller 1990).

Given these interpretations, saline endmember 2 waters are best explained as water from the Hosston Formation. The Hosston Formation is the principle unit of the Lower Trinity aquifer (Ashworth 1983, Hammond 1984) and is derived in part from the erosion of the metamorphic and igneous rocks of the Llano Uplift (Stricklin *et al*. 1971) that are composed primarily of granite, gneiss, and schist (Sellards 1932). Waters stored in the matrix of the Lower Trinity aquifer are thus likely to be more influenced by the silicate $^{87}Sr/^{86}Sr$ ratio than waters in other parts of the aquifer, where flow occurs primarily through carbonate rocks.

DETERMINING THE SOURCE OF FLOW TO JACOB'S WELL

The study results and interpretations above narrow down considerably the number of the sampled waters that could be within the source area providing baseflow to Jacob's Well. First, the water level in the source area must be higher than that at Jacob's Well. Most sites located south and east of the spring are thus not possible sources (Figure 12).

Second, all samples from Jacob's Well contain relatively low levels of the conservative ions Cl and B (Table 5, Figure 25). These elements do not typically interact with soil or rocks and are unlikely to come out of solution. They will become more concentrated in water through evaporation, and so will increase along a flowpath—therefore, source water cannot have a higher concentration of Cl or B than the spring water. In addition, the conservative isotope ^{18}O should become enriched relative to ^{16}O along the flowpath. The $\delta^{18}O$ measured in spring waters is more enriched than most well waters but less enriched than stream waters (Table 6, Figure 17).

Samples that contain lower concentrations of Cl, B, and $\delta^{18}O$ and have higher water elevations (if known) than all samples taken from the spring are LAN, LSR, MER, and NEW. Additional samples that meet these conditions for some, but not all, of the spring samples are HAR, KIN, LED, and POL (Tables 4, 5, and 6; Figure 11).

These possible sources, along with other sites that nearly met the constraints listed above, were further constrained by inverse modeling with PHREEQC. These models attempt to calculate phase changes in several aquifer minerals that could account for changes in major element concentrations between possible source waters and spring waters.

Successful models were able to explain the differences in sample chemistry from sites HAR, KIN, LED, LSR, MER, NEW, and WC22 and samples from Jacob's Well with phase changes that could be expected along a flowpath through the aquifer (Figure 11). Examples of successful model summaries are shown on Table 12. Additional modeling explored possible mixing between these waters and waters that could not be otherwise successfully modeled. This found that mixtures of fresher groundwaters with waters from sites LAN, POL, and several other sites could also be possible sources of spring discharge (Table 12).

These results suggest that during drought conditions, there are two possible contributing areas for water that discharges from Jacob's Well. First, several possible source waters, from sites HAR, KIN, LED, MER, NEW, and WC22, are nearby wells upgradient within the Cypress Creek watershed. Second, two other possible source waters, from sites LED and LSR, are located farther west, within the Upper Blanco River watershed (Figure 11).

Of the waters described above, the fresh groundwaters are the type that is providing baseflow to Jacob's Well. All possible source waters for which there is

construction information available are reported to be drilled within the Middle Trinity aquifer (Table 3). However, the lack of detailed well construction and stratigraphic information makes it difficult to determine whether these waters are more likely coming from the Cow Creek Limestone or the lower member of the Glen Rose Formation. Despite this uncertainty, several lines of evidence suggest that the Cow Creek Limestone is more likely the main source of flow to the spring. First, a geophysical log of the well at site LED, one of the possible sources to the spring, shows that it is screened within the Cow Creek Limestone (Hays Trinity Groundwater Conservation District, pers. comm. 2008). Second, the main conduit leading up to the spring is thought to be within the Cow Creek Limestone (Broun *et al*. in press). Third, the source area suggested above is mostly within the outcrop of the lower member of the Glen Rose Limestone (Figure 5), but the spring is artesian and thus under confining pressure—the Cow Creek Limestone is more likely to be under confined or semi-confined conditions and thus a more likely source of artesian flow.

In a karst aquifer undergoing dissolution, waters should become more saturated with respect to carbonate minerals along a flowpath. Saturation indices calculated for the likely source waters and spring waters show that they become more saturated with respect to anhydrite and barite along most of the possible flowpaths. The differences in saturation with respect to calcite and dolomite are less conclusive, indicating both increases and decreases in the saturation states of these minerals along possible flowpaths. This suggests that, at least during drought periods, secondary porosity might not significantly increase within the flow system that feeds discharge at Jacob's Well.

Two alternative models can explain the two possible contributing areas to Jacob's Well described above. In the first, groundwater travels along fracture and conduit paths across the surface watershed boundary between the Upper Blanco River and Cypress

Creek to provide baseflow to Jacob's Well (Figure 26a). In the second, groundwater follows the regional hydraulic gradient to the southeast, as shown in Figure 12, and a groundwater divide separates the Upper Blanco River watershed from the discharge at Jacob's Well (Figure 26b).

Available information indicates that both flowpath models are physically possible. Tracer tests have shown that groundwater movement across topographic divides can occur in karst aquifers (Winston and Criss 2004). In and near the study area, faults and joints trend northeast-southwest and northwest-southeast (DeCook 1960, Grimshaw 1970, Wermund 1978, Ogden *et al*. 1986, Veni 1994) and provide a possible mechanism for eastward movement across the surface water divide (Abbot 1977, Maclay and Small 1986, Domenico and Schwartz 1990).

Results of water chemistry analysis and modeling in this study indicate that waters along the flowpaths proposed by both models could be sources of baseflow at Jacob's Well. However, the presence of similar groundwater chemistry to the west of Jacob's Well could also indicate that waters flowing southeast along the regional gradient are interacting with similar host rocks, in which case these waters would not represent a source of baseflow to the spring.

One way to test the possibility that the Upper Blanco River watershed contributes to discharge at Jacob's Well is to use precipitation, spring discharge, and groundwater pumping data to estimate or model the recharge rates needed to account for measured spring discharge. Preliminary calculations indicate that unrealistically high recharge rates are required to account for discharge at Jacob's Well if all recharge occurs within the Cypress Creek watershed (HTGCD pers. comm. 2008). Continued recording of spring discharge and groundwater pumping will increase the accuracy of these calculations.

In addition, sampling spring, stream, well, and vadose zone waters during wetter than normal periods and storm events could provide more insight into flowpaths and how these might change under different conditions, particularly when there is an influx of dilute precipitation. While vadose zone waters were considered unlikely to be contributing significantly to flow during the low flow period studied here, they have been found to be a component of karst spring discharge, particularly during and after storm events (Lee and Krothe 2001, Perrin *et al*. 2003).

WATER MOVEMENT BETWEEN THE UPPER BLANCO RIVER AND JACOB'S WELL

While the measured stream water chemistry is generally similar to that in fresh groundwaters and spring waters, the Upper Blanco River does not appear to have been a source of flow at Jacob's Well during the study period. There was essentially no flow in losing parts of the stream, and the sampled stream waters appear to represent ponded, evaporatively concentrated surface water or nearby groundwater discharge.

However, the stream could provide baseflow to the spring during wetter periods. The Upper Blanco River is thought to lose significant amounts of water to the Trinity aquifer in stream segments within the study area during higher-flow periods (DeCook 1960, TBWE 1960, Slade *et al*. 2002, Steinhauer *et al*. 2006), and Steinhauer *et al*. (2006) determined that site UBR3 represented a possible source of Jacob's Well discharge in 2006. In addition, the first model described above (Figure 26a), in which water flows eastward across the surface watershed boundary between Cypress Creek and the Upper Blanco River, explains how the Upper Blanco River could be a source of flow to the spring.

Steinhauer *et al*. (2006) determined that site UBR3 represented a possible source of Jacob's Well discharge in 2006, when the Upper Blanco River was flowing. In 2006, water from this site contained less HCO_3 (151 mg/L) than in 2008 (189 mg/L) and had a

P_{CO_2} ($10^{-3.1}$ atm) closer to that of the atmosphere than in 2008 ($10^{-2.8}$ atm). This suggests that in 2006, the water contained a larger portion of recent precipitation than in 2008, and probably represented more normal conditions.

At Jacob's Well, the chemistry of the discharge in 2006 (Steinhauer *et al*. 2006) was very similar to that measured in 2008. The most significant difference is that all concentrations of Cl and NO_3 measured at the spring in 2006 are lower than all concentrations of these constituents measured in 2008. This might indicate more evaporation at the surface prior to surface infiltration in 2008. However, the lack of significant differences in the spring chemistry from 2006 and 2008 do not show evidence that the Upper Blanco River provided a distinct source of water that was cut off during the dry period in 2008.

The stream provides a possible tool for testing whether the Upper Blanco River watershed is contributing to flow at Jacob's Well. If storm waters in the Upper Blanco River and Cypress Creek have distinct chemistries, then the chemical composition of Upper Blanco River storm waters could be used as a natural tracer in the chemistry of storm discharge at Jacob's Well. If storm waters from the two streams cannot be easily distinguished, then dye tracer tests along losing reaches of the Upper Blanco River and near or upstream of the contributing area found in this study could evaluate whether surface water from the Upper Blanco River reaches Jacob's Well.

IMPLICATIONS FOR GROUNDWATER MANAGEMENT

The results of this study indicate that baseflow at Jacob's Well during low flow periods comes from groundwater in the Middle Trinity aquifer within the Cypress Creek watershed—additional discharge might be sourced from the Upper Blanco River watershed to the west of the spring. Residential developments are located around and

upgradient of Jacob's Well along both of these flowpaths (Figure 3) and are largely dependent on groundwater from this part of the aquifer. Groundwater pumping from the Middle Trinity aquifer within this area is likely capturing water that would otherwise flow to the spring. Projected growth in population and water demand in the area are likely to intensify stress on the aquifer if groundwater remains the primary source of water, increasing the possibility that the spring will dry up during future droughts.

Conclusions

Chemical and isotopic data collected in the study area show three major water types that appear to represent different parts of the aquifer. Fresh Ca-Mg-SO_4 surface, spring, and groundwaters are the most common type and most likely represent meteoric water interacting with carbonate rocks in the Middle Trinity aquifer. High TDS Ca-Mg-SO_4 groundwaters are found in the eastern part of the study area and are interpreted as waters from a part of the aquifer undergoing dedolomitization, most likely the Upper Trinity aquifer. High TDS Na-Mg-Ca-SO_4 waters are best explained as coming from the Lower Trinity aquifer.

The water chemistry in Jacob's Well showed little variation over the study period, suggesting a constant source or sources of baseflow dominated by diffuse flow under these low flow conditions. The two main conduits leading to the spring outlet show slight differences in water chemistry, and spring discharge constitutes a mixture of these two waters.

Analysis of water level elevations, chemical composition, and geochemical models suggests seven well sites located west of the spring that are potential source areas providing baseflow to Jacob's Well. Five of these sites are upgradient from the spring within the Cypress Creek watershed. Two others are located farther west, within the Upper Blanco River watershed.

The hydraulic gradient in the Trinity aquifer in the study area is generally to the southeast. However, fractures, faults, and conduits in the aquifer provide a mechanism by which groundwater flow directions could depart from this gradient. This presents the possibility of discharge to Jacob's Well coming from across the surface watershed boundary.

Future studies are needed to explore flowpaths in the study area, particularly the possibility of fast flowpaths through secondary porosity from west of the Cypress Creek watershed. Groundwater modeling or water-balance calculations could help to evaluate the likelihood of different contributing areas. In addition, analysis of spring, stream, well, and vadose zone waters sampled during wetter than normal periods and during storm events could be completed to assess whether differences in water chemistry can be used to identify flowpaths. Lastly, dye tracer tests in the Upper Blanco River could provide conclusive evidence of groundwater flow across the surface watershed boundary.

Tables

Table 1. Population of Hays County and the Wimberley area in 2000 and projections by decade for 2000–2060 (USCB, 2003; TWDB, 2007).

Area	2000	2010	2020	2030	2040	2050	2060	Percent growth
Hays County	97,589	166,342	242,051	302,795	363,678	436,388	493,320	406
Wimberley area	8,282	12,532	17,396	22,433	27,495	33,577	38,360	363

Table 2. Equilibrium solubility products constants (K_{sp}) at 25ºC of some minerals common to carbonate aquifers (Faure 1991).

Mineral	Composition	Ksp
calcite	$CaCO_3$	$10^{-8.35}$
dolomite	$CaMg(CO_3)_2$	$10^{-17.9}$
gypsum	$CaSO_4 \cdot 2H_2O$	$10^{-4.6}$
anhydrite	$CaSO_4$	$10^{-4.5}$

Table 3. Description of wells included in the study.

Well	Well depth (m)	Date drilled	Reported hydrostratigraphic unit	TWDB well no	TCEQ well no
BUL	112.8			5763902	G1050039D
MCM	204.2	2000	Lower Trinity		
CHA	~152.4	1993	Lower Trinity		
SUT	170.7 (pump at 146.3)	1985	Lower Trinity		
LSR	134.1	1997	Middle Trinity (Lower Glen Rose)	5763702	G1050135A
SWH	unknown				
SWM	unknown				
WC22	91.4 (pump at 57.6)	1980	Middle Trinity	5763903	G1050039B
WC21	121.9	1976	Middle Trinity	5763904	G1050039A
WC11	121.9	1977	Middle Trinity	5764702	G1050037A
WC12	179.8	1989	Middle Trinity		G1050037B
CYJ	76.2	1974	Middle Trinity		G1050060A
HOL	unknown	1987			
MTC	146.3 (pump at 109.7)	1987	Middle Trinity		G1050111A
GRA	46.6		Middle Trinity		
VAS	128.0	1983	Middle Trinity		
GOT	pump at 129.5	pre-1989	Middle Trinity		
HAR	97.5	2003	Middle Trinity		
SRT	unknown		Middle Trinity		
PAT	~48.8	mid-1970s	Middle Trinity		
ROH	61.0	2008	Middle Trinity (Lower Glen Rose)		
WC10	121.9		Middle Trinity		G1050037C
WCG	136.6		Middle Trinity	5764703	G1050037D
SAN	115.8	2005	Lower Trinity		
BUR	131.1	2002	Lower Trinity		
LED	93.0		Middle Trinity (Cow Creek)		
SPR	164.6	1998	Lower Trinity		
KIN	61.6	1995	Middle Trinity (Cow Creek)		
POL	131.1	1984	Lower Trinity		
WIL	unknown		unknown		
WIK	unknown	1979-1981	unknown		
LAN	115.8	1992	Lower Trinity		
WAR	103.6	2001	Middle Trinity		
MER	70.1	2002	Middle Trinity		
BRO	unknown		unknown		
NEW	pump at 54.9	1974	Middle Trinity (Lower Glen Rose)		
GLE	204.2	1996	Middle Trinity (Cow Creek)		
HOM	137.2 (pump at 67.0)	1986	Middle or Upper Trinity (Glen Rose)		
WS6	115.8 (pump at 91.4)				
WS4	167.6	1978		6808102	G1050018B
JAN	143.3		Middle Trinity (Lower Glen Rose)		G1050018

Table 4. Surveyed site locations and water levels. amsl=above mean sea level, MP=measuring point, na=not available.

Site	Date	Latitude (UTM)	Longitude (UTM)	Elevation of MP (m amsl)	Water level (m below MP)	Water level (m amsl)
Jacob's Well (JW)	5/19/08	3322928	584255	-	-	278.2
Upper Blanco River sites						
UBR1	6/17/08	3329055	557581	-	-	383.9
UBR3	6/17/08	3328778	565044	-	-	351.9
UBR2	6/17/08	3329962	563427	-	-	359.2
UBR6	6/17/08	3319125	577131	-	-	276.5
UBR5	7/2/08	3322840	575028	-	-	287.1
UBR4	7/2/08	3324195	571328	-	-	306.8
Well sites						
BUL	5/7/08	3322855	582309	309.1	30.9	278.2
MCM	5/7/08	3319963	579404	335.1	66.6	268.5
CHA	5/8/08	3327353	577247	376.0	100.1	275.9
SUT	5/8/08	3327302	577545	373.1	na	na
LSR	5/19/08	3323397	573735	346.5	57.7	288.8
SWH	5/19/08	3323247	571469	324.8	22.7	302.1
SWM	5/19/08	3325849	573322	342.2	34.1	308.1
WC22	5/20/08	3323435	581352	314.8	36.1	278.6
WC21	5/20/08	3322577	582880	302.8	24.2	278.5
WC11	5/20/08	3321812	585414	283.4	11.1	272.2
WC12	5/20/08	3321565	586565	312.7	52.3	260.4
CYJ	5/20/08	3322384	584968	290.3	11.8	278.5
HOL	5/21/08	3323968	586195	322.9	44.9	278.1
MTC	5/21/08	3323366	585831	355.1	76.2	278.9
GRA	5/21/08	3322800	584482	290.1	10.5	279.6
VAS	5/21/08	3323196	586798	353.0	86.8	266.2
GOT	5/22/08	3329098	576952	408.4	116.1	292.3
HAR	5/22/08	3324731	579614	352.1	72.7	279.5
SRT	5/22/08	3329104	580121	392.5	89.1	303.4
PAT	6/16/08	3316167	578276	315.4	na	na
ROH	6/16/08	3316358	576697	287.9	12.5	275.4
WC10	6/18/08	3321865	585478	288.4	13.5	274.9
WCG	6/18/08	3322268	585653	290.4	15.6	274.8
SAN	7/14/08	3324026	574501	324.1	na	na
BUR	7/14/08	3323933	575339	332.9	46.5	286.3
LED	7/14/08	3323620	576301	369.3	78.9	290.4
SPR	7/15/08	3322240	579705	354.1	92.7	261.4
KIN	7/15/08	3325193	579625	335.4	53.3	282.1
POL	7/15/08	3325014	577324	366.8	78.8	288.0
WIL	7/15/08	3323083	579257	358.3	74.4	283.8
WIK	7/15/08	3323300	579287	359.5	77.8	281.8
LAN	7/16/08	3323974	583831	315.1	33.5	281.6
WAR	7/16/08	3325508	583013	346.5	66.8	279.8
MER	7/16/08	3325424	582362	316.3	na	na

Table 4. continued.

Site	Date	Latitude (UTM)	Longitude (UTM)	Elevation of MP (m amsl)	Water level (m below MP)	Water level (m amsl)
BRO	7/16/08	3324414	584184	330.5	na	na
NEW	7/22/08	3325800	580655	327.3	na	na
GLE*	7/25/08	3315683	585386	332.0	na	na
HOM	9/16/08	3316200	583247	276.8	na	na
WS6*	9/19/08	3321140	584512	329.2	na	na
WS4*	9/19/08	3317628	587503	272.0	na	na
JAN	9/19/08	3315320	587731	316.4	na	na
Additional water level measurements						
GRA	6/16/08	3322800	584482	290.1	10.6	279.5
GRA	9/16/08	3322800	584482	290.1	10.5	279.6
SPR	9/15/08	3322240	579705	354.1	88.2	266.0
LED	9/15/08	3323620	576301	369.3	78.9	290.4
WC12	9/17/08	3321565	586565	312.7	72.2	240.4
HAR	9/17/08	3324731	579614	352.1	72.9	279.3
CHA	9/17/08	3327353	577247	376.0	99.5	276.5
VAS	9/19/08	3323196	586798	353.0	91.1	261.9

*Location is estimated.

Table 5a. Chemical description of water samples from Jacob's Well. All units are mmol/L unless labeled otherwise. bdl=below detection limit, na=not available, TDS=total dissolved solids.

Site	Date	pH	Temp (ºC)	Ca^{2+}	Mg^{2+}	Na^{+}	K^{+}	Sr^{2+}	HCO_3^{-}	Cl^{-}	SO_4^{2-}	NO_2^{-}	NO_3^{-}	F^{-}	Si	B	O_2	TDS (mg/L)	Water type
JW	5/19/08	6.8	22.7	2.25	0.81	0.33	0.04	0.01	5.25	0.34	0.27	bdl	0.042	0.013	0.16	0.007	0.210	497	Ca-Mg-HCO3
JW	6/16/08	6.9	21.1	2.23	0.78	0.29	0.03	0.01	5.18	0.36	0.25	bdl	0.036	0.009	0.16	0.005	0.183	487	Ca-Mg-HCO3
JW	6/18/08	6.8	23.1	2.21	0.77	0.29	0.03	0.01	5.30	0.37	0.23	bdl	0.037	0.007	0.16	0.005	0.250	495	Ca-Mg-HCO3
JW	7/2/08	7.1	20.7	2.24	0.78	0.29	0.03	0.01	4.95	0.36	0.21	bdl	0.038	0.016	0.16	0.005	0.181	470	Ca-Mg-HCO3
JW	7/14/08	6.8	22.0	2.18	0.81	0.31	0.04	0.01	5.27	0.36	0.22	bdl	0.041	0.019	0.17	0.006	0.187	490	Ca-Mg-HCO3
JW	7/22/08	7.1	20.8	2.16	0.82	0.31	0.04	0.01	5.21	0.35	0.23	bdl	0.049	0.015	0.17	0.005	0.179	487	Ca-Mg-HCO3
JW	7/25/08	7.0	21.4	2.14	0.82	0.32	0.04	0.01	5.19	0.36	0.21	bdl	0.046	0.019	0.16	0.005	0.178	483	Ca-Mg-HCO3
JW	8/10/08	7.4	21.0	2.25	0.81	0.31	0.03	0.01	5.00	0.36	0.23	bdl	0.038	0.014	0.17	0.005	na	471	Ca-Mg-HCO3
JW	9/15/08	7.2	20.6	2.25	0.85	0.32	0.03	0.01	5.22	0.37	0.22	0.002	0.043	0.014	0.17	0.005	0.203	482	Ca-Mg-HCO3
JW (A1)	8/10/08	7.1	21.0	2.20	0.82	0.31	0.03	0.01	5.52	0.37	0.23	bdl	0.047	0.014	0.17	0.005	na	502	Ca-Mg-HCO3
JW (A2)	8/10/08	7.1	21.0	2.23	0.87	0.33	0.03	0.01	4.96	0.37	0.23	bdl	0.041	0.014	0.17	0.005	na	467	Ca-Mg-HCO3
JW (B1)	8/10/08	7.1	21.0	2.25	0.83	0.31	0.03	0.01	5.24	0.37	0.26	bdl	0.037	0.015	0.18	0.005	na	490	Ca-Mg-HCO3

Table 5b. Chemical description of water samples from the Upper Blanco River. All units are mmol/L unless labeled otherwise. bdl=below detection limit, na=not available, TDS=total dissolved solids.

Site	Date	pH	Temp (ºC)	Ca^{2+}	Mg^{2+}	Na^{+}	K^{+}	Sr^{2+}	HCO_3^{-}	Cl^{-}	SO_4^{2-}	NO_2^{-}	NO_3^{-}	F^{-}	Si	B	O_2	TDS (mg/L)	Water type
UBR1	6/17/08	8.2	29.6	1.14	1.00	0.43	0.05	0.01	3.55	0.45	0.33	bdl	0.004	0.013	0.31	0.008	0.190	370	Ca-Mg-HCO3
UBR3	6/17/08	8.1	26.0	1.07	0.88	0.50	0.05	0.00	3.09	0.57	0.33	bdl	0.002	0.009	0.37	0.010	0.174	347	Ca-Mg-HCO3
UBR2	6/17/08	7.9	31.6	0.98	1.04	0.54	0.06	0.00	3.29	0.59	0.29	bdl	0.004	0.008	0.50	0.010	0.192	365	Mg-Ca-HCO3
UBR6	6/17/08	7.7	28.8	2.17	0.84	0.33	0.03	0.01	4.92	0.38	0.45	bdl	0.036	0.007	0.18	0.006	0.246	494	Ca-Mg-HCO3
UBR5	7/2/08	7.5	23.9	2.03	0.83	0.31	0.03	0.01	4.92	0.36	0.33	bdl	0.041	0.015	0.18	0.005	0.243	478	Ca-Mg-HCO3
UBR4	7/2/08	7.8	28.1	1.24	0.63	0.38	0.04	0.00	3.37	0.47	0.09	bdl	0.008	0.009	0.28	0.005	0.209	329	Ca-Mg-HCO3
Additional samples from stream sites																			
UBR1	7/2/08	8.2	28.4	1.08	1.41	0.62	0.07	0.01	3.50	0.49	0.33	bdl	0.004	0.017	0.38	0.009	0.227	387	Mg-Ca-HCO3
UBR1	9/15/08	8.5	25.9	0.90	0.98	0.43	0.06	0.01	2.94	0.43	0.27	bdl	0.005	0.015	0.46	0.008	0.241	327	Mg-Ca-HCO3

Table 5c. Chemical description of water samples from wells. All units are mmol/L unless labeled otherwise. bdl=below detection limit, na=not available, TDS=total dissolved solids.

Site	Date	pH	Temp (ºC)	Ca^{2+}	Mg^{2+}	Na^{+}	K^{+}	Sr^{2+}	HCO_3^{-}	Cl^{-}	SO_4^{2-}	NO_2^{-}	NO_3^{-}	F^{-}	Si	B	O_2	TDS (mg/L)	Water type
MCM	5/7/08	6.8	23.4	1.73	1.50	0.46	0.05	0.01	5.59	0.47	0.21	bdl	0.012	0.020	0.22	0.006	0.000	511	Ca-Mg-HCO3
CHA	5/8/08	7.2	24.4	4.41	4.57	9.62	0.32	0.06	3.46	5.03	8.43	0.002	0.012	0.045	0.22	0.232	0.006	1744	Na-Mg-Ca-SO4
SUT	5/8/08	7.1	24.1	1.82	1.13	0.33	0.03	0.01	5.06	0.39	0.22	bdl	0.033	0.017	0.17	0.006	0.230	474	Ca-Mg-HCO3
LSR	5/19/08	6.6	21.6	2.63	0.45	0.24	0.02	0.00	6.02	0.31	0.14	bdl	0.076	0.008	0.15	0.004	0.243	535	Ca-HCO3
SWH	5/19/08	7.0	21.3	3.14	0.23	0.58	0.05	0.00	5.27	0.66	0.19	bdl	0.684	0.008	0.14	0.004	0.275	569	Ca-HCO3
SWM	5/19/08	6.6	21.6	2.22	0.73	0.32	0.03	0.01	5.65	0.37	0.28	0.002	0.047	0.015	0.17	0.006	0.109	519	Ca-Mg-HCO3
WC22	5/20/08	6.8	21.8	2.34	0.80	0.30	0.03	0.00	5.41	0.36	0.20	bdl	0.044	0.015	0.17	0.006	0.201	503	Ca-Mg-HCO3
WC21	5/20/08	6.7	21.6	2.53	0.88	0.50	0.03	0.00	5.93	0.64	0.18	bdl	0.068	0.013	0.18	0.006	0.142	557	Ca-Mg-HCO3
WC11	5/20/08	6.9	23.5	2.23	0.99	0.33	0.03	0.00	5.80	0.38	0.19	0.002	0.029	0.011	0.16	0.005	0.142	524	Ca-Mg-HCO3
WC12	5/20/08	6.9	23.7	2.50	1.58	0.42	0.06	0.02	5.28	0.37	1.23	0.002	0.006	0.024	0.20	0.009	0.119	623	Ca-Mg-HCO3-SO4
CYJ	5/20/08	6.8	22.4	2.28	0.87	0.31	0.02	0.00	5.28	0.37	0.17	bdl	0.033	0.012	0.16	0.005	0.177	490	Ca-Mg-HCO3
HOL	5/21/08	6.8	23.5	1.99	1.04	0.28	0.04	0.00	5.44	0.34	0.19	0.002	0.040	0.017	0.18	0.005	0.162	494	Ca-Mg-HCO3
MTC	5/21/08	6.8	21.8	2.25	0.75	0.36	0.03	0.00	5.35	0.43	0.15	bdl	0.041	0.014	0.17	0.005	0.194	493	Ca-Mg-HCO3
VAS	5/21/08	6.7	23.6	13.72	4.06	0.44	0.22	0.19	4.95	0.33	14.19	bdl	0.004	0.042	0.19	0.019	0.016	2374	Ca-Mg-SO4
GOT	5/22/08	na	24.9	1.82	1.73	0.47	0.07	0.06	5.28	0.45	0.69	bdl	0.023	0.027	0.20	0.011	0.218	559	Ca-Mg-HCO3
HAR	5/22/08	6.9	24.8	2.00	0.94	0.27	0.03	0.01	5.37	0.33	0.19	bdl	0.043	0.015	0.18	0.005	0.151	487	Ca-Mg-HCO3
SRT	5/22/08	6.9	23.0	1.81	1.84	0.57	0.10	0.07	5.82	0.41	0.77	bdl	0.029	0.059	0.19	0.011	0.058	600	Mg-Ca-HCO3
PAT	6/16/08	7.1	23.0	1.49	1.68	0.38	0.09	0.04	5.47	0.38	0.33	bdl	0.007	0.079	0.21	0.010	0.001	510	Mg-Ca-HCO3
ROH	6/16/08	7.0	26.1	1.46	1.46	0.39	0.06	0.01	5.39	0.42	0.19	bdl	0.004	0.040	0.21	0.007	0.009	483	Ca-Mg-HCO3
GRA	6/16/08	6.4	21.1	2.95	2.01	1.03	0.79	0.01	7.30	1.37	1.23	0.001	0.131	0.001	0.23	0.008	0.018	857	Ca-Mg-HCO3-SO4
WC10	6/18/08	6.8	22.8	2.12	1.02	0.30	0.03	0.00	5.56	0.38	0.21	bdl	0.022	0.001	0.17	0.005	0.133	506	Ca-Mg-HCO3
SAN	7/14/08	7.0	25.2	2.03	1.17	0.86	0.11	0.04	4.97	0.57	0.66	bdl	0.032	0.021	0.20	0.027	0.099	541	Ca-Mg-HCO3
BUR	7/14/08	6.9	24.2	3.40	3.81	8.59	0.40	0.06	4.42	5.15	6.45	bdl	0.162	0.043	0.22	0.230	0.002	1546	Na-Mg-Ca-SO4-Cl
LED	7/14/08	6.7	26.2	2.23	0.77	0.31	0.04	0.01	6.17	0.34	0.22	bdl	0.031	0.013	0.17	0.006	0.106	544	Ca-Mg-HCO3
SPR	7/15/08	7.2	26.5	4.10	4.58	9.19	0.36	0.07	3.67	4.93	8.39	0.003	0.024	0.074	0.22	0.208	0.034	1731	Na-Mg-Ca-SO4
KIN	7/15/08	6.4	22.2	2.13	0.78	0.31	0.04	0.00	5.12	0.36	0.20	bdl	0.041	0.014	0.16	0.006	0.218	477	Ca-Mg-HCO3
POL	7/15/08	6.9	27.8	1.77	1.12	0.40	0.05	0.01	5.29	0.35	0.23	bdl	0.026	0.025	0.18	0.007	0.117	485	Ca-Mg-HCO3

Table 5c, continued.

Site	Date	pH	Temp (ºC)	Ca^{2+}	Mg^{2+}	Na^{+}	K^{+}	Sr^{2+}	HCO_3^{-}	Cl^{-}	SO_4^{2-}	NO_2^{-}	NO_3^{-}	F^{-}	Si	B	O_2	TDS (mg/L)	Water type
WIK	7/15/08	7.0	24.1	1.88	1.18	0.36	0.05	0.01	5.33	0.37	0.29	bdl	0.058	0.032	0.18	0.006	0.144	501	Ca-Mg-HCO3
LAN	7/16/08	7.0	23.6	1.91	1.20	0.27	0.05	0.01	5.75	0.34	0.12	bdl	0.034	0.026	0.18	0.004	0.044	504	Ca-Mg-HCO3
WAR	7/16/08	6.8	23.5	2.31	0.98	0.38	0.04	0.01	5.98	0.46	0.17	bdl	0.029	0.027	0.19	0.005	0.133	543	Ca-Mg-HCO3
MER	7/16/08	6.9	25.0	2.34	0.66	0.27	0.04	0.00	5.62	0.34	0.15	bdl	0.050	0.014	0.17	0.004	0.181	506	Ca-Mg-HCO3
BRO	7/16/08	6.9	23.9	2.07	1.05	0.37	0.04	0.01	5.56	0.46	0.19	bdl	0.027	0.024	0.17	0.005	0.146	510	Ca-Mg-HCO3
NEW	7/22/08	6.9	24.1	2.03	0.96	0.29	0.05	0.00	5.15	0.34	0.12	bdl	0.077	0.014	0.18	0.004	0.131	470	Ca-Mg-HCO3
GLE	7/25/08	6.9	22.5	4.94	2.69	0.91	0.24	0.15	5.62	0.50	4.52	bdl	0.010	0.041	0.19	0.020	0.002	1115	Ca-Mg-SO4-HCO3
HOM	9/16/08	7.3	24.6	1.27	1.84	0.95	0.17	0.05	5.16	0.54	0.53	bdl	0.004	0.114	0.21	0.016	0.003	528	Mg-Ca-HCO3
WS6	9/19/08	7.2	22.9	2.01	1.18	0.31	0.04	0.01	5.46	0.40	0.25	bdl	0.014	0.017	0.20	0.005	0.107	505	Ca-Mg-HCO3
WS4	9/19/08	7.3	24.7	1.67	1.78	0.64	0.15	0.04	5.42	0.50	0.65	bdl	0.004	0.062	0.23	0.012	0.055	561	Mg-Ca-HCO3
JAN	9/19/08	7.1	24.9	10.62	8.59	0.98	0.45	0.15	5.00	0.63	17.38	bdl	0.084	0.018	0.18	0.068	0.080	2703	Ca-Mg-SO4
Additional samples from well sites																			
SPR	9/15/08	7.4	24.4	4.08	4.74	9.68	0.35	0.07	3.57	5.19	8.38	0.018	0.030	0.049	0.24	0.222	0.098	1751	Na-Mg-Ca-SO4
NEW	9/15/08	7.2	21.9	2.07	0.93	0.29	0.03	0.00	5.29	0.36	0.13	bdl	0.078	0.013	0.18	0.005	0.156	483	Ca-Mg-HCO3
LED	9/15/08	7.1	21.7	2.35	0.80	0.32	0.03	0.01	5.22	0.37	0.23	0.002	0.037	0.012	0.18	0.005	0.127	495	Ca-Mg-HCO3
GRA	9/16/08	7.0	21.2	2.92	1.94	0.96	0.67	0.01	6.99	1.21	1.11	bdl	0.113	0.021	0.23	0.007	0.028	811	Ca-Mg-HCO3-SO4
WC12	9/17/08	7.2	24.5	2.72	1.67	0.37	0.07	0.02	5.06	0.39	1.53	bdl	0.010	0.029	0.21	0.005	0.053	646	Ca-Mg-HCO3-SO4
HAR	9/17/08	7.2	21.3	2.16	0.88	0.30	0.03	0.01	5.05	0.36	0.20	bdl	0.071	0.014	0.18	0.005	0.195	477	Ca-Mg-HCO3
CHA	9/17/08	7.2	24.7	4.16	4.09	8.26	0.29	0.05	3.68	5.24	7.88	bdl	0.014	0.033	0.22	0.192	0.018	1656	Ca-Na-Mg-SO4-Cl
VAS	9/19/08	6.9	24.3	12.61	3.86	0.41	0.20	0.16	4.76	0.26	13.74	bdl	0.010	0.028	0.19	0.014	0.014	2264	Ca-Mg-SO4

Table 6a. Additional chemical description of water samples from Jacob's Well. All units are mmol/L unless labeled otherwise. bdl=below detection limit, na=not available, OC=organic carbon.

						Field measured concentrations		
Site	Date	$\delta^{18}O$ (‰)	$\delta^{2}H$ (‰)	N	OC	H_2S	NH_3	Fe
JW	5/19/08	-3.50	-24.23	0.040	0.230	0.004	na	10.206
JW	6/16/08	na	na	0.034	0.066	0.001	0.000	0.000
JW	6/18/08	-3.57	-26.86	0.035	0.019	0.003	0.008	3.402
JW	7/2/08	na	na	0.049	0.065	0.001	0.000	0.000
JW	7/14/08	na	na	0.047	0.028	0.001	0.002	bdl
JW	7/22/08	na	na	0.047	0.027	0.001	na	0.000
JW	7/25/08	na	na	na	0.081	0.002	0.004	0.000
JW	8/10/08	na	na	na	0.039	na	na	na
JW	9/15/08	na	na	na	0.078	0.001	0.008	0.000
JW (A1)	8/10/08	na	na	na	0.036	na	na	na
JW (A2)	8/10/08	na	na	na	0.005	na	na	na
JW (B1)	8/10/08	na	na	na	0.033	na	na	na

Table 6b. Additional chemical description of water samples from the Upper Blanco River. All units are mmol/L unless labeled otherwise. bdl=below detection limit, na=not available, OC=organic carbon.

						Field measured concentrations		
Site	Date	$\delta^{18}O$ (‰)	$\delta^{2}H$ (‰)	N	OC	H_2S	NH_3	Fe
UBR1	6/17/08	1.24	-5.08	0.030	0.276	0.002	0.015	0.000
UBR3	6/17/08	3.16	3.52	0.021	0.344	0.001	0.004	0.000
UBR2	6/17/08	3.57	6.52	0.027	0.362	0.002	0.009	bdl
UBR6	6/17/08	-3.50	-25.81	0.037	0.064	0.001	0.004	0.000
UBR5	7/2/08	-3.28	-26.01	0.056	0.035	0.001	0.002	0.000
UBR4	7/2/08	0.33	-11.81	0.032	0.133	0.006	0.008	3.223
Additional samples from stream sites								
UBR1	7/2/08	na	na	0.041	0.165	0.003	0.010	1.432
UBR1	9/15/08	na	na	na	0.343	0.003	0.015	0.358

Table 6c. Additional chemical description of water samples from wells. All units are mmol/L unless labeled otherwise. bdl=below detection limit, na=not available, OC=organic carbon.

						Field measured concentrations		
Site	Date	$\delta^{18}O$ (‰)	$\delta^{2}H$ (‰)	N	OC	H_2S	NH_3	Fe
MCM	5/7/08	-3.68	-26.64	0.003	0.086	0.004	na	0.000
CHA	5/8/08	-4.27	-29.31	0.031	0.165	0.001	na	0.716
SUT	5/8/08	-3.91	-27.99	0.068	0.086	0.002	na	0.000
LSR	5/19/08	-3.84	-26.33	0.079	0.080	0.002	na	0.716
SWH	5/19/08	-3.92	-26.76	0.775	0.113	0.002	na	0.000
SWM	5/19/08	-3.35	-25.59	0.064	0.111	0.006	na	5.909
WC22	5/20/08	-3.48	-25.19	0.047	0.082	0.001	na	0.537
WC21	5/20/08	-3.73	-26.04	0.080	0.188	0.002	na	1.253
WC11	5/20/08	-3.85	-26.13	0.061	0.223	na	na	1.791
WC12	5/20/08	-3.90	-27.56	0.011	0.116	na	na	15.936
CYJ	5/20/08	-3.73	-27.04	0.034	0.088	na	na	2.149
HOL	5/21/08	-4.08	-30.10	0.050	0.083	na	na	0.000
MTC	5/21/08	-4.06	-26.91	0.044	0.087	na	na	3.223
VAS	5/21/08	-4.22	-29.37	0.207	0.375	0.003	na	0.000
GOT	5/22/08	-4.07	-29.01	0.017	0.671	0.002	na	0.000
HAR	5/22/08	-3.99	-28.03	0.041	0.130	0.003	na	bdl
SRT	5/22/08	-3.63	-27.70	0.023	0.047	0.010	na	1.791
PAT	6/16/08	-3.77	-28.68	0.004	0.014	0.001	0.019	0.000
ROH	6/16/08	-4.28	-28.37	0.001	1.250	0.003	0.265	3.760
GRA	6/16/08	-3.87	-27.68	0.120	0.247	0.004	0.028	2.865
WC10	6/18/08	-3.86	-27.96	0.022	0.035	0.001	0.004	0.000
SAN	7/14/08	-3.70	-26.77	0.042	0.030	0.002	0.006	4.118
BUR	7/14/08	-4.12	-30.51	0.063	0.030	0.002	0.015	bdl
LED	7/14/08	-3.82	-28.18	0.047	0.027	0.002	0.002	bdl
SPR	7/15/08	-4.47	-30.16	0.063	0.015	0.001	0.318	0.000
KIN	7/15/08	-4.49	-28.44	0.050	0.023	0.022	0.000	28.469
POL	7/15/08	-4.12	-28.19	0.037	0.019	0.029	0.014	16.294
WIK	7/15/08	-4.11	-27.58	0.069	0.022	0.014	0.007	26.321
LAN	7/16/08	-3.92	-26.70	0.040	0.023	0.001	0.003	0.000
WAR	7/16/08	-4.00	-27.02	0.039	0.027	0.002	0.006	0.000
MER	7/16/08	-4.14	-27.07	0.059	0.018	0.003	0.021	0.179
BRO	7/16/08	-3.84	-25.92	0.039	0.029	0.003	0.012	1.074
NEW	7/22/08	-4.21	-28.50	0.089	0.022	0.002	0.004	0.000
GLE	7/25/08	na	na	na	0.044	0.003	na	3.402
HOM	9/16/08	na	na	na	0.027	0.003	0.047	1.611
WS6	9/19/08	na	na	na	0.043	0.001	na	0.000
WS4	9/19/08	na	na	na	0.040	0.001	na	0.000
JAN	9/19/08	na	na	na	0.088	0.004	na	3.044

Table 6c, continued.

Site	Date	$\delta^{18}O$ (‰)	$\delta^{2}H$ (‰)	N	OC	Field measured concentrations		
						H_2S	NH_3	Fe
Additional samples from well sites								
SPR	9/15/08	na	na	na	0.018	0.001	0.066	0.000
NEW	9/15/08	na	na	na	0.025	0.001	0.004	0.000
LED	9/15/08	na	na	na	0.077	0.001	0.006	na
GRA	9/16/08	na	na	na	0.090	0.002	0.032	0.179
WC12	9/17/08	na	na	na	0.082	0.001	0.021	0.000
HAR	9/17/08	na	na	na	0.185	0.000	0.011	0.537
CHA	9/17/08	na	na	na	0.179	0.000	na	1.253
VAS	9/19/08	na	na	na	0.030	0.003	na	4.834

Table 7a. Concentrations of trace elements in water samples from Jacob's Well. All units are μmol/L. All measurements of Ag, Bi, Cd, Mo, PO4, and Th are below detection limit. Only one or two measurements of Co, Cs, Sb, Se, and Tl are above detection limit. bdl=below detection limit, na=not available.

Site	Date	Al	Mn	Fe	Ni	Ba	Zn	Pb	Cr	Cu	Sn	As	P	Rb	Ti	U	V
JW	5/19/08	bdl	0.16	bdl	0.08	0.31	0.87	bdl	bdl	0.59	0.17	bdl	bdl	bdl	0.12	0.004	bdl
JW	6/16/08	bdl	bdl	bdl	bdl	0.23	0.05	bdl	bdl	bdl	0.07	bdl	bdl	bdl	na	bdl	bdl
JW	6/18/08	bdl	bdl	bdl	bdl	0.22	bdl	bdl	bdl	bdl	bdl	bdl	bdl	bdl	na	bdl	bdl
JW	7/2/08	bdl	bdl	bdl	bdl	0.23	0.02	bdl	bdl	bdl	0.09	bdl	bdl	bdl	na	bdl	bdl
JW	7/14/08	bdl	bdl	bdl	bdl	0.20	bdl	bdl	bdl	bdl	0.17	bdl	bdl	bdl	bdl	bdl	bdl
JW	7/22/08	bdl	bdl	0.24	bdl	0.21	bdl	bdl	bdl	bdl	0.07	bdl	bdl	bdl	bdl	bdl	bdl
JW	7/25/08	bdl	bdl	bdl	bdl	0.24	bdl	bdl	bdl	bdl	0.07	bdl	bdl	bdl	bdl	bdl	bdl
JW	8/10/08	bdl	0.03	bdl	bdl	0.24	0.03	bdl	bdl	bdl	bdl	bdl	bdl	bdl	0.02	0.003	bdl
JW	9/15/08	bdl	bdl	bdl	bdl	0.23	0.30	bdl	bdl	bdl	0.07	bdl	bdl	bdl	0.02	0.003	bdl
JW (A2)	8/10/08	bdl	bdl	bdl	bdl	0.23	0.02	bdl	bdl	bdl	bdl	bdl	bdl	bdl	0.02	0.004	0.03
JW (A1)	8/10/08	bdl	bdl	bdl	bdl	0.23	0.03	bdl	bdl	bdl	bdl	bdl	bdl	bdl	0.02	0.004	bdl
JW (B1)	8/10/08	bdl	bdl	bdl	0.03	0.23	0.00	bdl	bdl	bdl	bdl	bdl	bdl	bdl	0.02	0.003	bdl

Table 7b. Concentrations of trace elements in water samples from the Upper Blanco River. All units are μmol/L. All measurements of Ag, Bi, Cd, Mo, PO4, and Th are below detection limit. Only one or two measurements of Co, Cs, Sb, Se, and Tl are above detection limit. bdl=below detection limit, na=not available.

Site	Date	Al	Mn	Fe	Ni	Ba	Zn	Pb	Cr	Cu	Sn	As	P	Rb	Ti	U	V
UBR1	6/17/08	bdl	0.09	bdl	bdl	0.26	bdl	bdl	bdl	bdl	bdl	bdl	0.28	0.02	0.09	bdl	0.07
UBR3	6/17/08	bdl	0.16	bdl	bdl	0.23	bdl	bdl	bdl	bdl	bdl	bdl	0.10	bdl	bdl	bdl	bdl
UBR2	6/17/08	bdl	0.15	bdl	bdl	0.23	0.21	bdl	bdl	bdl	bdl	bdl	bdl	0.02	bdl	bdl	0.07
UBR6	6/17/08	bdl	bdl	bdl	bdl	0.27	bdl	bdl	bdl	bdl	bdl	bdl	bdl	bdl	na	bdl	bdl
UBR5	7/2/08	bdl	0.39	17.33	bdl	0.34	0.01	bdl	bdl	0.10	bdl	11.03	0.72	bdl	bdl	bdl	bdl
UBR4	7/2/08	bdl	0.27	bdl	bdl	0.23	bdl	bdl	bdl	bdl	bdl	bdl	bdl	bdl	na	bdl	bdl
Additional samples from stream sites																	
UBR1	7/2/08	bdl	0.08	bdl	bdl	0.25	bdl	bdl	bdl	bdl	bdl	bdl	bdl	0.02	bdl	bdl	0.12
UBR1	9/15/08	0.76	0.07	0.28	bdl	0.23	0.07	bdl	bdl	0.04	bdl	34.53	bdl	0.02	0.05	bdl	0.10

Table 7c. Concentrations of trace elements in water samples from wells. All units are μmol/L. All measurements of Ag, Bi, Cd, Mo, PO4, and Th are below detection limit. Only one or two measurements of Co, Cs, Sb, Se, and Tl are above detection limit. bdl=below detection limit, na=not available.

Site	Date	Al	Mn	Fe	Ni	Ba	Zn	Pb	Cr	Cu	Sn	As	P	Rb	Ti	U	V
MCM	5/7/08	bdl	bdl	bdl	bdl	0.37	0.15	bdl	bdl	bdl	0.01	bdl	bdl	0.02	na	bdl	bdl
CHA	5/8/08	bdl	bdl	bdl	bdl	bdl	0.33	bdl	bdl	bdl	0.08	bdl	bdl	0.11	na	bdl	bdl
SUT	5/8/08	bdl	bdl	bdl	bdl	0.31	0.71	bdl	bdl	0.13	0.22	bdl	0.20	bdl	na	0.004	bdl
LSR	5/19/08	bdl	bdl	bdl	bdl	0.23	0.24	bdl	bdl	0.14	bdl	bdl	bdl	bdl	bdl	bdl	bdl
SWH	5/19/08	bdl	bdl	bdl	bdl	0.45	0.13	bdl	bdl	bdl	bdl	bdl	bdl	bdl	bdl	bdl	bdl
SWM	5/19/08	bdl	2.35	6.60	bdl	0.27	13.13	bdl	bdl	1.44	bdl	bdl	bdl	bdl	bdl	bdl	bdl
WC22	5/20/08	bdl	bdl	bdl	bdl	0.27	0.25	0.01	bdl	0.43	bdl	bdl	bdl	bdl	na	bdl	bdl
WC21	5/20/08	bdl	bdl	bdl	bdl	0.32	0.16	0.01	bdl	0.35	bdl	bdl	bdl	bdl	na	bdl	bdl
WC11	5/20/08	bdl	bdl	bdl	bdl	0.27	0.17	bdl	bdl	bdl	0.17	bdl	bdl	bdl	na	bdl	bdl
WC12	5/20/08	bdl	bdl	bdl	0.07	0.64	3.49	bdl	bdl	0.08	0.02	bdl	0.19	0.02	bdl	bdl	bdl
CYJ	5/20/08	bdl	bdl	bdl	bdl	0.24	2.21	0.03	bdl	0.25	bdl	bdl	bdl	bdl	na	bdl	bdl
HOL	5/21/08	bdl	bdl	bdl	bdl	0.23	0.98	0.01	bdl	0.61	0.01	bdl	0.29	bdl	na	bdl	bdl
MTC	5/21/08	bdl	bdl	bdl	bdl	0.24	0.40	bdl	bdl	0.11	bdl	bdl	bdl	bdl	na	bdl	bdl
VAS	5/21/08	bdl	bdl	bdl	bdl	bdl	0.31	bdl	bdl	bdl	bdl	bdl	bdl	0.09	bdl	bdl	bdl
GOT	5/22/08	bdl	bdl	bdl	bdl	0.89	1.88	bdl	bdl	0.15	0.01	bdl	bdl	0.02	bdl	0.004	bdl
HAR	5/22/08	bdl	bdl	bdl	bdl	0.30	0.21	0.01	bdl	0.17	0.20	bdl	bdl	bdl	bdl	bdl	bdl
SRT	5/22/08	bdl	bdl	bdl	bdl	0.40	0.37	bdl	bdl	0.21	bdl	bdl	bdl	0.04	bdl	0.004	bdl
PAT	6/16/08	bdl	bdl	bdl	bdl	0.17	0.14	bdl	bdl	0.13	bdl	bdl	bdl	0.04	na	bdl	bdl
ROH	6/16/08	bdl	0.26	bdl	bdl	0.23	3.24	0.06	bdl	0.44	0.04	bdl	bdl	0.02	na	bdl	bdl
GRA	6/16/08	bdl	0.06	bdl	0.07	0.50	0.97	bdl	bdl	0.06	bdl	bdl	bdl	0.14	na	0.013	bdl
WC10	6/18/08	bdl	bdl	bdl	bdl	0.17	bdl	bdl	bdl	bdl	bdl	bdl	bdl	bdl	na	bdl	bdl
SAN	7/14/08	bdl	bdl	0.61	bdl	0.59	1.42	bdl	bdl	0.20	bdl	bdl	bdl	0.04	bdl	bdl	bdl
BUR	7/14/08	bdl	0.13	0.96	bdl	bdl	bdl	bdl	bdl	bdl	0.08	bdl	bdl	0.12	bdl	bdl	bdl
LED	7/14/08	bdl	bdl	0.42	0.85	0.23	13.58	bdl	bdl	0.70	bdl	bdl	bdl	bdl	bdl	bdl	bdl
SPR	7/15/08	bdl	bdl	0.29	bdl	0.13	bdl	bdl	bdl	0.08	bdl	bdl	bdl	0.12	bdl	bdl	bdl
KIN	7/15/08	bdl	bdl	bdl	bdl	0.21	bdl	bdl	bdl	0.11	bdl	bdl	bdl	bdl	bdl	bdl	bdl
POL	7/15/08	bdl	bdl	1.52	0.19	0.16	bdl	bdl	0.56	0.23	bdl	bdl	bdl	bdl	bdl	bdl	bdl
WIK	7/15/08	bdl	bdl	bdl	bdl	0.20	bdl	bdl	bdl	0.18	bdl	bdl	bdl	bdl	bdl	bdl	bdl

Table 7c, continued.

Site	Date	Al	Mn	Fe	Ni	Ba	Zn	Pb	Cr	Cu	Sn	As	P	Rb	Ti	U	V
LAN	7/16/08	bdl	bdl	0.39	bdl	0.18	10.86	bdl	bdl	0.11	bdl	bdl	bdl	bdl	bdl	bdl	bdl
WAR	7/16/08	bdl	bdl	bdl	0.07	0.24	bdl	bdl	bdl	0.22	bdl	bdl	bdl	bdl	bdl	0.019	bdl
MER	7/16/08	bdl	bdl	bdl	bdl	0.18	0.63	bdl	bdl	0.14	bdl	bdl	bdl	bdl	bdl	bdl	bdl
BRO	7/16/08	bdl	bdl	bdl	bdl	0.20	bdl	bdl	bdl	0.07	bdl	bdl	bdl	bdl	bdl	bdl	bdl
NEW	7/22/08	bdl	bdl	bdl	bdl	0.18	bdl	bdl	bdl	0.07	0.16	bdl	bdl	bdl	bdl	bdl	bdl
GLE	7/25/08	bdl	bdl	0.82	bdl	bdl	bdl	bdl	bdl	0.14	bdl	bdl	bdl	0.12	bdl	bdl	bdl
HOM	9/16/08	bdl	bdl	0.76	bdl	0.15	1.10	bdl	bdl	0.02	bdl	bdl	bdl	0.07	0.02	bdl	bdl
WS6	9/19/08	bdl	bdl	bdl	0.03	0.20	0.74	0.01	bdl	0.13	0.01	bdl	bdl	0.02	0.02	0.003	bdl
WS4	9/19/08	bdl	bdl	0.52	0.04	0.13	0.66	0.01	bdl	0.03	bdl	bdl	bdl	0.07	0.03	bdl	bdl
JAN	9/19/08	bdl	bdl	0.22	0.15	bdl	1.03	0.03	bdl	0.38	bdl	bdl	bdl	0.30	0.02	bdl	bdl
Additional samples from well sites																	
SPR	9/15/08	bdl	0.03	0.14	0.06	0.11	0.68	0.01	0.02	0.16	bdl	bdl	bdl	0.12	0.03	bdl	bdl
NEW	9/15/08	bdl	bdl	bdl	bdl	0.23	0.69	0.01	bdl	0.19	bdl	bdl	bdl	bdl	0.02	0.003	0.05
LED	9/15/08	0.12	bdl	0.45	0.53	0.25	11.62	0.02	bdl	0.49	0.01	bdl	bdl	bdl	0.02	0.004	bdl
GRA	9/16/08	bdl	bdl	0.07	0.10	0.50	0.84	bdl	bdl	0.02	bdl	bdl	bdl	0.13	0.03	0.012	bdl
WC12	9/17/08	bdl	bdl	0.20	0.07	0.20	1.08	0.01	bdl	0.14	bdl	bdl	bdl	0.03	0.03	bdl	bdl
HAR	9/17/08	0.22	bdl	bdl	0.03	0.22	0.39	0.01	bdl	0.19	0.22	bdl	bdl	bdl	0.02	0.003	0.03
CHA	9/17/08	bdl	0.61	1.82	0.06	bdl	3.00	0.01	0.02	0.10	0.20	bdl	bdl	0.10	0.03	bdl	bdl
VAS	9/19/08	bdl	0.07	1.30	0.17	bdl	0.61	bdl	bdl	0.04	bdl	bdl	bdl	0.09	0.02	bdl	bdl

Table 8a. Calculated values from water samples taken at Jacob's Well. CB=charge balance, SI=saturation index. Charge balance is from PHREEQC speciation.

Site	Date	pe	Ionic strength	pP_{CO2}	SI calcite	SI anhydrite	SI dolomite	SI barite	CB (%)	Ca/Mg	Na/Cl
JW	5/19/08	8.5	0.0093	-1.357	-0.227	-2.334	-0.793	-0.543	1.4	2.8	1.0
JW	6/16/08	8.4	0.0091	-1.472	-0.157	-2.362	-0.686	-0.662	1.0	2.9	0.8
JW	6/18/08	8.6	0.0091	-1.300	-0.271	-2.395	-0.890	-0.755	-0.1	2.9	0.8
JW	7/2/08	8.2	0.0090	-1.675	0.002	-2.435	-0.376	-0.733	3.9	2.9	0.8
JW	7/14/08	8.5	0.0091	-1.349	-0.256	-2.426	-0.848	-0.791	0.5	2.7	0.9
JW	7/22/08	8.2	0.0091	-1.622	-0.022	-2.413	-0.384	-0.745	0.6	2.6	0.9
JW	7/25/08	8.2	0.0090	-1.570	-0.069	-2.449	-0.467	-0.728	0.6	2.6	0.9
JW	8/10/08	-	0.0091	-1.559	-0.098	-2.395	-0.558	-0.680	3.8	2.8	0.8
JW	9/15/08	8.1	0.0093	-1.713	0.081	-2.429	-0.186	-0.722	2.6	2.7	0.9
JW (A1)	8/10/08	-	0.0093	-1.516	-0.069	-2.413	-0.484	-0.708	-1.5	2.7	0.8
JW (A2)	8/10/08	-	0.0092	-1.563	-0.108	-2.408	-0.543	-0.713	4.8	2.6	0.9
JW (B1)	8/10/08	-	0.0093	-1.539	-0.082	-2.346	-0.515	-0.653	1.6	2.7	0.9

Table 8b. Calculated values from water samples taken at Upper Blanco River sites. CB=charge balance, SI=saturation index.

Site	Date	pe	Ionic strength	pP_{CO2}	SI calcite	SI anhydrite	SI dolomite	SI barite	CB (%)	Ca/Mg	Na/Cl
UBR1	6/17/08	7.1	0.0067	-2.836	0.743	-2.469	1.614	-0.606	1.0	1.1	0.9
UBR3	6/17/08	7.2	0.0063	-2.812	0.525	-2.479	1.107	-0.572	1.4	1.2	0.9
UBR2	6/17/08	7.4	0.0065	-2.566	0.412	-2.562	1.050	-0.723	2.0	0.9	0.9
UBR6	6/17/08	7.7	0.0091	-2.214	0.657	-2.115	1.077	-0.492	0.2	2.6	0.9
UBR5	7/2/08	7.9	0.0088	-2.031	0.366	-2.280	0.462	-0.441	-0.1	2.5	0.9
UBR4	7/2/08	7.5	0.0059	-2.463	0.387	-2.980	0.649	-1.161	1.6	2.0	0.8
Additional samples from stream sites											
UBR1	7/2/08	7.1	0.0075	-2.917	0.742	-2.521	1.777	-0.612	10.4	0.8	0.9
UBR1	9/15/08	6.8	0.0059	-3.296	0.842	-2.648	1.868	-0.655	4.2	0.9	0.9

Table 8c. Calculated values from water samples taken at well sites. CB=charge balance, SI=saturation index.

Site	Date	pe	Ionic strength	pP_{CO2}	SI calcite	SI anhydrite	SI dolomite	SI barite	CB (%)	Ca/Mg	Na/Cl
MCM	5/7/08	8.3	0.0098	-1.257	-0.378	-2.565	-0.704	-0.596	3.4	1.2	1.0
CHA	5/8/08	7.3	0.0346	-1.958	0.042	-0.919	0.213	0.140	5.9	1.0	1.9
SUT	5/8/08	8.2	0.0089	-1.675	-0.001	-2.495	-0.086	-0.638	2.1	1.6	0.9
LSR	5/19/08	8.7	0.0095	-1.115	-0.306	-2.553	-1.286	-0.944	-4.1	5.8	0.8
SWH	5/19/08	8.4	0.0115	-1.499	0.012	-2.372	-1.019	-0.537	-12.1	13.5	0.9
SWM	5/19/08	8.6	0.0093	-1.072	-0.478	-2.323	-1.350	-0.566	-3.9	3.0	0.9
WC22	5/20/08	8.5	0.0094	-1.360	-0.199	-2.449	-0.772	-0.722	1.9	2.9	0.8
WC21	5/20/08	8.5	0.0104	-1.224	-0.239	-2.477	-0.845	-0.699	0.9	2.9	0.8

Table 8c, continued.

Site	Date	pe	Ionic strength	pP_{CO2}	SI calcite	SI anhydrite	SI dolomite	SI barite	CB (%)	Ca/Mg	Na/Cl
WC11	5/20/08	8.3	0.0097	-1.361	-0.131	-2.485	-0.500	-0.769	0.7	2.3	0.9
WC12	5/20/08	8.3	0.0123	-1.387	-0.185	-1.705	-0.457	0.300	3.5	1.6	1.1
CYJ	5/20/08	8.4	0.0093	-1.368	-0.212	-2.518	-0.742	-0.831	3.9	2.6	0.8
HOL	5/21/08	8.5	0.0092	-1.297	-0.292	-2.536	-0.749	-0.845	0.3	1.9	0.8
MTC	5/21/08	8.5	0.0091	-1.294	-0.287	-2.574	-0.957	-0.870	0.9	3.0	0.8
VAS	5/21/08	8.1	0.0459	-1.285	0.062	-0.347	-0.302	-0.260	5.9	3.4	1.3
GOT	5/22/08	-	0.0109	-1.516	-0.144	-2.060	-0.179	0.218	3.8	1.1	1.1
HAR	5/22/08	8.3	0.0090	-1.404	-0.164	-2.532	-0.523	-0.743	-0.5	2.1	0.8
SRT	5/22/08	8.1	0.0115	-1.396	-0.227	-2.026	-0.341	-0.056	1.0	1.0	1.4
PAT	6/16/08	7.0	0.0097	-1.599	-0.132	-2.439	-0.105	-0.731	2.1	0.9	1.0
ROH	6/16/08	7.6	0.0090	-1.505	-0.172	-2.654	-0.199	-0.877	0.7	1.0	0.9
GRA	6/16/08	8.4	0.0163	-0.808	-0.498	-1.693	-1.080	0.184	0.2	1.5	0.7
WC10	6/18/08	8.4	0.0094	-1.282	-0.276	-2.478	-0.766	-0.917	1.4	2.1	0.8
SAN	7/14/08	8.2	0.0103	-1.499	-0.151	-2.011	-0.408	0.034	3.3	1.7	1.5
BUR	7/14/08	7.4	0.0302	-1.555	-0.221	-1.093	-0.281	-0.074	0.8	0.9	1.7
LED	7/14/08	8.5	0.0095	-1.146	-0.237	-2.417	-0.787	-0.823	-5.5	2.9	0.9
SPR	7/15/08	7.7	0.0338	-1.909	0.055	-0.944	0.291	0.002	3.5	0.9	1.9
KIN	7/15/08	8.9	0.0088	-0.930	-0.701	-2.480	-1.742	-0.821	0.9	2.7	0.9
POL	7/15/08	8.3	0.0089	-1.401	-0.173	-2.487	-0.382	-0.974	0.0	1.6	1.1
WIK	7/15/08	8.2	0.0094	-1.513	-0.111	-2.383	-0.303	-0.739	-0.1	1.6	1.0
LAN	7/16/08	8.0	0.0094	-1.494	-0.065	-2.763	-0.215	-1.142	0.6	1.6	0.8
WAR	7/16/08	8.4	0.0100	-1.288	-0.164	-2.528	-0.586	-0.879	0.5	2.4	0.8
MER	7/16/08	8.4	0.0092	-1.404	-0.057	-2.554	-0.525	-1.055	-1.4	3.5	0.8
BRO	7/16/08	8.3	0.0095	-1.396	-0.152	-2.512	-0.481	-0.904	0.8	2.0	0.8
NEW	7/22/08	8.3	0.0089	-1.467	-0.143	-2.732	-0.491	-1.157	2.1	2.1	0.9
GLE	7/25/08	7.3	0.0225	-1.446	0.064	-1.030	-0.040	-0.098	5.7	1.8	1.8
HOM	9/16/08	7.2	0.0101	-1.777	-0.053	-2.309	0.181	-0.646	4.1	0.7	1.8
WS6	9/19/08	8.0	0.0095	-1.711	0.109	-2.426	0.095	-0.775	2.5	1.7	0.8
WS4	9/19/08	7.8	0.0107	-1.766	0.087	-2.118	0.330	-0.642	3.1	0.9	1.3
JAN	9/19/08	8.0	0.0509	-1.719	0.376	-0.412	0.775	-0.622	-1.1	1.2	1.6
Additional samples from well sites											
SPR	9/15/08	7.8	0.0345	-2.086	0.160	-0.954	0.499	-0.026	4.8	0.9	1.9
NEW	9/15/08	8.1	0.0091	-1.700	0.074	-2.693	-0.105	-0.983	0.7	2.2	0.8
LED	9/15/08	8.1	0.0094	-1.658	0.064	-2.386	-0.250	-0.685	3.6	2.9	0.9
GRA	9/16/08	7.9	0.0101	-1.436	0.095	-1.732	0.096	0.154	2.0	1.5	0.8
WC12	9/17/08	7.9	0.0130	-1.703	0.130	-1.592	0.172	-0.149	4.4	1.6	0.9
HAR	9/17/08	8.1	0.0091	-1.743	0.081	-2.482	-0.141	-0.789	2.3	2.4	0.8
CHA	9/17/08	7.6	0.0324	-1.876	0.009	-0.952	0.127	-0.173	1.0	1.0	1.6
VAS	9/19/08	7.8	0.0435	-1.505	0.235	-0.378	0.064	-0.350	2.8	3.3	1.6

Table 9. Measured values of $^{87}Sr/^{86}Sr$ in water samples. Internal precision represents the 95% confidence interval for individual samples.

Sample	Date	$^{87}Sr/^{86}Sr$	Internal precision
JW	7/22/08	0.70777	0.0000040
NEW	9/15/08	0.70778	0.0000045
LED	9/15/08	0.70776	0.0000043
UBR1	9/15/08	0.70777	0.0000042
CHA	9/17/08	0.70866	0.0000041
CHA (duplicate)	9/17/08	0.70865	0.0000043
VAS	9/19/08	0.70797	0.0000038
NIST-SRM-987 (1)	standard	0.71024	0.0000041
NIST-SRM-987 (2)	standard	0.71025	0.0000043

Table 10. Parameters measured by gauging equipment at Jacob's Well during sampling times (USGS 2008).

Date	Time	Discharge (L/s)	Temp (ºC)	SC (µS/cm)	Water level (m amsl)
05/19/08	15:00	68.0	20.93	563	278.237
06/16/08	7:45	34.0	20.92	565	278.221
06/18/08	12:30	24.4	20.91	566	278.215
07/02/08	7:35	48.1	20.94	573	278.221
07/14/08	18:30	48.1	20.93	572	278.227
07/22/08	8:15	42.5	20.93	572	278.224
07/25/08	10:15	82.1	20.94	574	278.243
08/10/08	12:00	73.6	21.00	559	278.227
09/15/08	7:20	28.3	20.94	569	278.227

Table 11. Average total monthly precipitation at Blanco, Texas, 1971–2008, and total monthly precipitation in 2008 (NCDC 2008).

Month	Average precipitation (mm)	2008 precipitation (mm)
January	48	18
February	50	8
March	69	49
April	65	22
May	108	28
June	104	3
July	60	59
August	64	-
September	82	-
October	108	-
November	72	-
December	57	-

Table 12. Summary of mass transfer results calculated with inverse models. All values are in mmol/kg. Positive indicates dissolution, negative indicates precipitation. Where more than one successful model was calculated, the model with minimal mass transfer is shown.

Site 1 (start)	Site 2 (start)	Site (end)	Calculated mass transfers										Mix	
			Calcite	Anhydrite	Dolomite	Albite	K-feldspar	Illite	Kaolinite	Quartz	Halite	$CO_2(g)$	1	2
JW(A2)	JW(B1)	JW	0.2433	0	0	-	-	-	-	-	-	0	90	10
NEW	-	CHA	-9.4220	8.3190	3.6470	2.1140	0.2847	0	-1.199	-4.7590	6.6900	0	-	-
HAR	-	JW	0	0	0	0	0.0052	0	-0.0026	0	0	0	-	-
KIN	-	JW	0	0	0	0	0	0	0	0	0	-2.5260	-	-
LED	-	JW	0	0	0	0	0	0	0	0	0	0	-	-
LSR	-	JW	-0.9995	0.0942	0.3200	0	0.0104	-0.0045	0	0	0	-1.6850	-	-
MER	-	JW	-0.2291	0.0818	0	0.0540	0	-0.0235	0	-0.0879	0	0	-	-
NEW	-	JW	-0.1404	0.0851	0	0.0314	0	-0.0137	0	-0.0685	0	0	-	-
WC22	-	JW	0	0	0	0	0.0090	0	-0.0045	0	0	0	-	-
LAN	MER	JW	0.2168	0.0857	0	0	0	0	0	0	0	0	18	82
POL	MER	JW	0	0	0	0	0	0	0	0	0	0	38	62
BRO	MER	JW	0	0	0	0	0	0	0	0	0	0	54	46
HOL	MER	JW	0	0	0.0656	0	0	0	0	0	0	0	62	38
SUT	MER	JW	0	0	0	0	0	0	0	0	0	0	58	42
UBR1	LSR	JW	-0.1314	0	0.1576	0	0	0	0	0	0	0	30	70
WAR	MER	JW	0	0.0533	0.0621	0	0	0	0	0	0	0	41	59
WC21	MER	JW	0	0.0544	0.0772	0	0	0	0	0	0	0	25	75

Table 13. Optimized mixing models from Aquachem, modeling mixing between cave conduits A and B to reach measured chemistry at the spring outlet.

Element	JW (A2)	JW (B1)	JW (ledge) modeled	JW (ledge) actual
Na	7.7	7.2	7.6	7.1
K	1.1	1.1	1.1	1.1
Ca	89.2	90.0	89.3	90.2
Mg	21.1	20.2	20.9	19.7
Cl	13.0	13.0	13.0	12.9
HCO_3	302.5	320.0	305.3	305.3
SO_4	22.0	25.3	22.5	22.3
Percentage of solution in mix	84.0	16.0		

Element	JW (A2)	JW (B1)	JW (ledge) modeled	JW (ledge) actual
Na	7.7	7.2	7.6	7.1
HCO_3	302.5	320.0	305.3	305.3
SO_4	22.0	25.3	22.5	22.3
NO_3	2.6	2.3	2.5	2.3
Percentage of solution in mix	84.0	16.0		

Table 14. Summary of mass transfer results calculated with forward models. All values are in mmol/kg. Positive indicates dissolution, negative indicates precipitation.

		Calculated mass transfers				Percent difference between modeled and actual element concentrations					
Site (start)	Site (end)	Calcite	Anhydrite	Dolomite	$CO_2(g)$	Ca	Cl	Mg	SO_4	pH	HCO_3
Sonora	NEW	0.0147	-0.0043	0.0097	0.0336	-2	0	-6	1	0	-6
Sonora	VAS	-0.0554	0.1614	0.0453	0.0410	-2	0	-1	3	0	1

Figures

Figure 1. Map showing the study area. The blue shaded area indicates the extent of the Trinity aquifer.

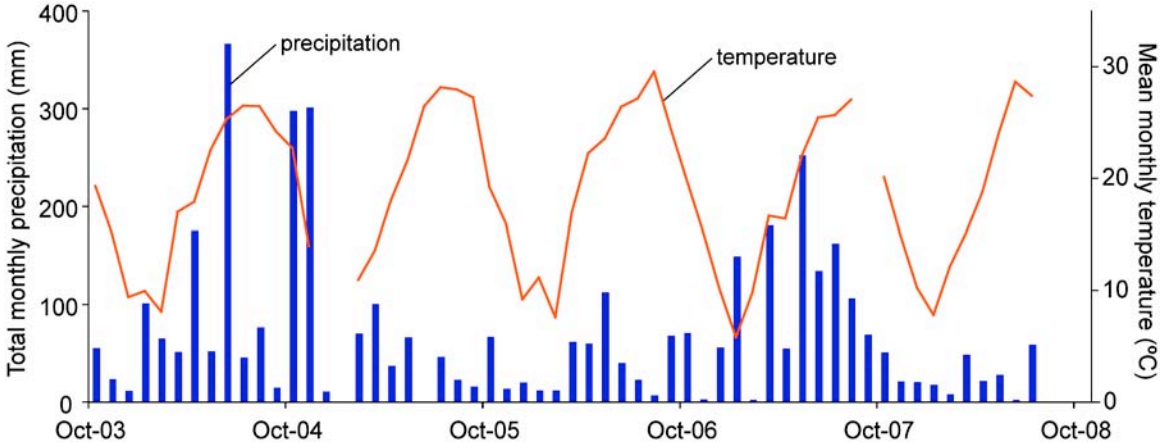

Figure 2. Monthly total precipitation and average temperature in Blanco, Texas from October 2003–July 2008 (NCDC 2008).

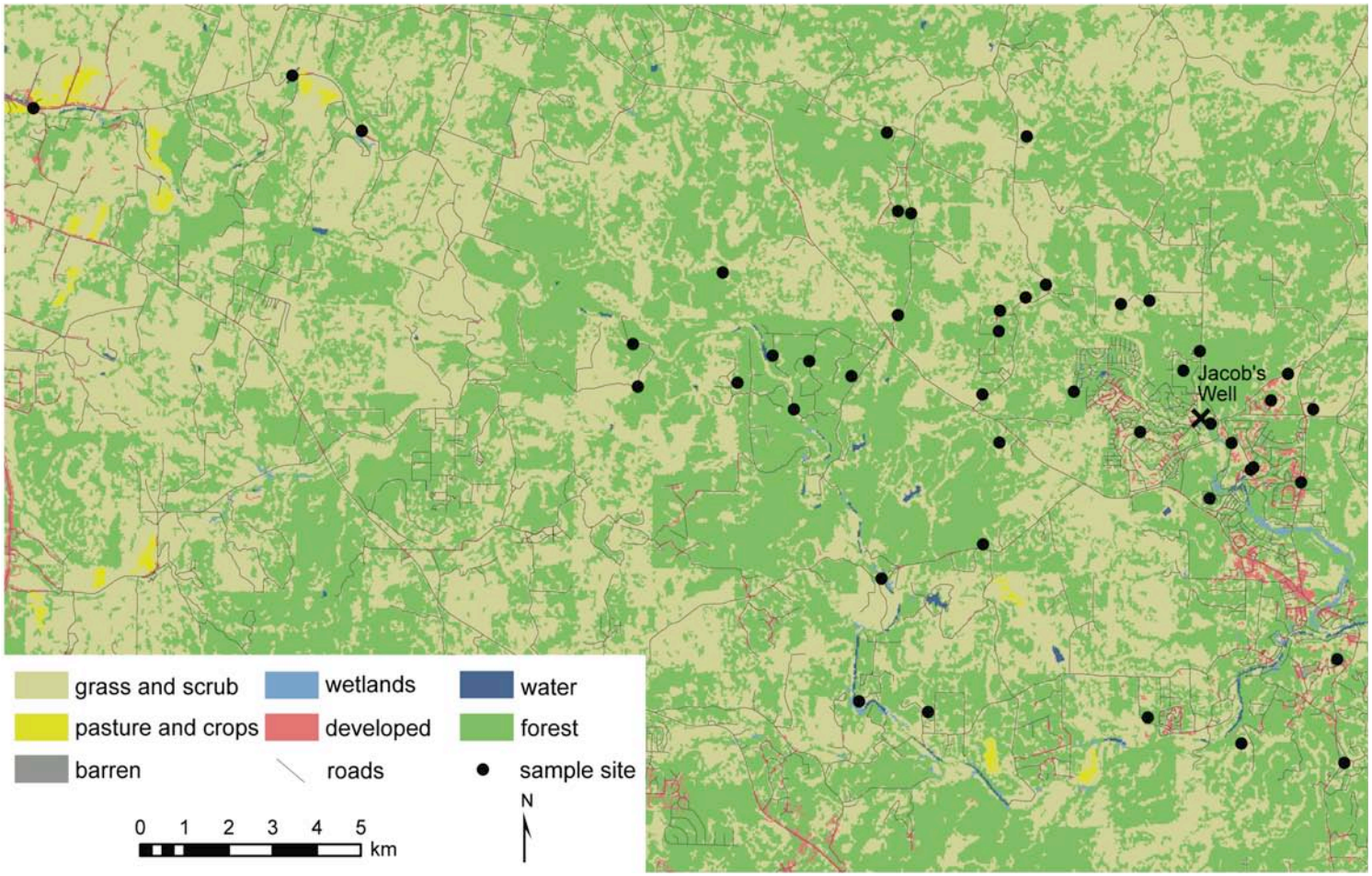

Figure 3. Map showing land use in the study area in 2001 (USGS 2003, Homer *et al*. 2004, TNRIS 2006).

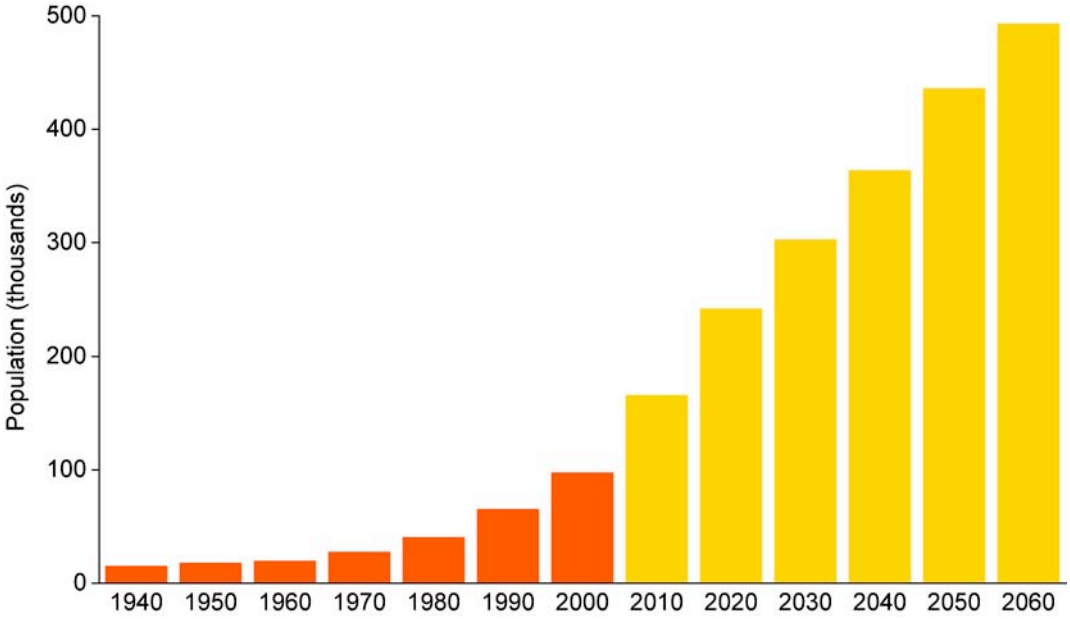

Figure 4. Historical (1940–2000) and projected (2010–2060) population in Hays County, Texas (USCB 1993, 2003).

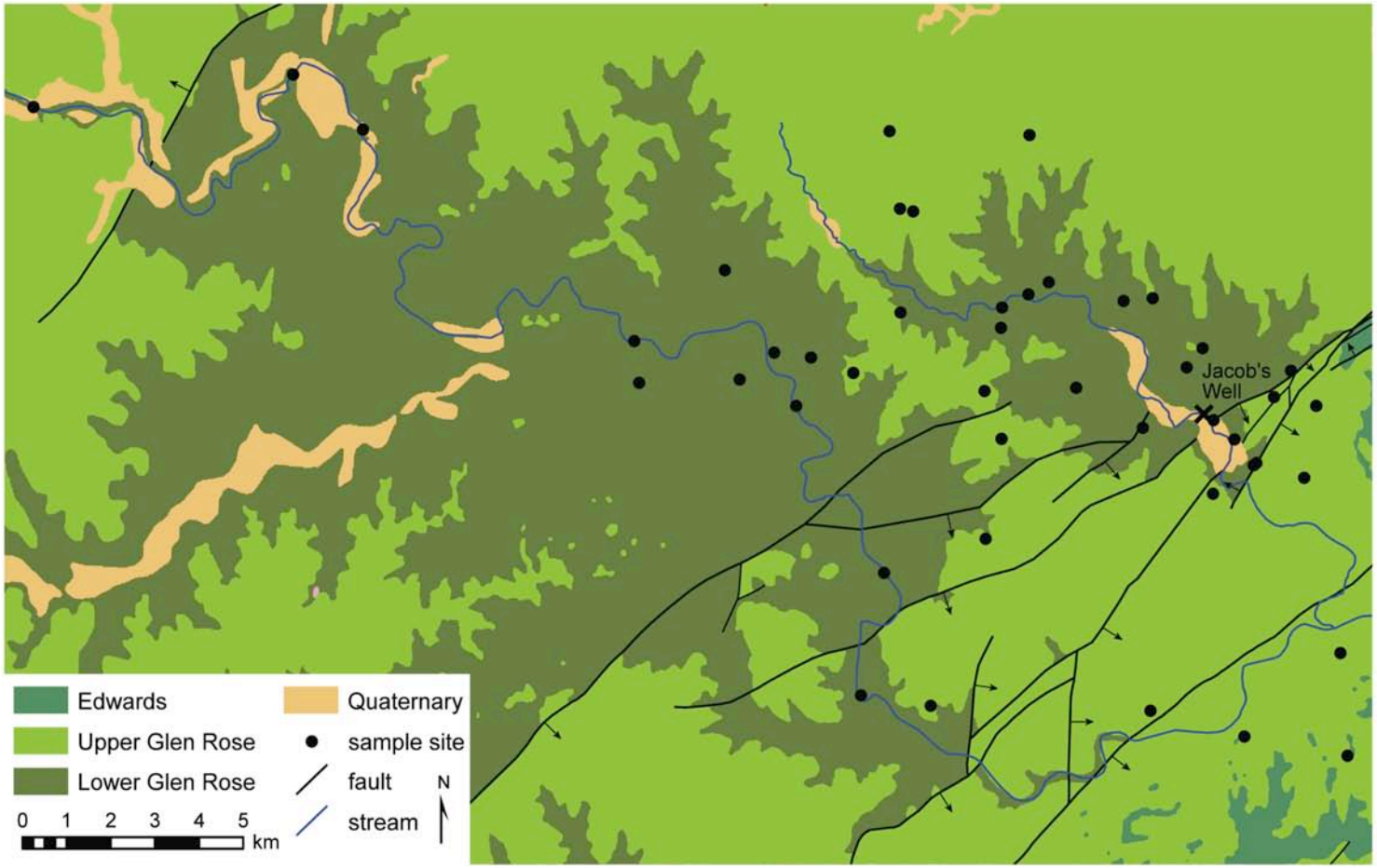

Figure 5. Map showing the general geology of the study area (USGS undated) and locations of water samples.

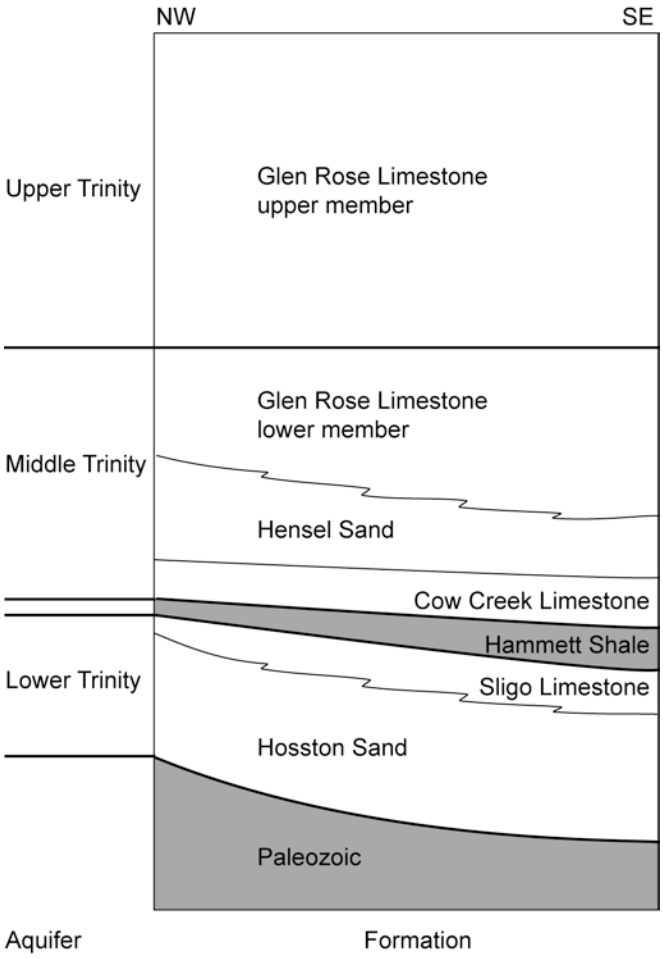

Figure 6. Diagram of the stratigraphy and hydrostratigraphy of the study area (after Sticklin *et al*. 1971, Ashworth 1983).

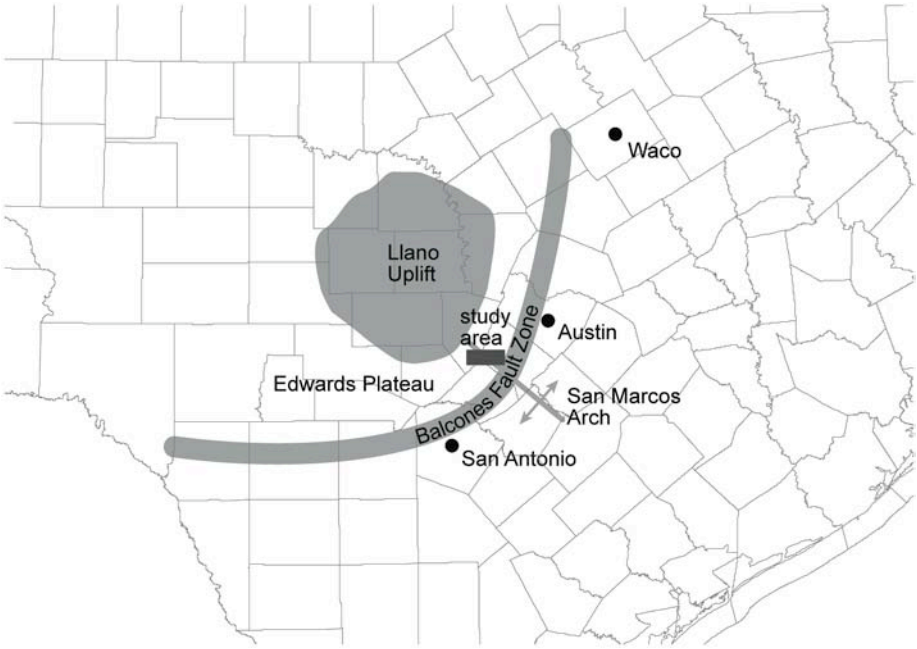

Figure 7. Map indicating major structural features in and near the study area (after DeCook 1960, Ashworth 1983, Barker and Ardis 1992).

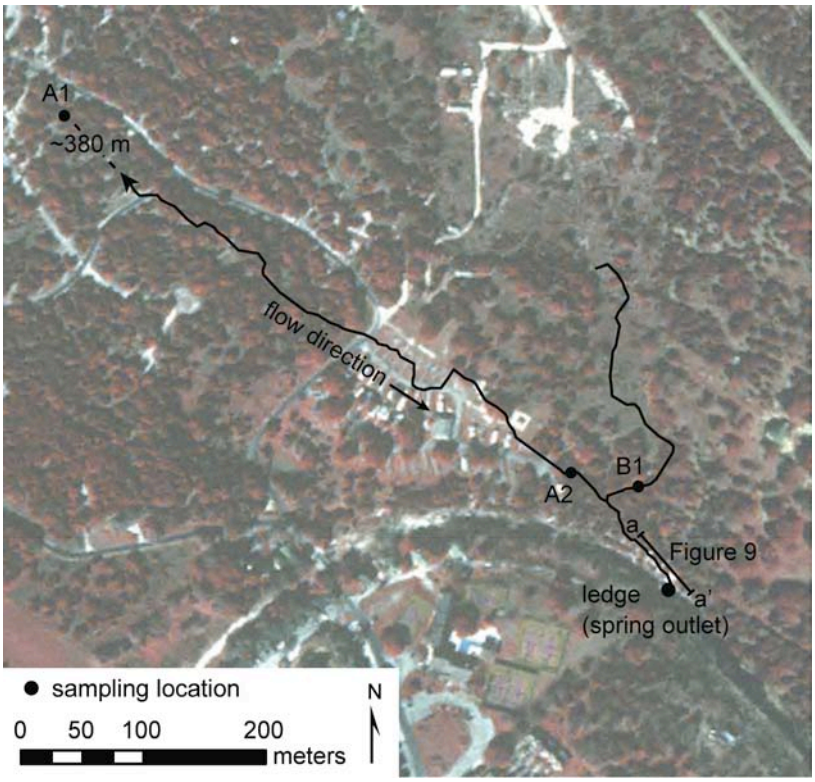

Figure 8. Mapped conduit passages leading to Jacob's Well spring and approximate locations of spring and cave samples (after Gary 2007, USDA/FSA 2003). Sample location A2 is located about 380 m beyond the end of the mapped portion of the passageway.

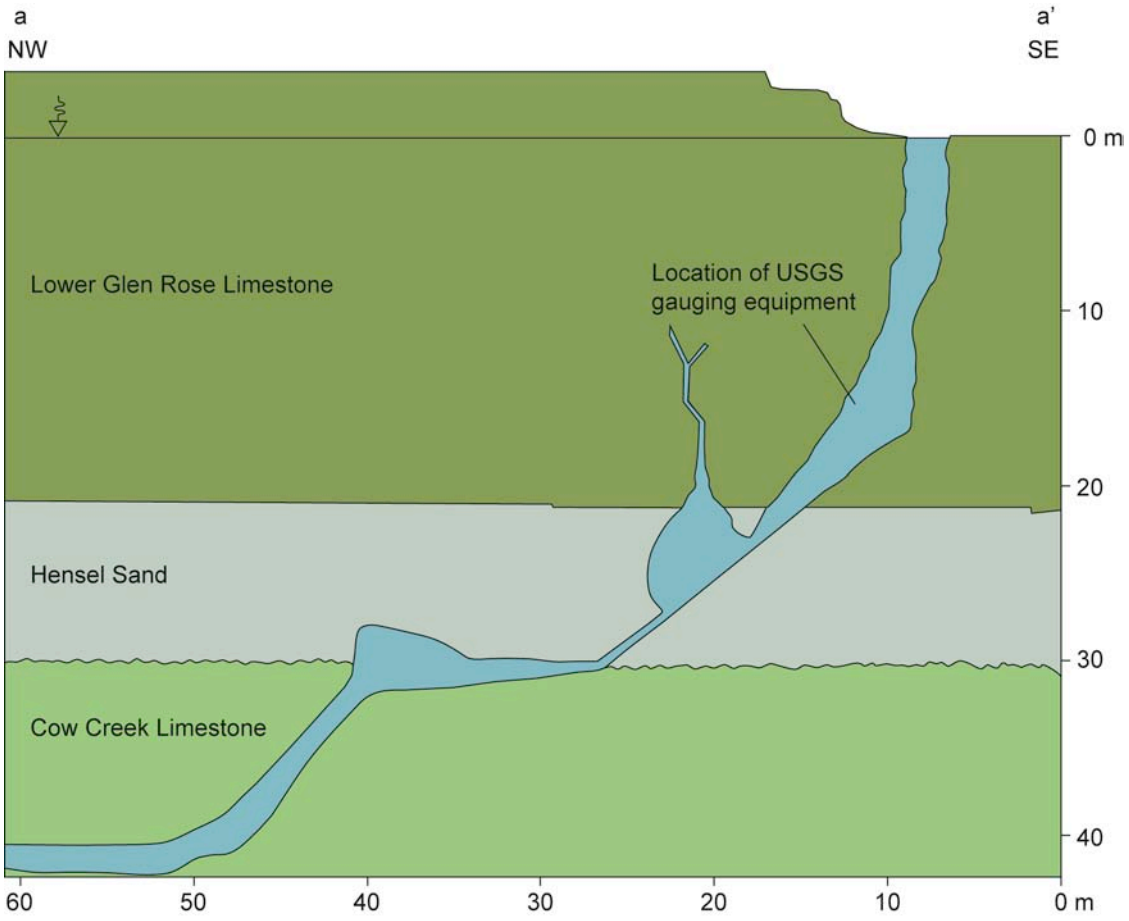

Figure 9. Cross-sectional diagram of Jacob's Well (modified from Broun *et al*. in press).

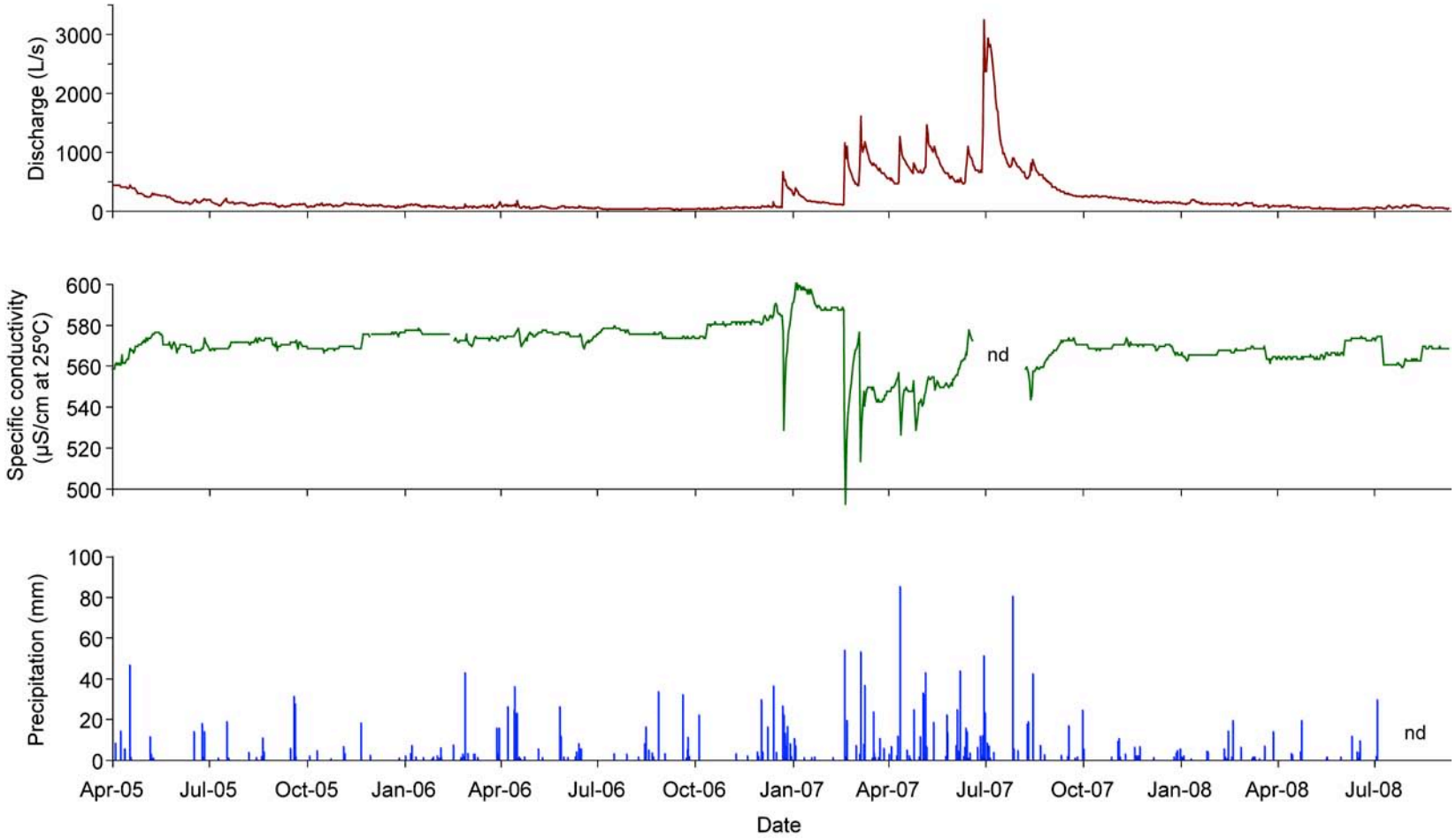

Figure 10. Daily average discharge and specific conductivity for the period of record at Jacob's Well (USGS gauge 08170990) and total daily precipitation at Blanco, Texas (NCDC 2008, USGS 2008). nd=no data.

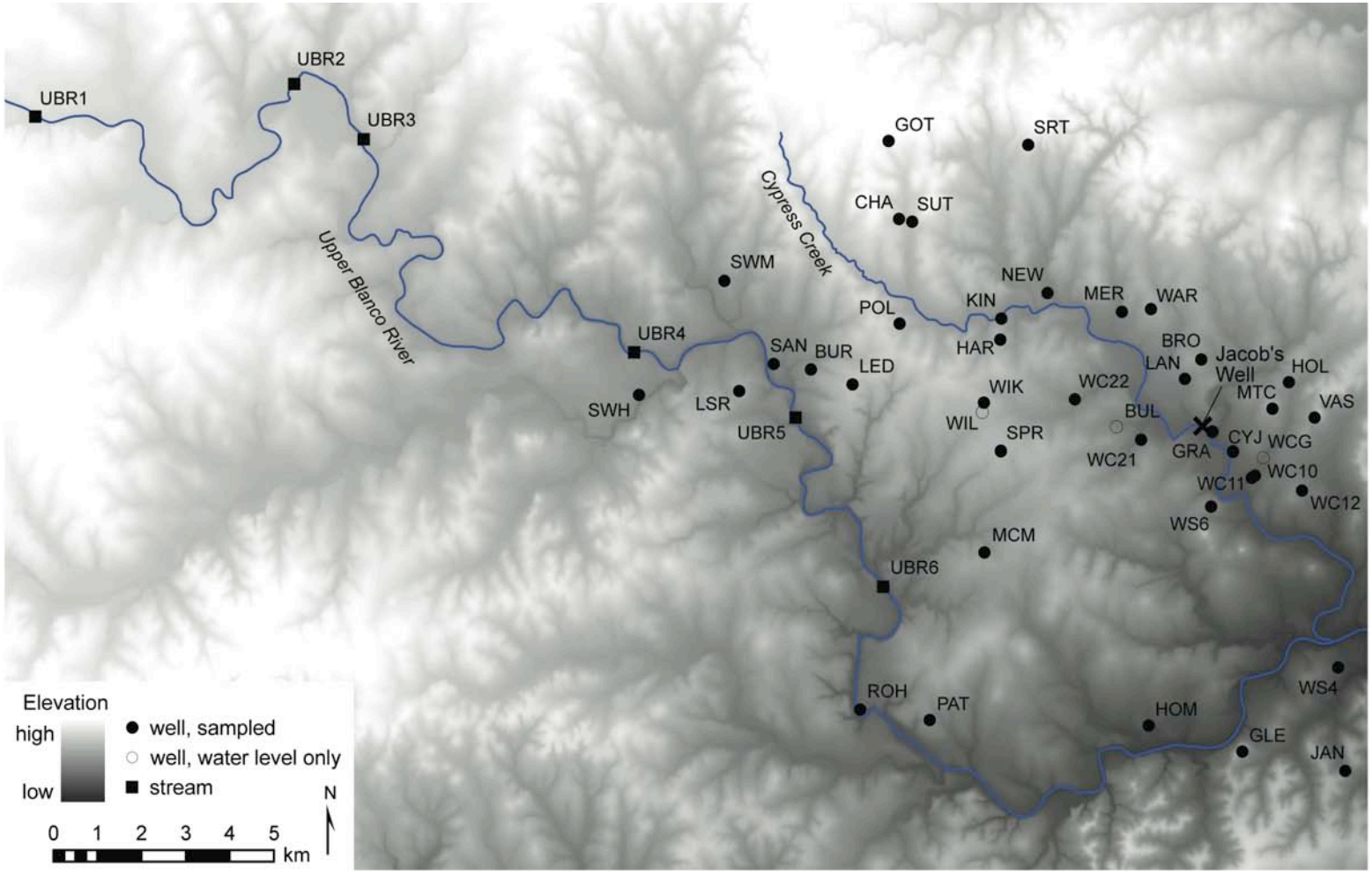

Figure 11. Map showing elevation and drainages in the study area and locations of water sample and water level measurements (USDA/NRCS 2000). Elevations range from about 250 to 470 m amsl.

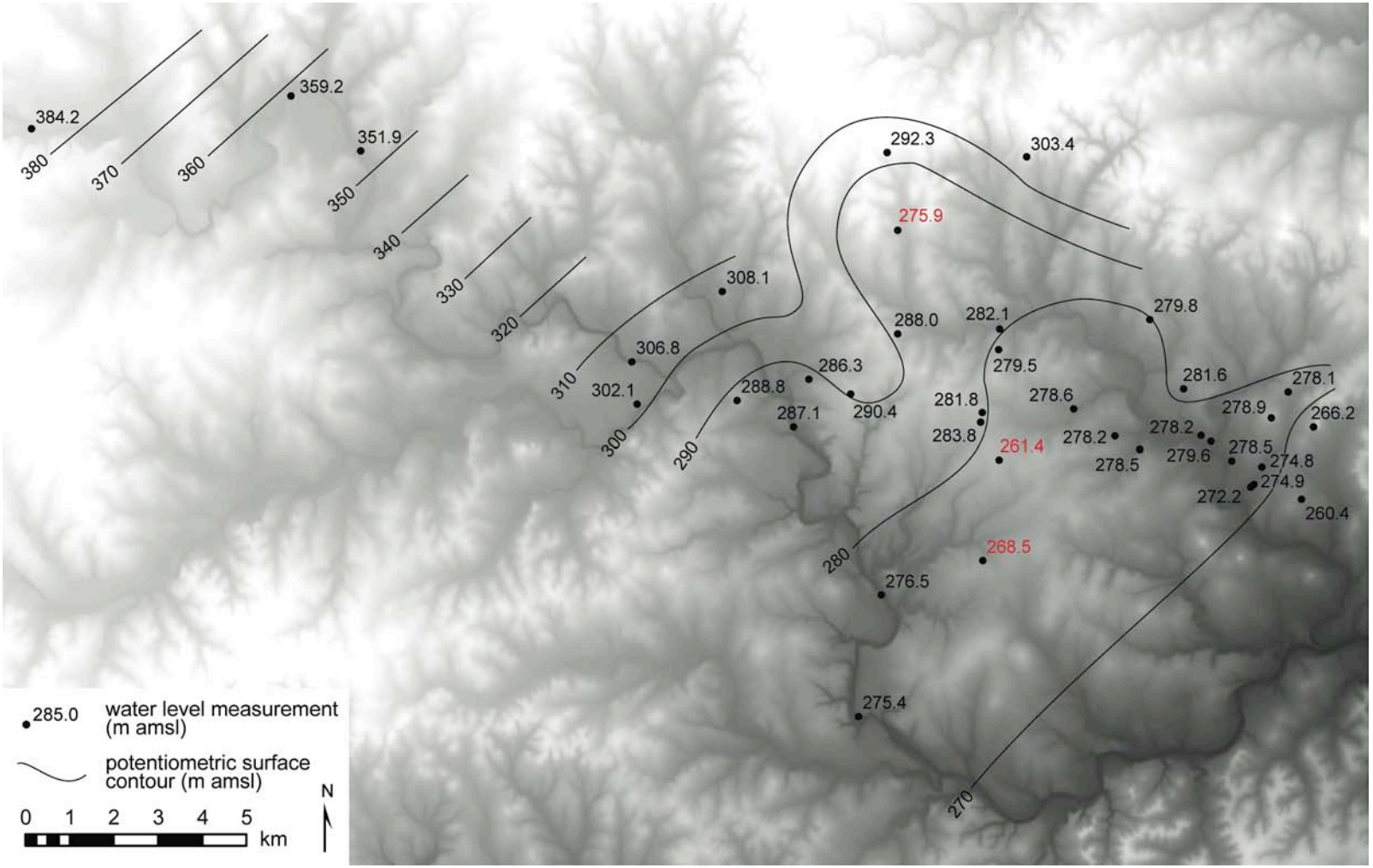

Figure 12. Map showing measured water levels and contours of the approximate water level elevation in the study area. Elevations marked in red were not used to draw contours (see discussion in text).

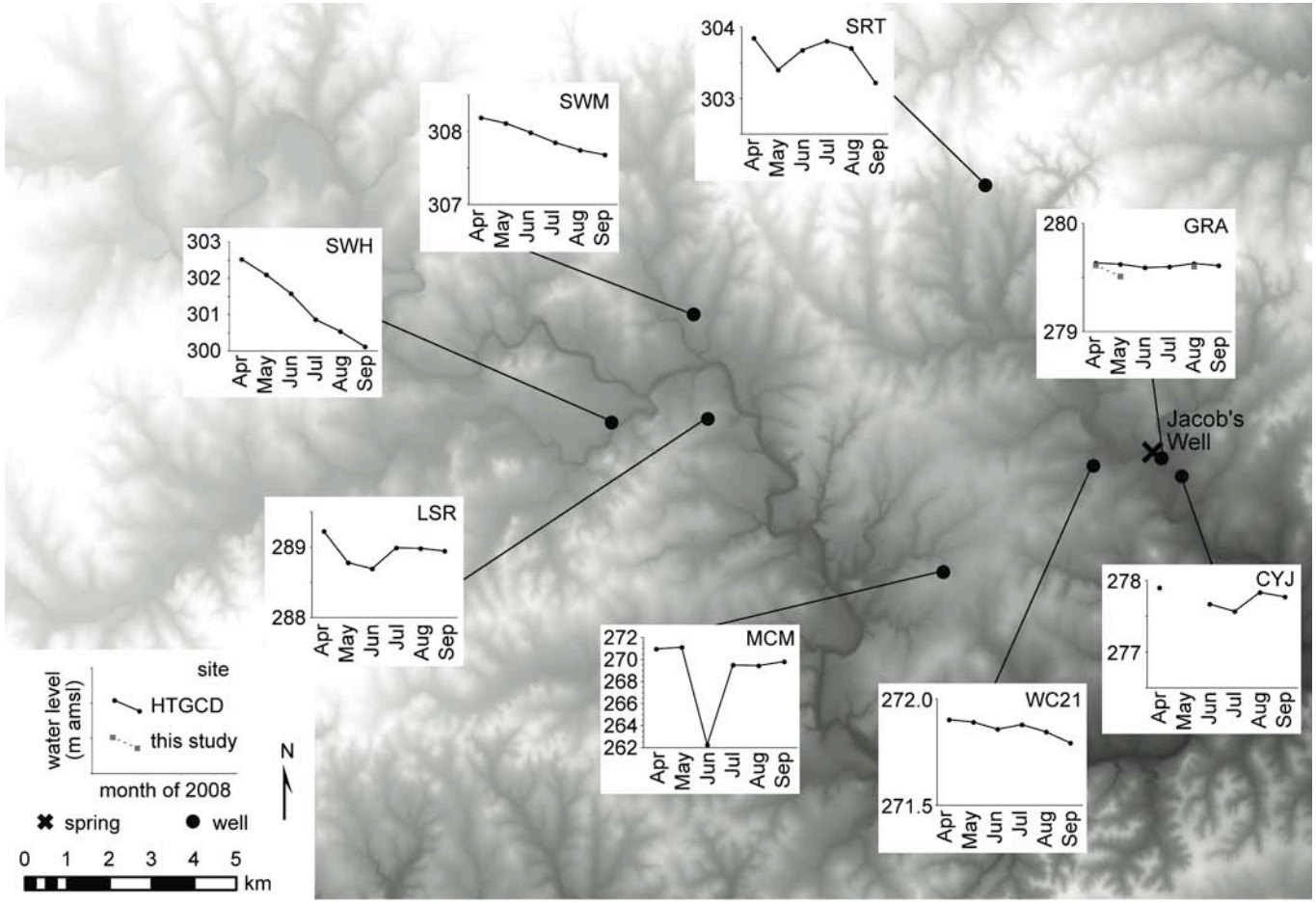

Figure 13. Map showing hydrographs for study wells with more than two water level measurements available for the study period (HTGCD 2008).

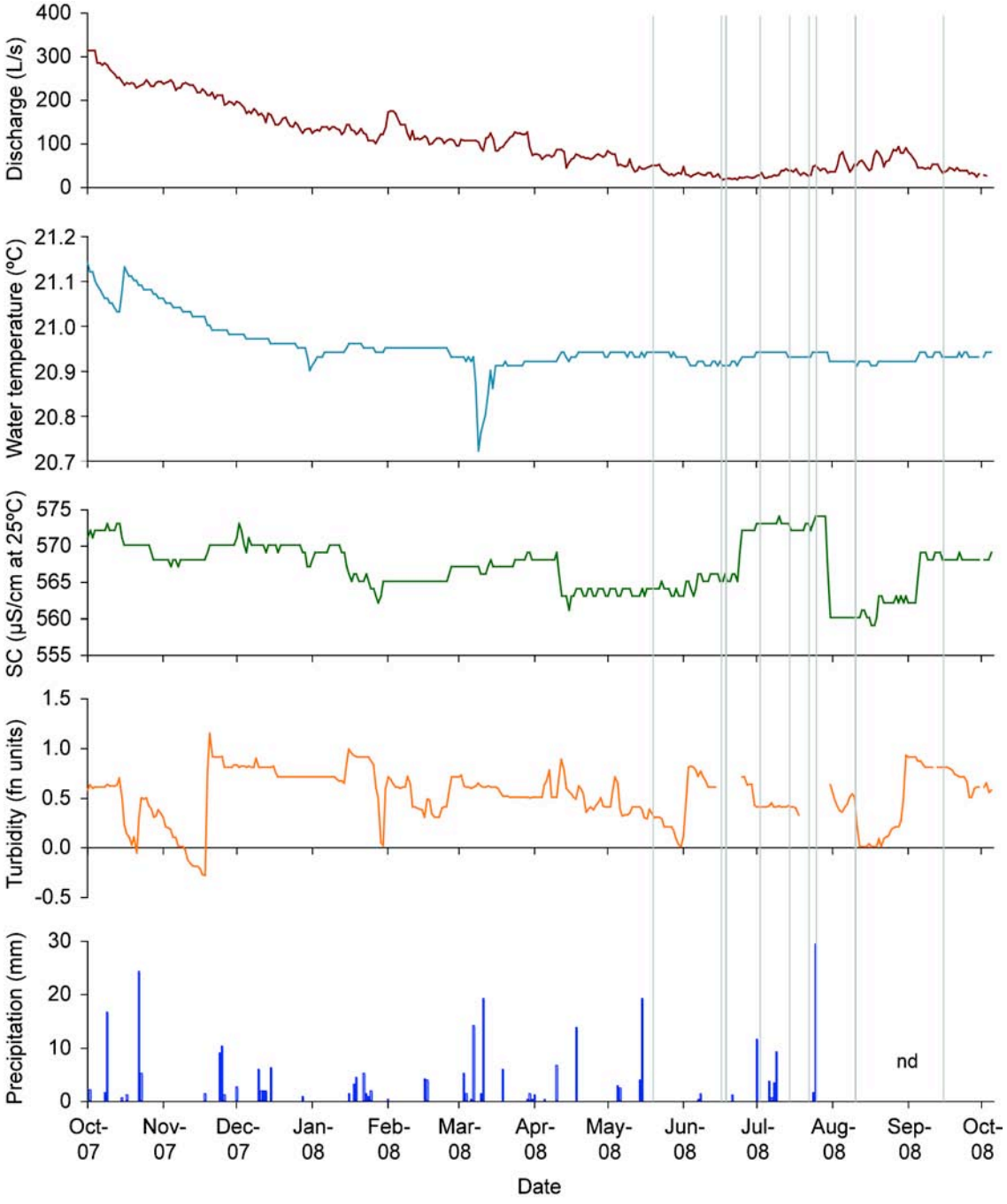

Figure 14. Daily mean measured parameters at Jacob's Well and daily total precipitation in Blanco, Texas over the study period (NCDC 2008, USGS 2008). fn units=formazin nephelometric units, nd=no data, SC=specific conductivity. Gray lines indicate days on which samples were taken at the spring.

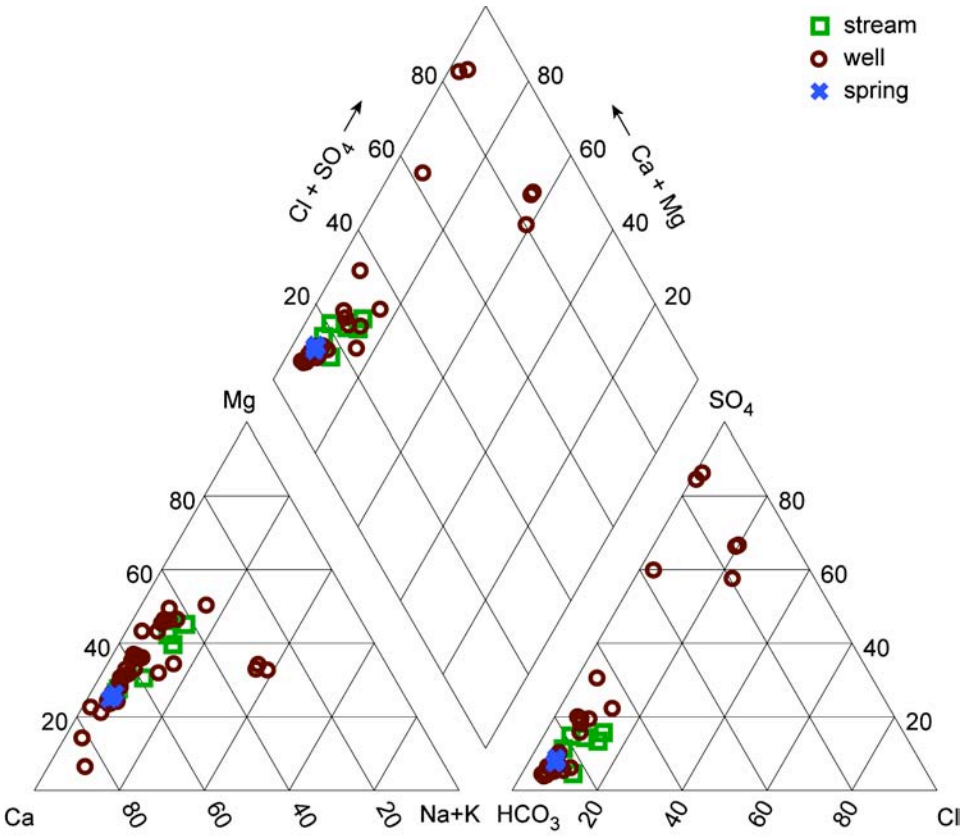

Figure 15. Piper diagram showing major ion geochemistry of study samples.

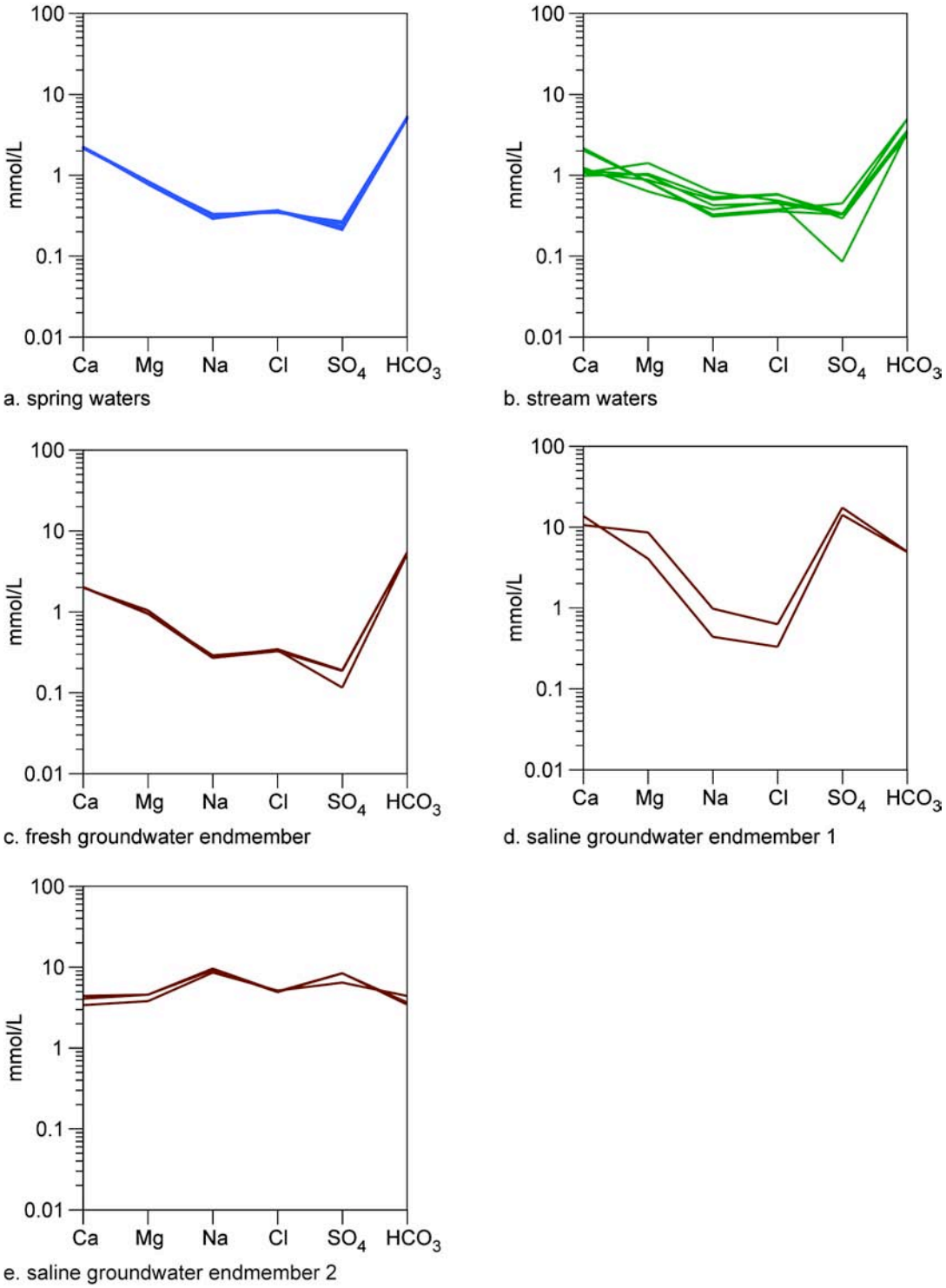

Figure 16. Schoeller diagrams showing the concentrations of major cations and anions in spring, stream, and surface waters in the study area.

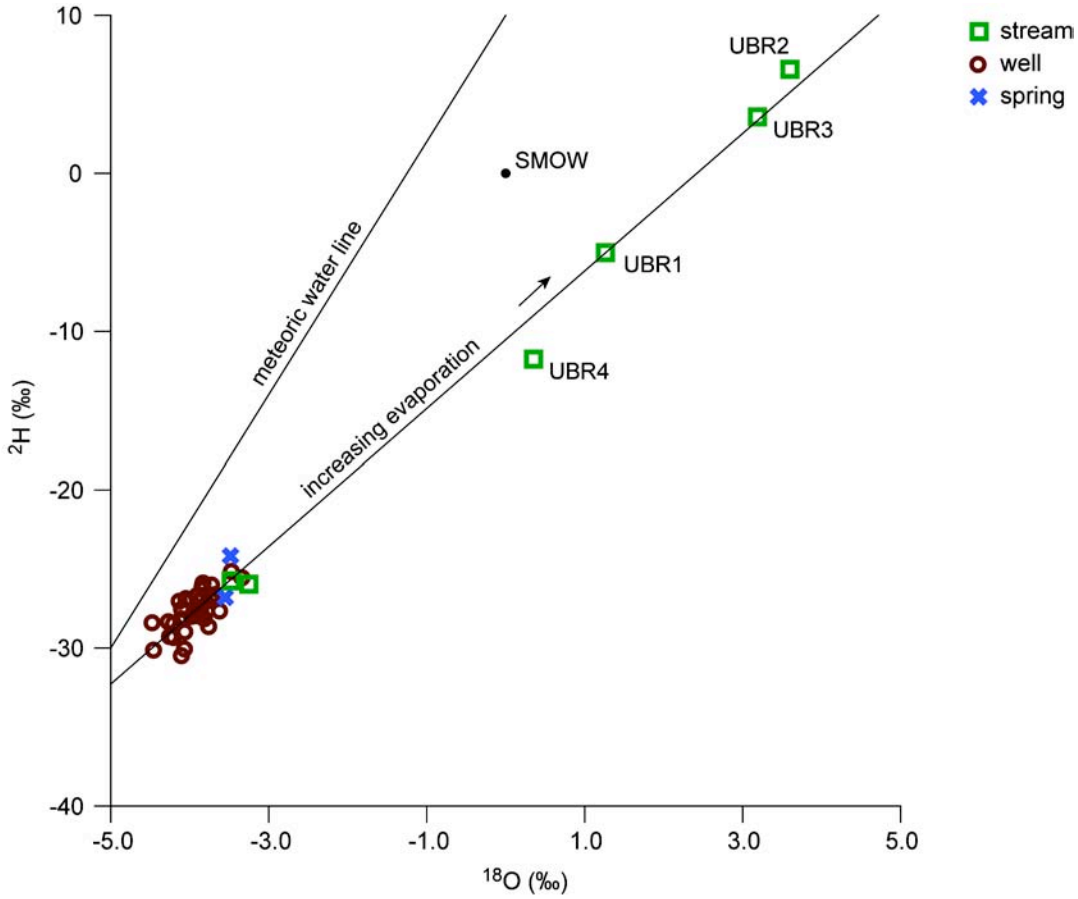

Figure 17. Plot of oxygen isotope ratios relative to standard mean ocean water (SMOW).

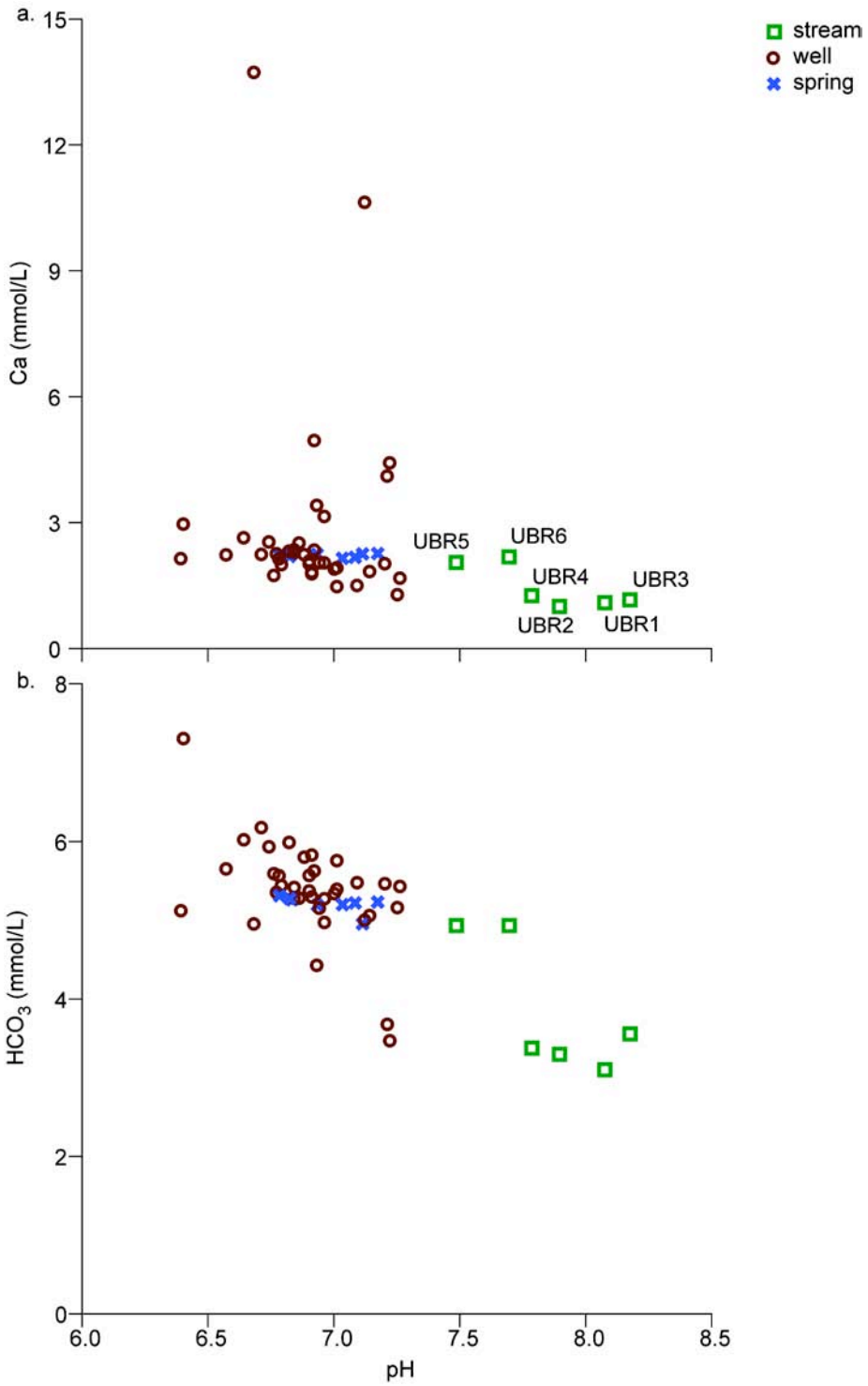

Figure 18. Plot of pH with (a) Ca and (b) HCO_3 in the study samples.

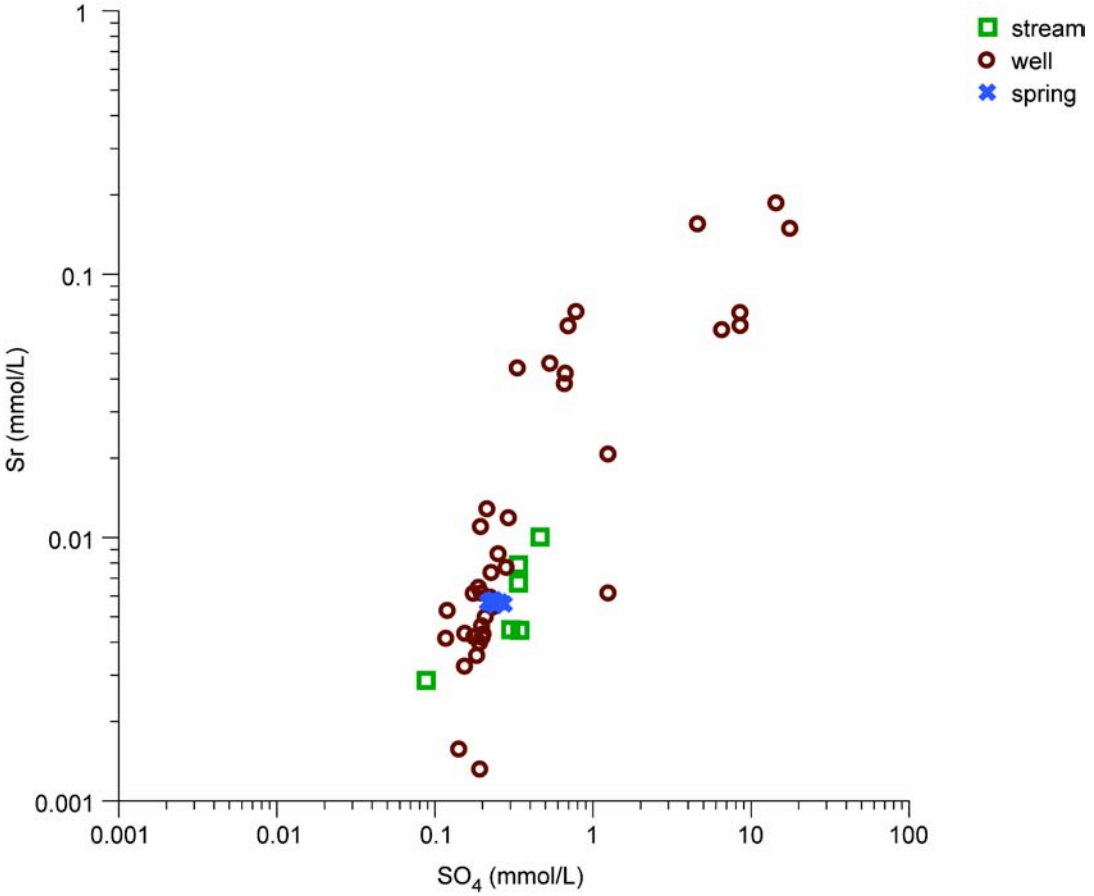

Figure 19. Plot of SO_4 and Sr concentrations in study samples.

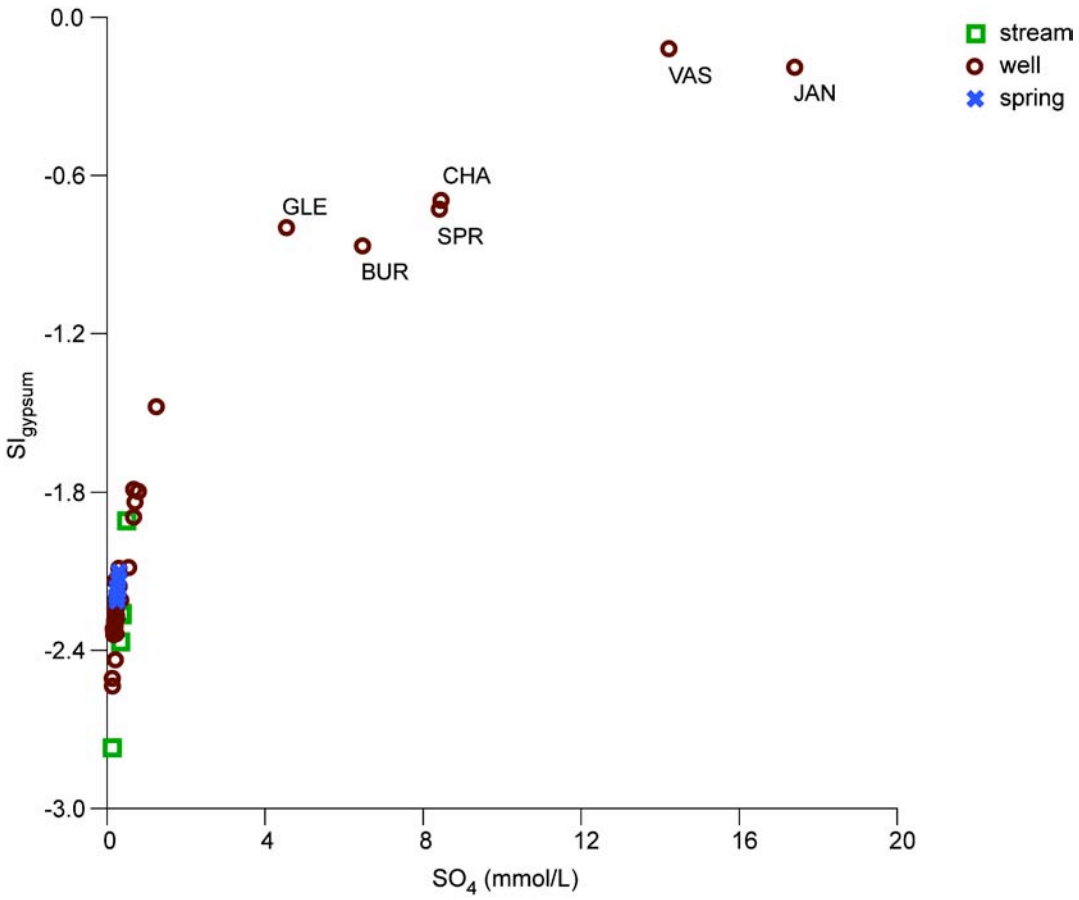

Figure 20. Plot of SO_4 concentrations and gypsum saturation indices (SI_{gypsum}) of study samples.

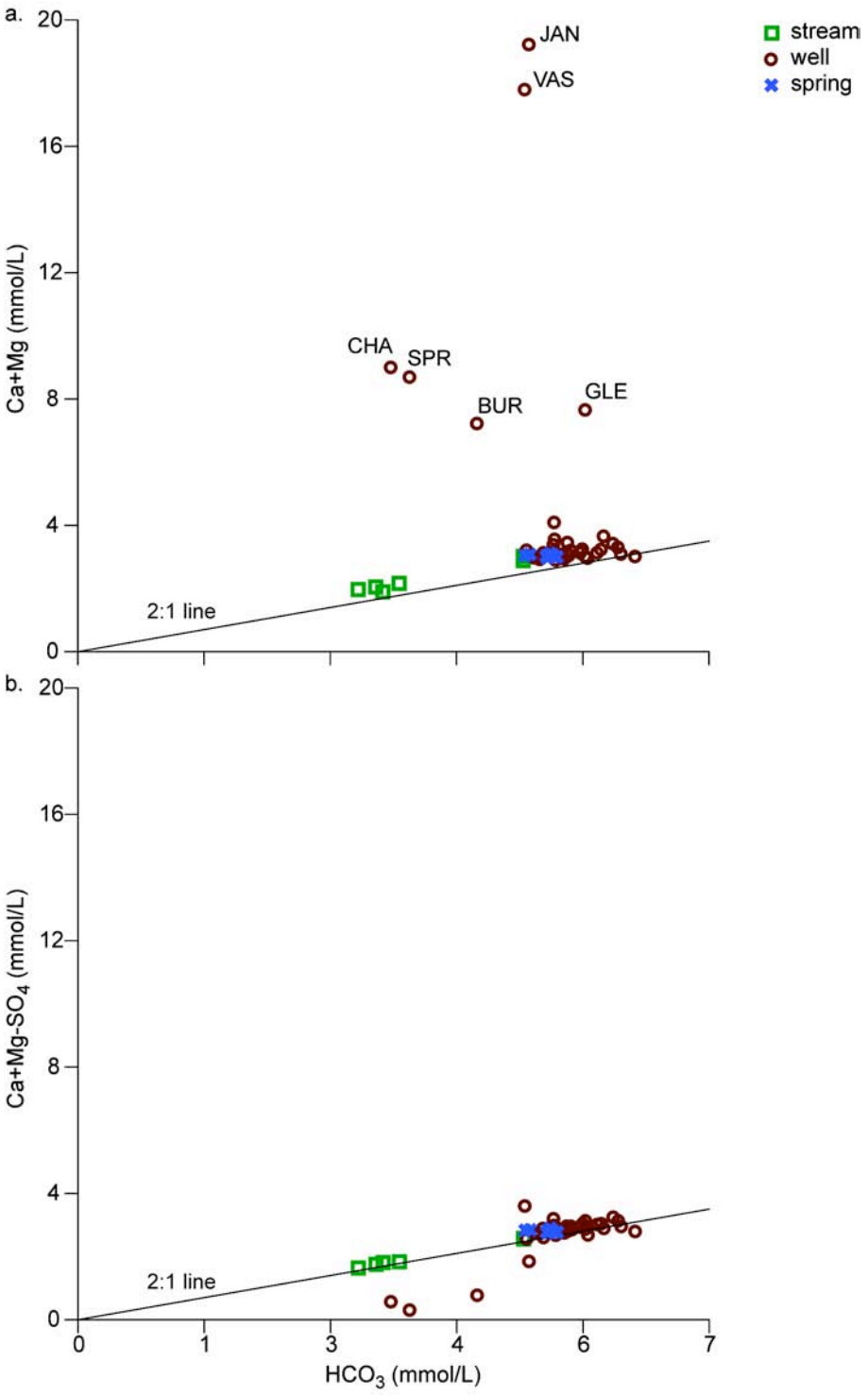

Figure 21. (a) Plot of HCO_3 and Ca+Mg concentrations in study samples. (b) Plot of HCO_3 and Ca+Mvg-SO_4 concentrations in study samples.

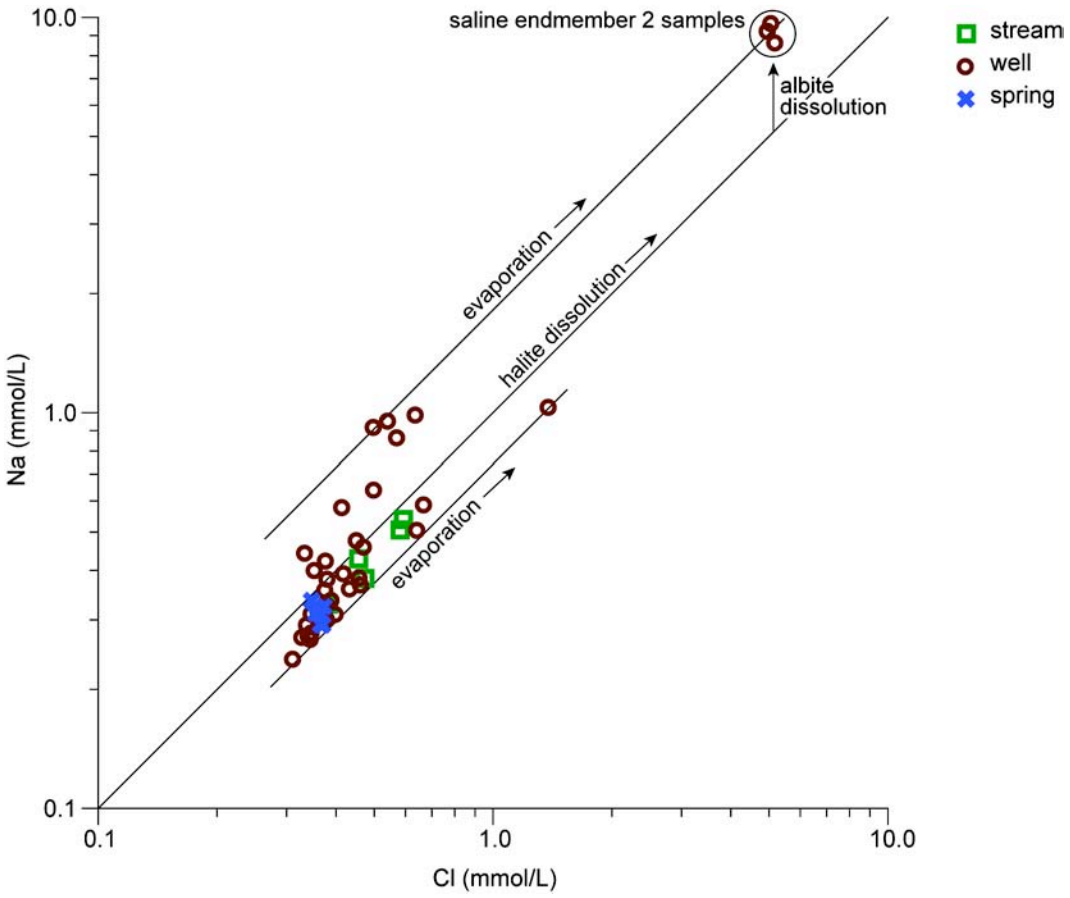

Figure 22. Plot of Cl and Na concentrations in study samples.

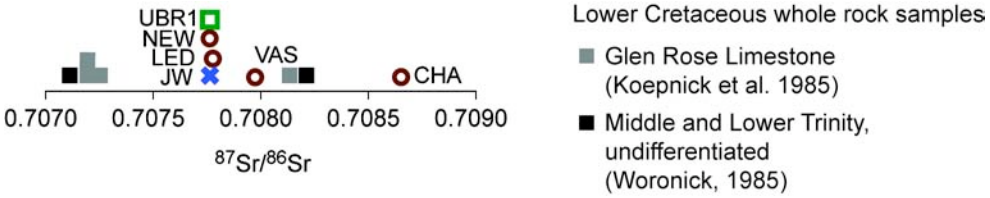

Figure 23. Graph of measured $^{87}Sr/^{86}Sr$ ratios in study samples representing chemical endmembers and in Lower Cretaceous host rocks.

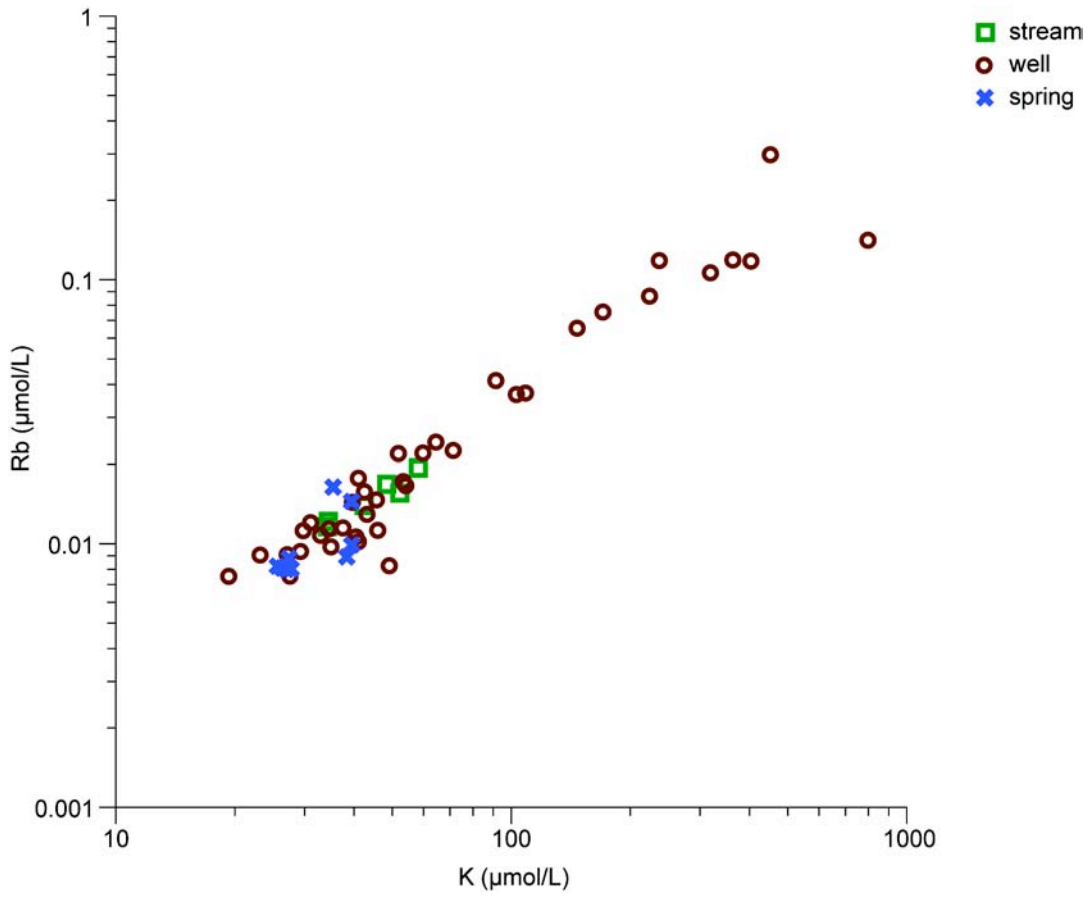

Figure 24. Plot of K and Rb in study samples.

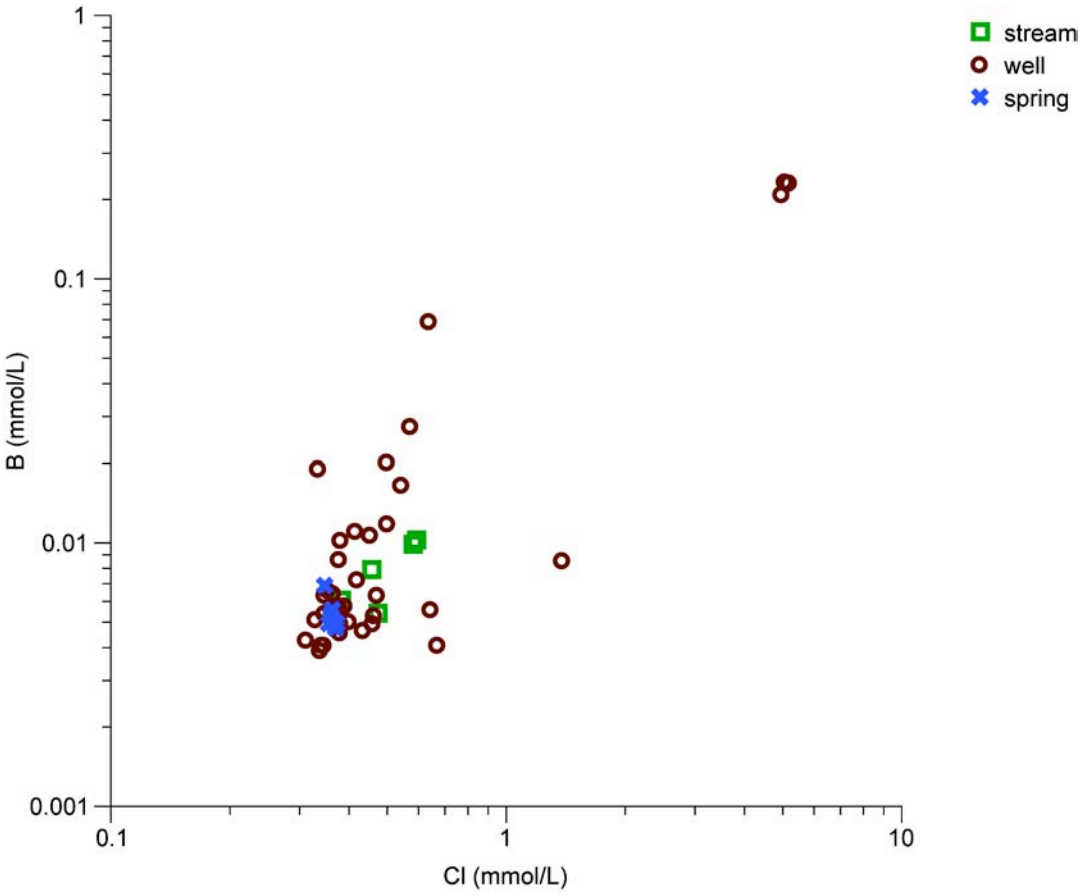

Figure 25. Plot of Cl and B concentrations in study samples.

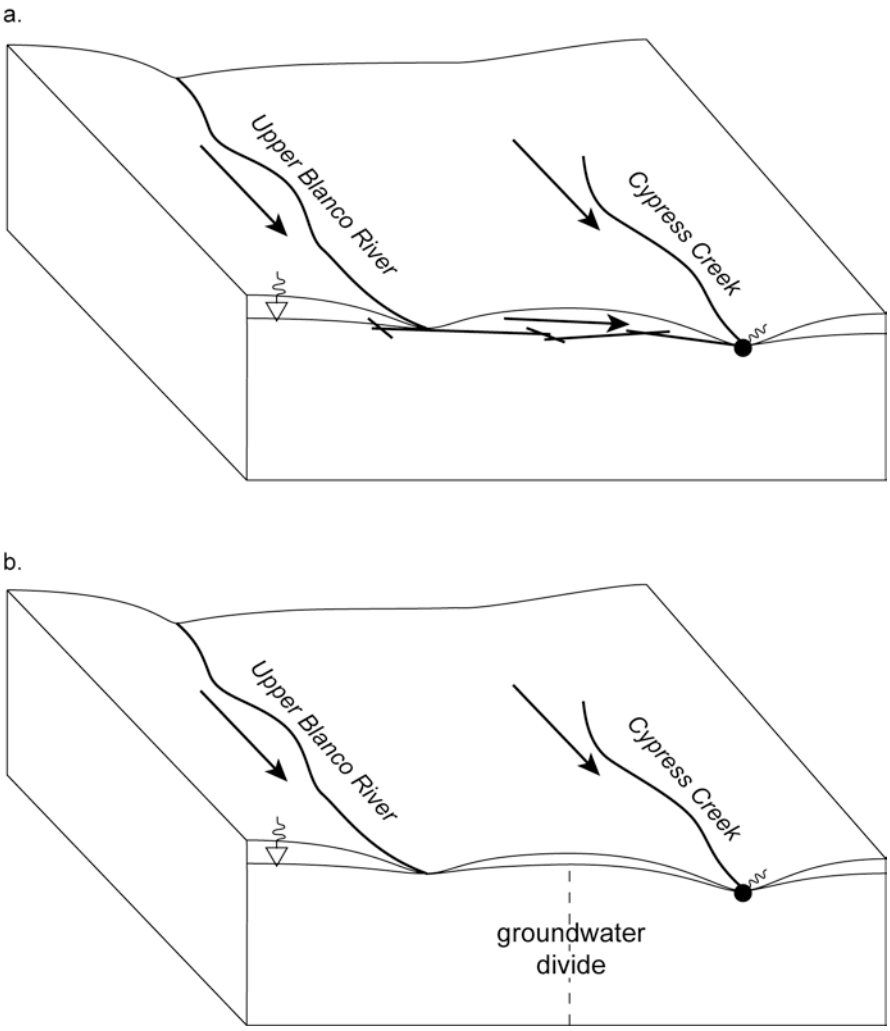

Figure 26. Diagrams showing two possible models for groundwater flow in the vicinity of Jacob's Well.

References

Abbott, P.L., 1977. Effect of Balcones faults on groundwater movement, south central Texas. Texas Journal of Science, 29(1–2): 5–14.

Adkins, W.S., 1932. Part 2—The Mesozoic systems in Texas. In: E.H. Sellards, W.S. Adkins, F.B. Plummer, The Geology of Texas, Volume 1—Stratigraphy. The University of Texas, Austin, Texas, pp. 239–518.

Anderson, C.W., 2008. Turbidity. In: U.S. Geological Survey (Editor), National field manual for the collection of water-quality data. Handbooks for water-resources investigations, Book 9, var. pag.

APHA (American Public Health Association), American Water Works Association and Water Pollution Control Federation, 1976. Standard methods for the examination of water and wastewater. American Public Health Association, Washington, DC, 1193 pp.

Appelo, C.A.J. and Postma, D., 2005. Geochemistry, groundwater and pollution. A.A. Balkema Publishers, Philadelphia, PA, 649 pp.

Ardis, A.F. and Barker, R.A., 1993. Historical saturated thickness of the Edwards-Trinity aquifer system and selected contiguous hydraulically connected units, west-central Texas. U.S. Geological Survey Water-Resources Investigations Report 92-4125, 2 sheets.

Ashworth, J.B., 1983. Ground-water availability of the Lower Cretaceous formations in the Hill Country of south-central Texas. Texas Department of Water Resources Report 273, 65 pp.

Atkinson, T.C., 1977. Diffuse flow and conduit flow in limestone terrain in the Mendip Hills, Somerset (Great Britain). Journal of Hydrology, 35: 93–110.

Back, W. and Hanshaw, B.B., 1971. Rates of physical and chemical processes in a carbonate aquifer. In: R.F. Gould (Editor), Nonequilibrium systems in natural water chemistry. Advances in Chemistry Series 106. American Chemical Society, Washington, D.C., pp. 77–93.

Back, W., Hanshaw, B.B., Plummer, L.N., Rahn, P.H., Rightmire, C.T. and Rubin, M., 1983. Process and rate of dedolomitization—Mass transfer and ^{14}C dating in a regional carbonate aquifer. Geological Society of America Bulletin, 94: 1415–1429.

Bakalowicz, M., Blavoux, B. and Mangin, A., 1974. Apports du traçage isotopique naturel a la connaissance du fonctionnement d'un systeme karstique—Teneurs en oxygene-18 de trois systemes des Pyrenees, France. Journal of Hydrology, 23: 141–158.

Banner, J.L., Musgrove, M. and Capo, R.C., 1994. Tracing groundwater evolution in a limestone aquifer using Sr Isotopes—Effects of multiple sources of dissolved ions and mineral-solution reactions. Geology, 22(8): 687–690.

Barbieri, M., Boschetti, T., Petitta, M. and Tallini, M., 2005. Stable isotope (^{2}H, ^{18}O and $^{87}Sr/^{86}Sr$) and hydrochemistry monitoring for groundwater hydrodynamics analysis in a karst aquifer (Gran Sasso, Central Italy). Applied Geochemistry, 20(11): 2063–2081.

Barker, R.A. and Ardis, A.F., 1992. Configuration of the base of the Edwards-Trinity aquifer system and hydrogeology of the underlying pre-Cretaceous rocks, west-central Texas. U.S. Geological Survey Water-Resources Investigations Report 91-4071, 25 pp.

Barker, R.A., Bush, P.W. and E. T. Baker, J., 1994. Geologic history and hydrogeologic setting of the Edwards-Trinity aquifer system, west-central Texas. U.S. Geological Survey Water-Resources Investigations Report 94-4039, 51 pp.

Barnes, V.E., 1948. Ouachita facies in central Texas. Bureau of Economic Geology—Report of Investigations, 2: 12 pp.

Bickle, M.J., Chapman, H.J., Bunbury, J., Harris, N.B.W., Fairchild, I.J., Ahmad, T. and Pomies, C., 2005. Relative contributions of silicate and carbonate rocks to riverine Sr fluxes in the headwaters of the Ganges. Geochimica Et Cosmochimica Acta, 69(9): 2221–2240.

Birk, S., Liedl, R. and Sauter, M., 2004. Identification of localised recharge and conduit flow by combined analysis of hydraulic and physico-chemical spring responses. Journal of Hydrology, 286(1–4): 179–193.

Bishop, P.K., Smalley, P.C., Emery, D. and Dickson, J.A.D., 1994. Strontium isotopes as indicators of the dissolving phase in a carbonate aquifer—Implications for ^{14}C dating of groundwater. Journal of Hydrology, 154: 301–321.

Broun, A.S., Llado, L., Wierman, D.A. and Backus, A.A., in press. The geology of the Cypress Creek watershed, Wimberley area, Texas. Austin Geological Society Bulletin, 3.

Brune, G., 1981. Springs of Texas, 1. Branch-Smith, Inc., Fort Worth, Texas, 566 pp.

Bush, P.W., Ardis, A.F. and Wynn, K.H., 1993. Historical potentiometric surface of the Edwards-Trinity aquifer system and contiguous hydraulically connected units, west-central Texas. U.S. Geological Survey Water-Resources Investigations Report 92-4055, 3 sheets.

Bush, P.W., Ardis, A.F., Fahlquist, L., Ging, P.B., Hornig, C.E. and Lanning-Rush, J., 2000. Water quality in south-central Texas, Texas, 1996–98, U.S. Geological Survey Circular 1212, 32 pp.

Craig, H., 1961a. Standard for reporting concentrations of deuterium and oxygen-18 in natural waters. Science, 133(3467): 1833–1834.

Craig, H., 1961b. Isotopic variations in meteoric waters. Science, 133(3465): 1702–1703.

Cuyler, R.H., 1931. Vegetation as an indicator of geologic formations. AAPG Bulletin, 15: 67–78.

DeCook, K.J., 1960. Geology and ground-water resources of Hays County, Texas. Texas Board of Water Engineers Bulletin 6004, 157 pp.

Deines, P., Langmuir, D. and Harmon, R.S., 1974. Stable carbon isotope ratios and the existence of a gas phase in the evolution of carbonate ground waters. Geochimica et Cosmochimica Acta, 38(7): 1147–1164.

Desmarais, K. and Rojstaczer, S., 2002. Inferring source waters from measurements of carbonate spring response to storms. Journal of Hydrology, 260(1–4): 118–134.

Doctor, D.H. Alexander, E.C., Jr., Petric, M., Kogovsek, J., Urbanc, J., Lojen, S. and Stichler, W., 2006. Quantification of karst aquifer discharge components during storm events through end-member mixing analysis using natural chemistry and stable isotopes as tracers. Hydrogeology Journal, 14(7): 1171–1191.

Domenico, P.A. and Schwartz, F.W., 1990. Physical and chemical hydrogeology. John Wiley and Sons, New York, NY, 824 pp.

Dreiss, S.J., 1989. Regional scale transport in a karst aquifer 1. Component separation of spring flow hydrographs. Water Resources Research, 25(1): 117–125.

Engel, A.S., Stern, L.A. and Bennett, P.C., 2004. Microbial contributions to cave formation—New insights into sulfuric acid speleogenesis. Geology, 32(5): 369–372.

Fahlquist, L. and Ardis, A.F., 2004. Quality of water in the Trinity and Edwards aquifers, south-central Texas, 1996–1998. U.S. Geological Survey Scientific Investigations Report 2004-5201. 17 pp.

Faure, G., 1991. Principles and applications of inorganic geochemistry—A comprehensive textbook for geology students. MacMillan Publishing Company, New York, NY, 626 pp.

Faure, G. and Powell, J.L., 1972. Strontium isotope geology. Springer-Verlag, New York, NY, 188 pp.

Flawn, P.T., Goldstein, A., Jr., King, P.B. and Weaver, C.E., 1961. The Ouachita System. Bureau of Economic Geology Publication 6120, 401 pp.

Forgotson, J.M., Jr., 1957. Stratigraphy of Comanchean Cretaceous Trinity Group. AAPG Bulletin, 41(10): 2328–2363.

Franklyn, M.T., McNutt, R.H., Kamineni, D.C., Gascoyne, M. and Frape, S.K., 1991. Groundwater 87Sr/86Sr values in the Eye-Dashwa Lakes pluton, Canada—Evidence for plagioclase-water reaction. Chemical Geology (Isotope Geoscience Section), 86: 111–122.

Gary, M.O., 2007. Establishing temporal trends—The first two years of continuous monitoring at Jacob's Well spring, Woodcreek, Texas. Texas Commission for Environmental Quality, 15th National Nonpoint Source Monitoring Workshop, Austin, TX.

Grimshaw, T.W., 1970. Geology of the Wimberley area, Hays and Comal counties, Texas. M.A. Thesis, The University of Texas, Austin, Texas, 104 pp.

Hammond, W.W., Jr., 1984. Hydrogeology of the lower Glen Rose aquifer, south-central Texas. Dissertation, The University of Texas, Austin, Texas, 243 pp.

Harrington, G.A. and Herczeg, A.L., 2003. The importance of silicate weathering of a sedimentary aquifer in arid Central Australia indicated by very high $^{87}Sr/^{86}Sr$ ratios. Chemical Geology, 199: 281–292.

Hill, R.T., 1891. The Comanche Series of the Texas-Arkansas region. Geological Society of America Bulletin, 2: 503–524.

Hill, R.T., 1901. Geography and geology of the Black and Grand prairies, Texas, with detailed descriptions of the Cretaceous formations and special reference to artesian waters. 21st annual report, United States Geological Survey, Washington, D.C., 666 pp.

Homer, C., Huang, C., Yang, L., Wylie, B. and Coan, M., 2004. Development of a 2001 national land cover database for the United States. Photogrammetric Engineering and Remote Sensing, 70(7): 829–840.

HTGCD (Hays Trinity Groundwater Conservation District), 2008. Well monitoring program data, <www.haysgroundwater.com>, accessed 2008.

Imlay, R.W., 1945. Subsurface Lower Cretaceous formations of south Texas. AAPG Bulletin, 29(10): 1416–1469.

Jones, I.C., Banner, J.L. and Humphrey, J.D., 2000. Estimating recharge in a tropical karst aquifer. Water Resources Research, 36(5): 1289–1299.

Jørgensen, N.O. and Banoeng-Yakubo, B.K., 2001. Environmental isotopes (^{18}O, ^{2}H, and $^{87}Sr/^{86}Sr$) as a tool in groundwater investigations in the Keta Basin, Ghana. Hydrogeology Journal, 9(2): 190–201.

Katz, B.G. and Bullen, T.D., 1996. The combined use of $^{87}Sr/^{86}Sr$ and carbon and water isotopes to study the hydrochemical interaction between groundwater and lakewater in mantled karst. Geochimica et Cosmochimica Acta, 60(24): 5075–5087.

Kendall, C., Sklash, M.G. and Bullen, T.D., 1995. Isotope tracers of water and solute sources in catchments. In: S.T. Trudgill (Editor), Solute modelling in catchment systems. John Wiley and Sons, New York, NY, pp. 261–303.

Kennedy, V.C., Kendall, C., Zellweger, G.W., Wyerman, T.A. and Avanzino, R.J., 1986. Determination of the components of stormflow using water chemistry and environmental isotopes, Mattole River Basin, California. Journal of Hydrology, 84(1–2): 107–140.

Koepnick, R.B., Burke, W.H., Denison, R.E., Hetherington, E.A., Nelson, H.F., Otto, J.B. and Waite, L.E., 1985. Construction of the seawater $^{87}Sr/^{86}Sr$ curve for the Cenozoic and Cretaceous—Supporting data. Chemical Geology (Isotope Geoscience Section), 58: 55–81.

Krothe, N.C. and Libra, R.D., 1983. Sulfur isotopes and hydrochemical variations in spring waters of southern Indiana, USA. Journal of Hydrology, 61(1–3): 267–283.

Kunianski, E.L., 1990. Potentiometric surface of the Edwards-Trinity aquifer system and contiguous hydraulically connected units, west-central Texas, winter 1974–75. U.S. Geological Survey Water-Resources Investigations Report 89-4208, 2 sheets.

Lakey, B. and Krothe, N.C., 1996. Stable isotopic variation of storm discharge from a perennial karst spring, Indiana. Water Resources Research, 32(3): 721–731.

Lambert, R.B., Grimm, K.C. and Lee, R.W., 2000. Hydrogeology, hydrologic budget, and water chemistry of the Medina Lake area, Texas. U.S. Geological Survey Water-Resources Investigations Report 00-4148, 54 pp.

Langmuir, D., 1997. Aqueous environmental geochemistry. Prentice-Hall, Inc., Upper Saddle River, NJ, 600 pp.

Lee, E.S. and Krothe, N.C., 2001. A four-component mixing model for water in a karst terrain in south-central Indiana, USA. Using solute concentration and stable isotopes as tracers. Chemical Geology, 179(1–4): 129–143.

Li, Q., Sun, H., Han, J., Liu, Z. and Yu, L., 2008. High-resolution study on the hydrochemical variation caused by the dilution of precipitation in the epikarst spring—An example spring of Landiantang at Nongla, Mashan, China. Environmental Geology, 54: 347–354.

Lozo, F.E. and F. L. Stricklin, J., 1956. Stratigraphic notes on the outcrop basal Cretaceous, central Texas. Gulf Coast Association of Geological Societies Transactions, 6: 67–78.

Mace, R.E., Chowdhury, A.H., Anaya, R. and Way, S.-C., 2000. Groundwater availability of the Trinity aquifer, Hill Country area, Texas—Numerical simulations through 2050. Texas Water Development Board Report 353, 117 pp.

Maclay, R.W. and Small, T.A., 1986. Carbonate geology and hydrology of the Edwards aquifer in the San Antonio area, Texas. Texas Water Development Board Report 296, 90 pp.

Maloszewski, P., Stichler, W., Zuber, A. and Rank, D., 2002. Identifying the flow systems in a karstic-fissured-porous aquifer, the Schneealpe, Austria, by modelling of environmental ^{18}O and ^{3}H isotopes. Journal of Hydrology, 256(1–2): 48–59.

McNutt, R.H., 2000. Strontium isotopes. In: P.G. Cook and A.L. Herczeg (Editors), Environmental tracers in subsurface hydrology. Kluwer Academic Publishers, Boston, MA, pp. 233–260.

Moser, H. and Stichler, W., 1975. Use of environmental isotope methods as a reconnaissance tool in groundwater exploration near San Antonio de Pichincha, Ecuador. Water Resources Research, 11(3): 501–505.

Muller, D.A., 1990. Ground-water evaluation in and adjacent to Dripping Springs, Texas. Texas Water Development Board Report 322, 61 pp.

Muller, D.A. and McCoy, W., 1987. Ground-water conditions of the Trinity Group aquifer in western Hays County. Texas Water Development Board LP-205, 62 pp.

Musgrove, M. and Banner, J.L., 1993. Regional ground-water mixing and the origin of saline fluids—Midcontinent, United States. Science, 259(5103): 1877–1882.

Musgrove, M. and Banner, J.L., 2004. Controls on the spatial and temporal variability of vadose dripwater chemistry—Edwards Aquifer, central Texas. Geochimica et Cosmochimica Acta, 68(5): 1007–1020.

NADP (National Atmospheric Deposition Program), 2007. National Trends Network Site TX16 (Sonora, TX), <nadp.sws.uiuc.edu>, accessed 2008.

NCDC (National Climatic Data Center), 2008. Climate data online, daily surface data for Blanco station, cooperative station ID 410832, <cdo.ncdc.noaa.gov>, accessed 2008.

Nernst, W., 1904. Theorie der reaktionsgeschwindigkeit in heterogenen systemen. Zeitschrift für Physikalische Chemie, 47: 52–55.

Oetting, G.C., Banner, J.L. and John M. Sharp, J., 1996. Regional controls on the geochemical evolution of saline groundwaters in the Edwards aquifer, central Texas. Journal of Hydrology, 181: 251–283.

Ogden, A.E., Quick, R.A., Rothermel, S.R., Lunsford, D.L. and Snider, C.C., 1986. Hydrogeological and hydrochemical investigation of the Edwards aquifer in the San Marcos area, Hays County, Texas. Edwards Aquifer Research and Data Center R1-86, 364 pp.

Padilla, A., Pulidobosch, A. and Mangin, A., 1994. Relative importance of baseflow and quickflow from hydrographs of karst spring. Ground Water, 32(2): 267–277.

Parkhurst, D.L. and Appelo, C.A.J., 1999. User's guide to PHREEQC (Version 2)—A computer program for speciation, batch-reaction, one-dimensional transport, and inverse geochemical calculations. U.S. Geological Survey Water-Resources Investigations Report 99-4259, 312 pp.

Parkhurst, D.L. and Plummer, F.B., 1993. Geochemical models. In: W.M. Alley (Editor), Regional ground-water quality. Van Nostrand Reinhold, New York, NY, pp. 199–225.

Peel, M.C., Finlayson, B.L. and McMahon, T.A., 2007. Updated world map of the Köppen-Geiger climate classification. Hydrology and Earth System Sciences, 11: 1633–1644.

Perrin, J., Jeannin, P.Y. and Cornaton, F., 2007. The role of tributary mixing in chemical variations at a karst spring, Milandre, Switzerland. Journal of Hydrology, 332(1–2): 158–173.

Perrin, K., Jeannin, P.Y. and Zwahlen, F., 2003. Epikarst storage in a karst aquifer—A conceptual model based on isotopic data, Milandre test site, Switzerland. Journal of Hydrology, 279(1–4): 106–124.

Playá, E. and Rosell, L., 2005. The celestite problem in gypsum Sr geochemistry—An evaluation of purifying methods of gypsiferous samples. Chemical Geology, 221: 102–116.

Plummer, L.N., 1977. Defining reactions and mass transfer in part of the Floridan aquifer. Water Resources Research, 13(5): 801–812.

Plummer, L.N. and Back, W.W., 1980. The mass balance approach—Application to interpreting the chemical evolution of hydrologic systems. American Journal of Science, 280: 130–142.

Plummer, L.N., Busby, J.F., Lee, R.W. and Hanshaw, B.B., 1990. Geochemical modeling of the Madison aquifer in parts of Montana, Wyoming, and South Dakota. Water Resources Research, 26(9): 1981–2014.

Price, A., October 29, 2008. Central Texas still in grips of drought, Austin American-Statesman, Austin, TX.

Rauch, H.W. and White, W.B., 1977. Dissolution kinetics of carbonate rocks 1. Effects of lithology on dissolution rate. Water Resources Research, 13(2): 381–394.

Scanlon, B.R. and Thrailkill, J., 1987. Chemical similarities among physically distinct spring types in a karst terrain. Journal of Hydrology, 89: 259–279.

Schlumberger Water Services, 2007. AquaChem v.5.1 user's manual—Water quality data analysis, plotting, and modeling. Schlumberger Water Services, 384 pp.

Sellards, E.H., 1932. Part 1—The pre-Paleozoic and Paleozoic systems in Texas. In: E.H. Sellards, W.S. Adkins, F.B. Plummer, The Geology of Texas, Volume 1—Stratigraphy. The University of Texas, Austin, Texas, pp. 15–238.

Shuster, E.T. and White, W.B., 1971. Seasonal fluctuations in the chemistry of limestone springs—A possible means for characterizing carbonate aquifers. Journal of Hydrology, 14: 93–128.

Simsek, C., Elci, A., Gunduz, O. and Erdogan, B., 2008. Hydrogeological and hydrogeochemical characterization of a karstic mountain region. Environmental Geology, 54: 291–308.

Slade, R.M., Jr., Bentley, J.T. and Michaud, D., 2002. Results of streamflow gain-loss studies in Texas, with emphasis on gains from and losses to major and minor aquifers. U.S. Geological Survey Open-File Report 02-068, 131 pp.

Smalley, P.C., Raheim, A., Dickson, J.A.D. and Emery, D., 1988. $^{87}Sr/^{86}Sr$ in waters from the Lincolnshire Limestone aquifer, England, and the potential of natural strontium isotopes as a tracer for a secondary recovery seawater injection process in oilfields. Applied Geochemistry, 3: 591–600.

Smart, P.L., Dawans, J.M. and Whitaker, F., 1988. Carbonate dissolution in a modern mixing zone. Nature, 335: 811–813.

Steinhauer, E.S., Neill, M.F., DeMott, L.M., Landrum, J.T., Schumacher, W. and Bennett, P.C., 2006. Hydrogeochemical and hydrogeologic evidence for Blanco River recharge of Jacob's Well, a karst spring in Hays County, Texas. Geological Society of America Abstracts with Programs, 38(7): 435.

Stricklin, J., F. L., Smith, C.I. and Lozo, F.E., 1971. Stratigraphy of Lower Cretaceous Trinity deposits of central Texas. Bureau of Economic Geology—Report of Investigations, 71: 63.

Stringfield, V.T. and Le Grand, H.E., 1966. Hydrology of limestone terranes in the coastal plain of the southeastern United States. Geological Society of America Special Paper 93, 46 pp.

Stumm, W. and Morgan, J.J., 1996. Aquatic chemistry—Chemical equilibria and rates in natural waters. John Wiley and Sons, New York, NY, 1022 pp.

Taff, J.A., 1892. Reports on the Cretaceous area north of the Colorado River. In: E. T. Dumble (Editor), Third Annual Report of the Geological Survey of Texas (1891). Henry Hutchings, state printer, Austin, pp. 269–379.

TBWE (Texas Board of Water Engineers), 1960. Channel gain and loss investigations, Texas streams, 1918–1958. Texas Board of Water Engineers Bulletin 5807-D, 270 pp.

TCEQ (Texas Commission on Environmental Quality), 2007. Public water supply database.

Teledyne Tekmar Co., 2002. Apollo 9000 with Total Nitrogen. Tekmar Company, Mason, OH, 154 pp.

Teledyne Tekmar Co., 2003. Apollo 9000 TOC Combustion Analyzer user manual. Tekmar Company, Mason, OH, 135 pp.

Thrailkill, J., 1968. Chemical and hydrologic factors in the excavation of caves. Geological Society of America Bulletin, 79: 19–46.

TNRIS (Texas Natural Resource Information System), 2006. StratMap transportation phase 2 feature layer, digital vector data.

Turner, S.F., 1938. Hays County Texas—Records of wells and springs, drillers' logs, water analyses and map showing location of wells. Texas State Board of Water Engineers, 31 pp.

TWDB (Texas Water Development Board), 2007. Water for Texas—2007, 3: Regional water planning information database, <www.twdb.state.tx.us>.

TWDB (Texas Water Development Board), 2008. Groundwater database, <www.twdb.state.tx.us>.

USCB (United States Census Bureau), 1993. 1990 census of population and housing—Population and housing unit counts, CPH-2-1, United States. In: United States Department of Commerce, Economics and Statistics Administration and United States Census Bureau (Editors). 1990 census of population and housing. U.S. Government Printing Office, 777 pp.

USCB (United States Census Bureau), 2003. 2000 census of population and housing—Population and housing unit counts, PHC-3-45, Texas. In: United States Department of Commerce, Economics and Statistics Administration and United States Census Bureau (Editors). 2000 census of population and housing. U.S. Government Printing Office, 98 pp.

USDA/FSA (United States Department of Agriculture Farm Service Agency, Aerial Photography Field Office), 2003. Digital ortho MrSID mosaic, remote sensing image.

USDA/NRCS (United States Department of Agriculture and Natural Resources Conservation Service National Cartography and Geospatial Data Center), 2000-present. National elevation data 10 meter or better, digital raster data.

USDA SCS (United States Department of Agriculture Soil Conservation Service), 1984. Soil survey of Comal and Hays counties Texas, 136 pp.

Usdowski, E., Hoefs, J. and Menschel, G., 1979. Relationship between 13C and 18O fractionation and changes in major element composition in a recent calcite-depositing spring—A model of chemical variations with inorganic CaCO3 precipitation. Earth and Planetary Science Letters, 42: 267–276.

USGS (United States Geological Survey), undated. Statewide digital geologic atlas of Texas—Geology 250k, digital vector data.

USGS (United States Geological Survey), 2003. National land cover database 2001, remote sensing image.

USGS (United States Geological Survey), 2008. National water information system data, gauge 08170990, <waterdata.usgs.gov/nwis>, accessed 2008.

Veni, G., 1994. Geomorphology, hydrodeology, geochemistry, and evolution of the karstic lower Glen Rose aquifer, south-central Texas. Dissertation, Pennsylvania State University, 720 pp.

Vesper, D.J. and White, W.B., 2004. Storm pulse chemographs of saturation index and carbon dioxide pressure—Implications for shifting recharge sources during storm events in the karst aquifer at Fort Campbell, Kentucky/Tennessee, USA. Hydrogeology Journal, 12(2): 135–143.

Weeks, A.W., 1945. Balcones, Luling, and Mexia fault zones in Texas. AAPG Bulletin, 29(12): 1733–1737.

Wermund, E.G., Cepeda, J.C. and Luttrell, P.E., 1978. Regional distribution of fractures in the southern Edwards Plateau and their relationship to tectonics and caves. Bureau of Economic Geology—Geological Circular, 78-2: 14 pp.

Whitney, M.I., 1952. Some zone marker fossils of the Glen Rose Formation of central Texas. Journal of Paleontology, 26(1): 66–73.

Wigley, T.M.L. and Plummer, L.N., 1976. Mixing of carbonate waters. Geochimica et Cosmochimica Acta, 40: 989–995.

Winston, W.E. and Criss, R.E., 2004. Dynamic hydrologic and geochemical response in a perennial karst spring. Water Resources Research, 40(5): W05106, doi:10.1029/2004WR003054.

Woronick, R.E., 1985. Burial diagenesis of the Lower Cretaceous Pearsall and Lower Glen Rose formations, south Texas—A petrographic and geochemical study, The University of Texas at Austin, Austin, TX, 91 pp.

Zhu, C. and Anderson, G., 2002. Environmental applications of geochemical modeling. Cambridge University Press, New York, NY, 284 pp.

Vita

Sarah Cain Davidson was born on October 25, 1981 in Minneapolis, Minnesota to J. Warren Davidson and Rachel R. Cain. Prior to attending The University of Texas at Austin, Sarah completed coursework at the University of Minnesota in Minneapolis, Minnesota; Beloit College in Beloit, Wisconsin; and Marmara University in Istanbul, Turkey. She graduated from Beloit College in 2004 with a B.S. in environmental geology and a minor in political science. Over the past nine years, she has worked for the Minnesota Geological Survey, the Austin consulting firm Loomis Partners, the Texas Water Development Board, and the Bureau of Economic Geology.

Permanent address: 5594 Sheldon Street, Shoreview, Minnesota 55126

This thesis was typed by Sarah Cain Davidson.